

Maximizing the Interaction Strength

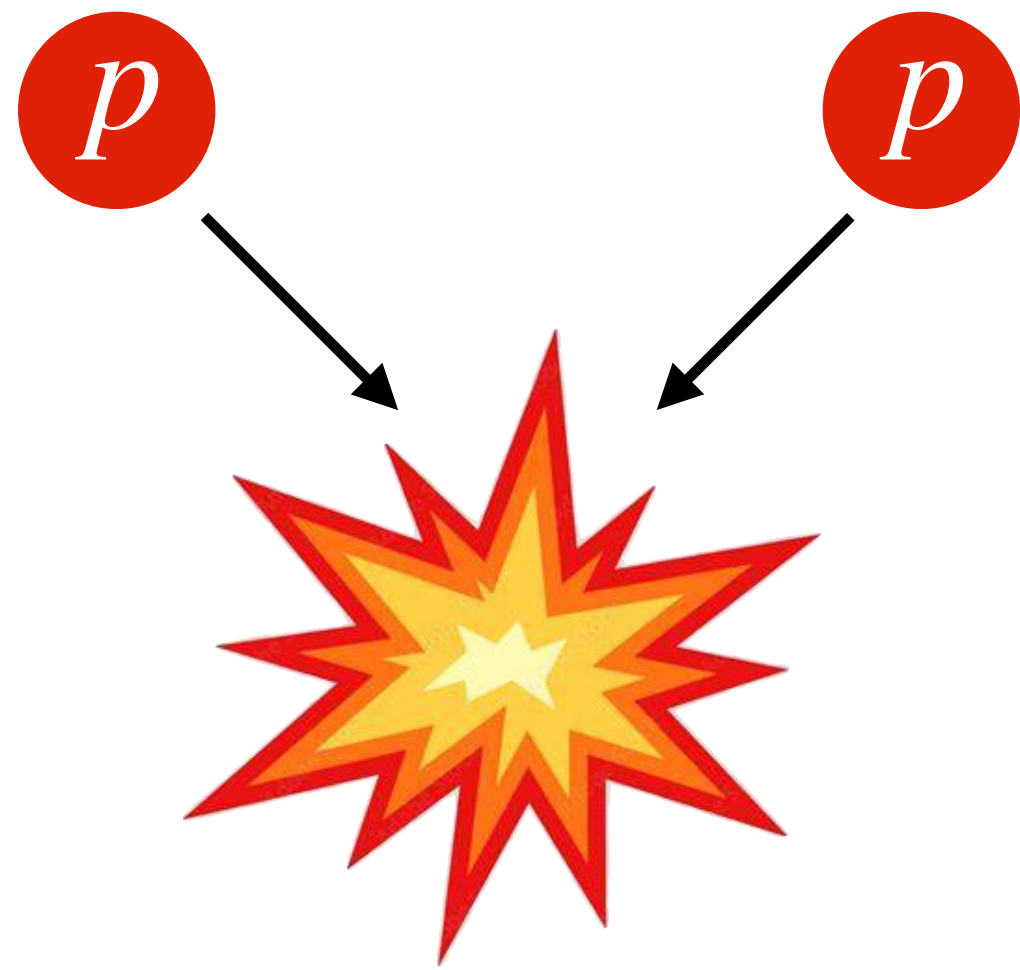
Miguel Correia



Based on **2506.04313** w/ **Alessandro Georgoudis** and **Andrea Guerrieri**

New Frontiers of Quantum Field and Gravity, PKU 2026

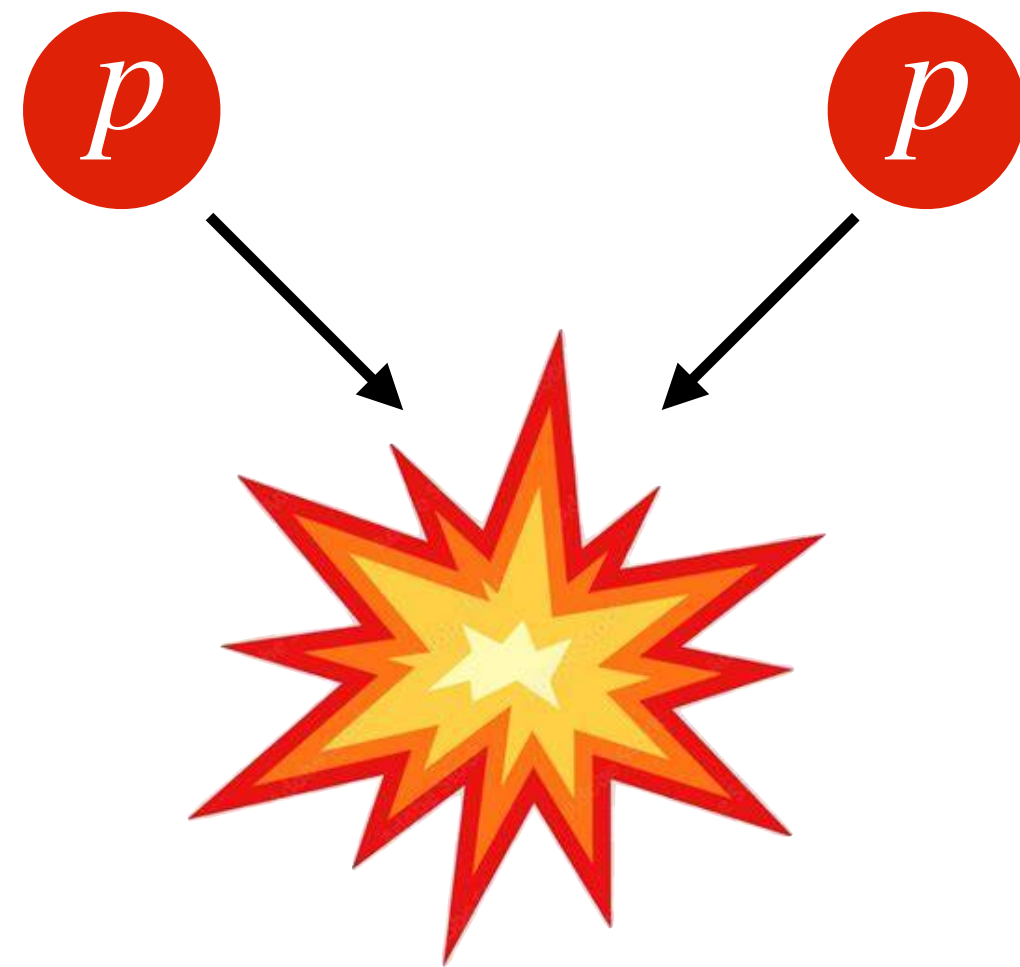
Total Proton-Proton Cross-Section



$$\sigma_{tot}(s) = ?$$

Total Proton-Proton Cross-Section

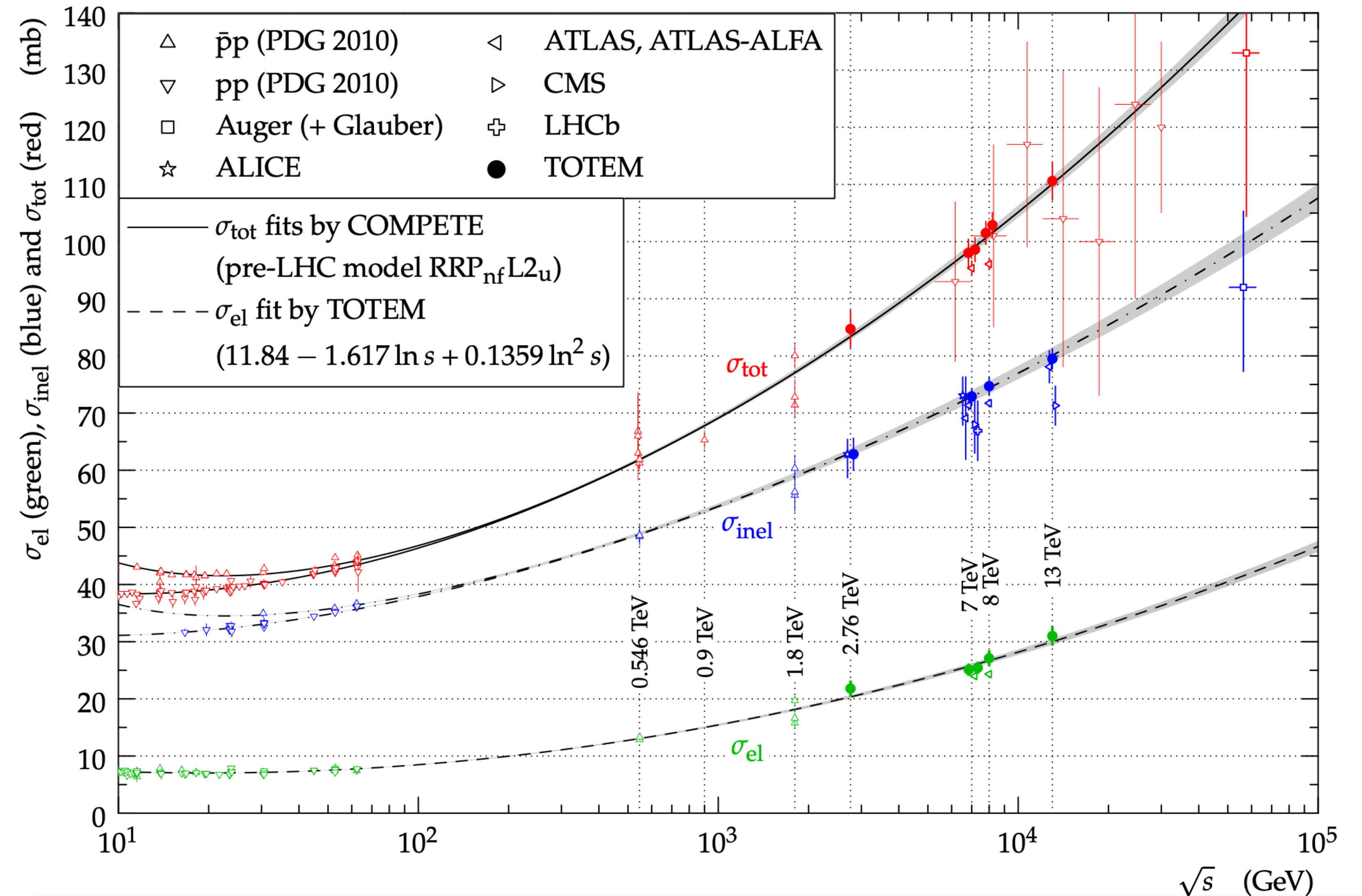
[PDG, 2024]



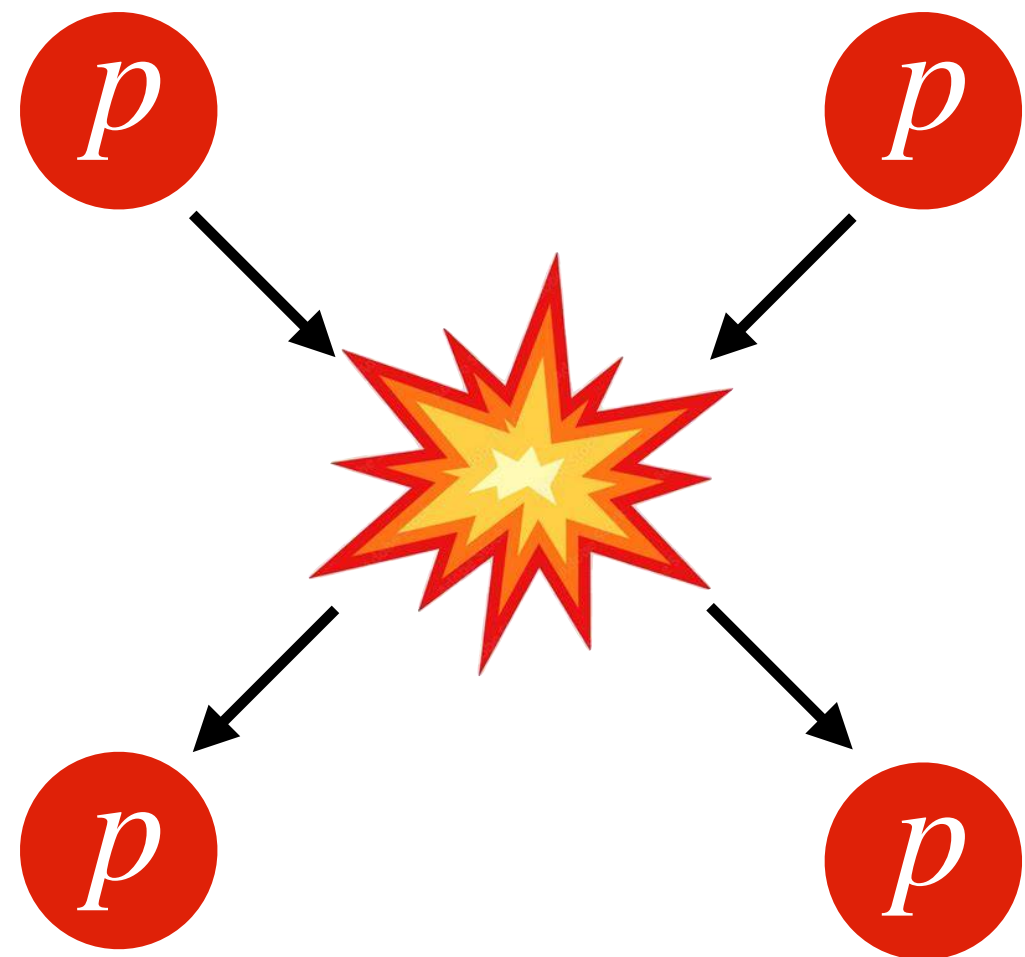
$$\sigma_{tot}(s) = ?$$

Cross-section grows!
Distinctive feature of
the strong force.

No theory/model that
explains this behavior.



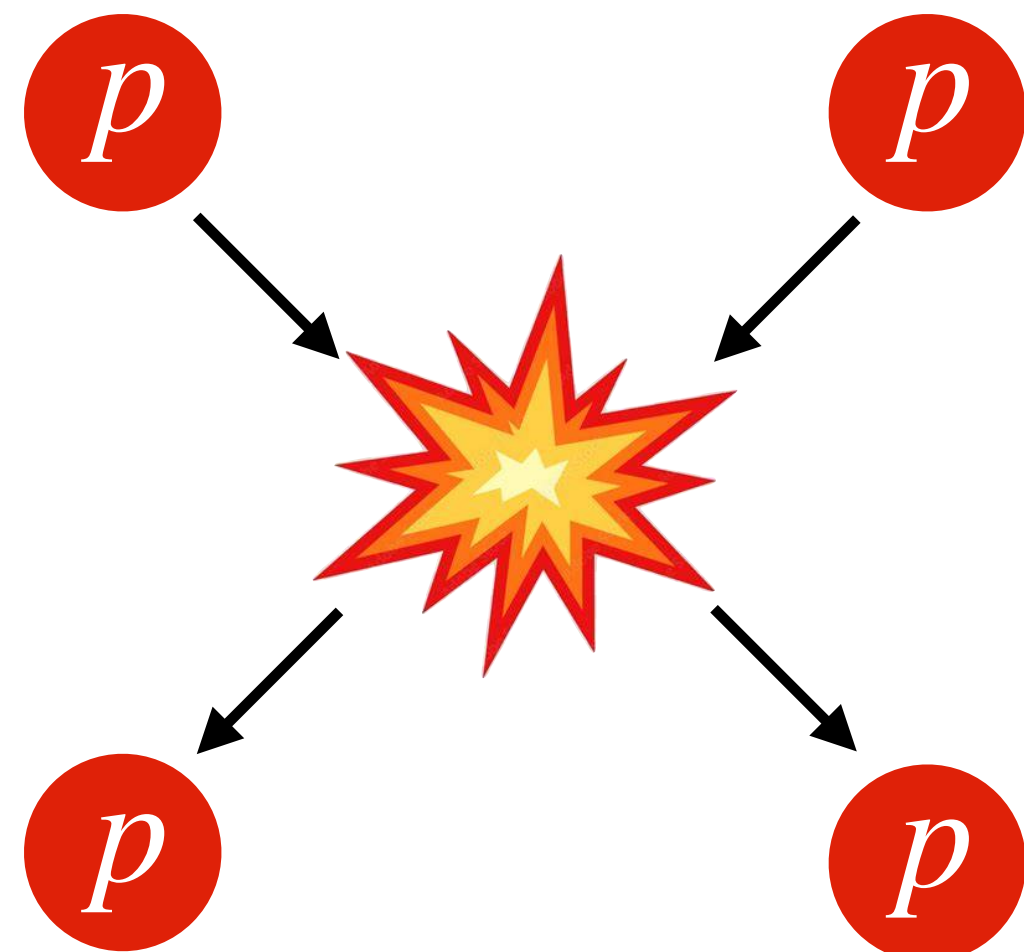
Elastic Proton-Proton Differential Cross-Section



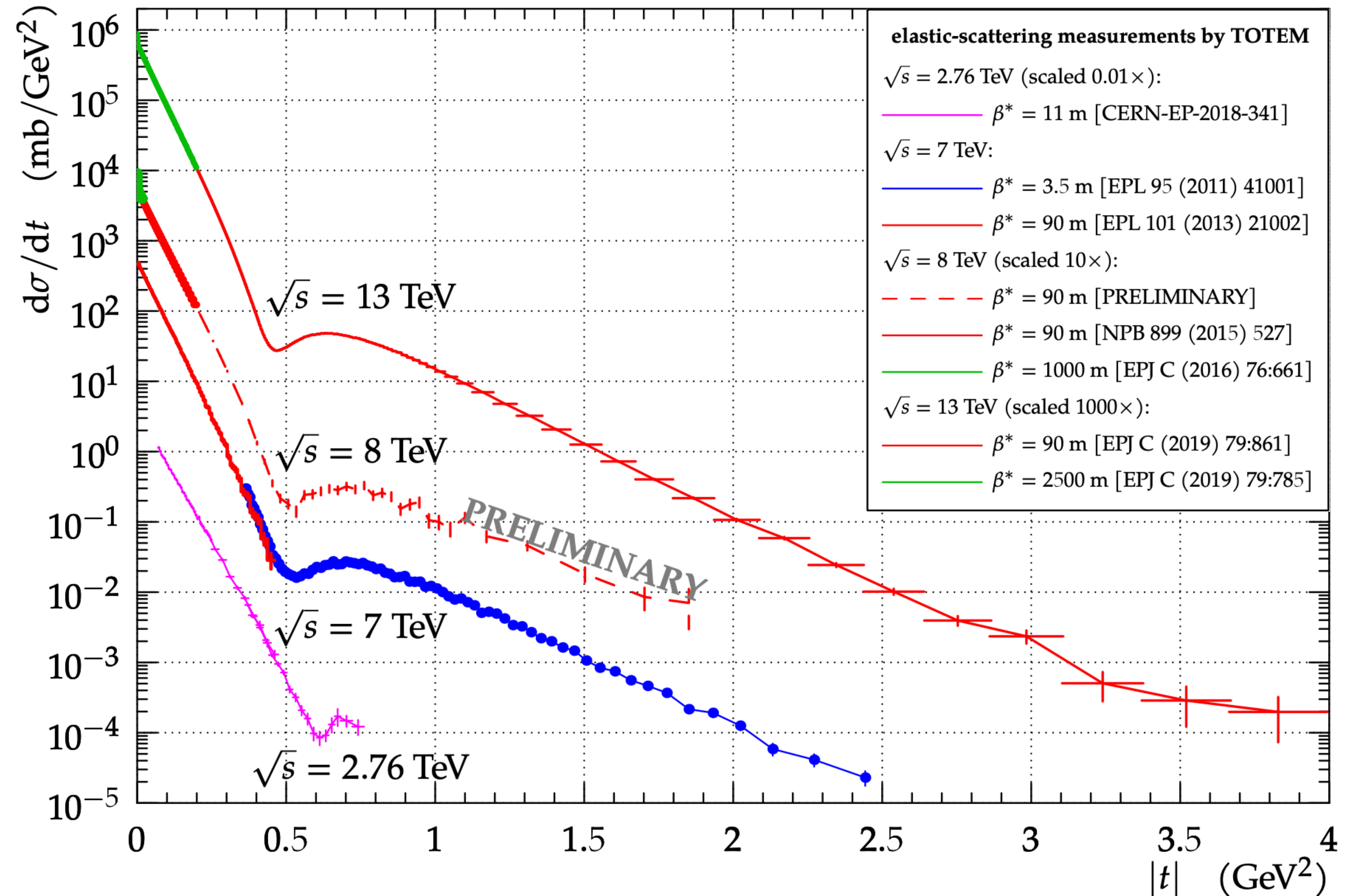
$$\frac{d\sigma_{el}}{d\Omega}(s, t) = ?$$

Elastic Proton-Proton Differential Cross-Section

[PDG, 2024]

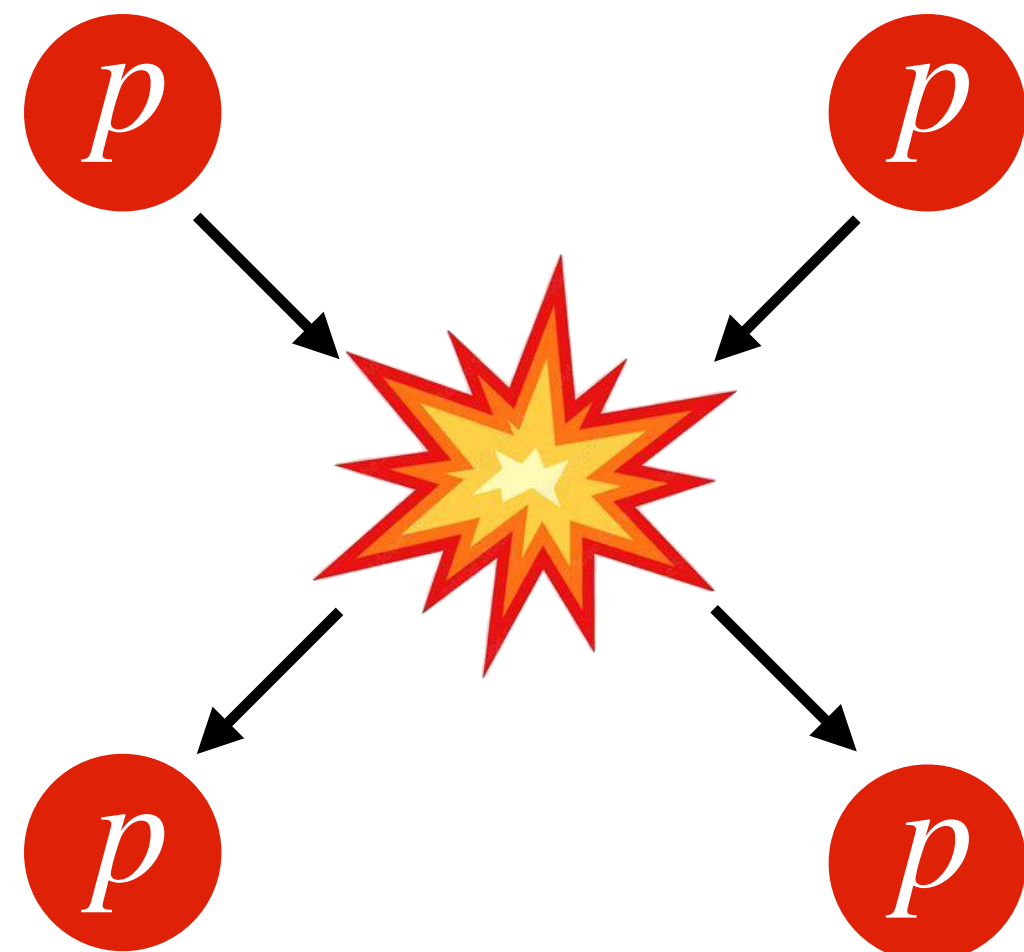


$$\frac{d\sigma_{el}}{d\Omega}(s, t) = ?$$

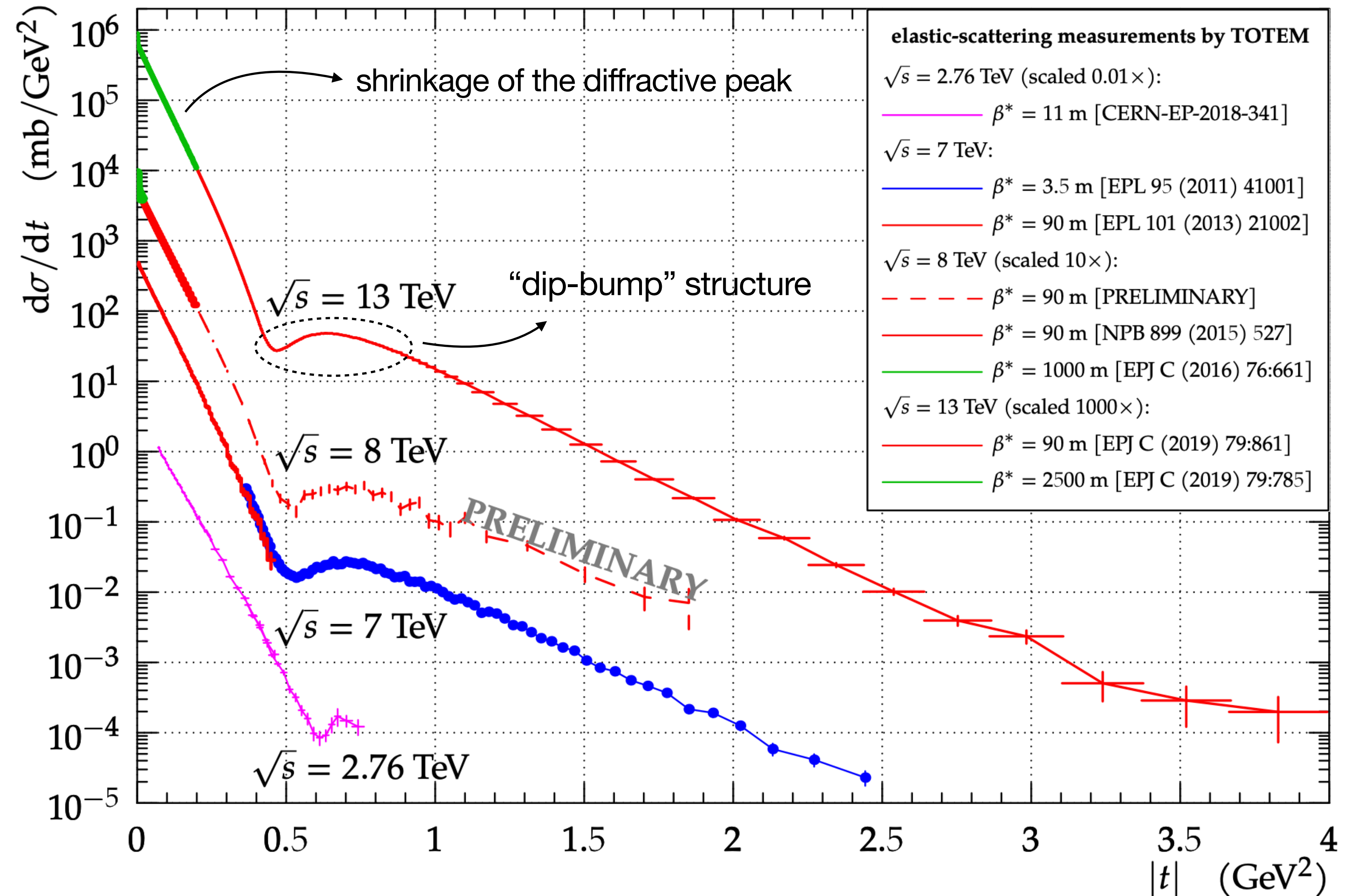


Elastic Proton-Proton Differential Cross-Section

[PDG, 2024]

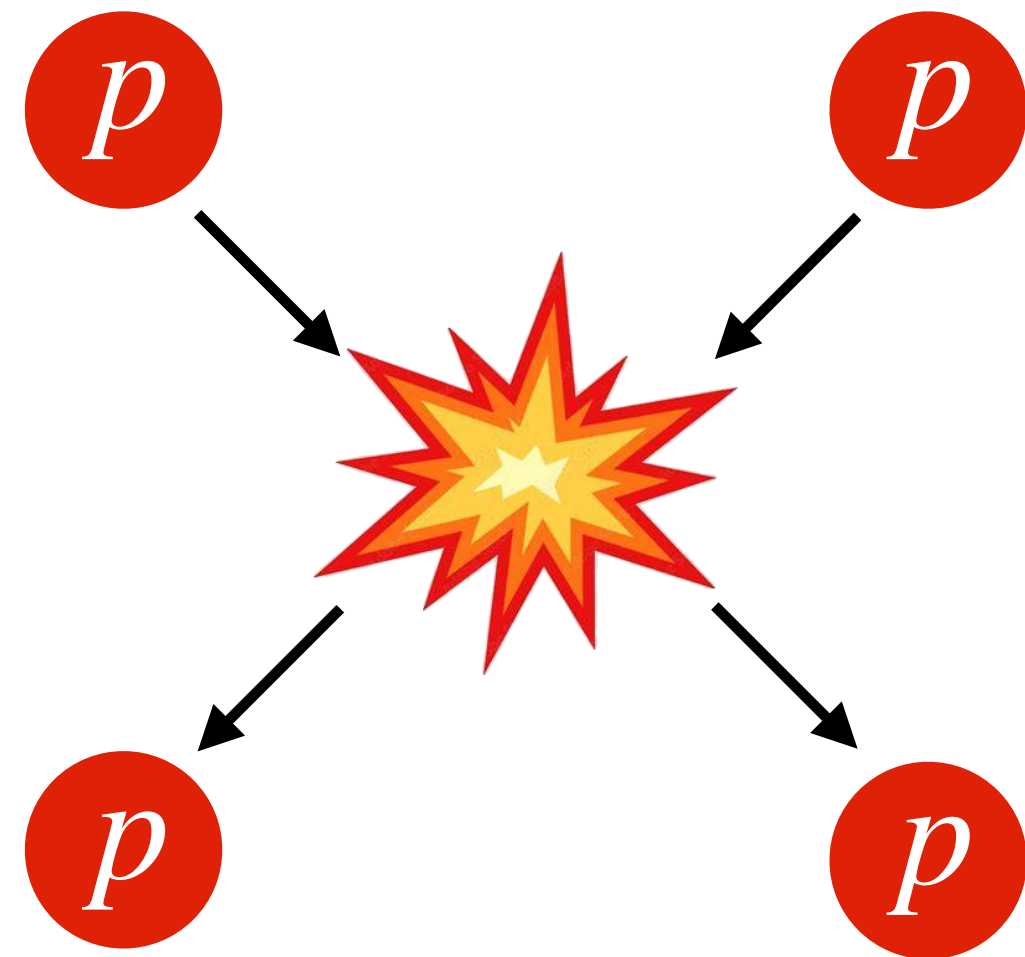


$$\frac{d\sigma_{el}}{d\Omega}(s, t) = ?$$



Elastic Proton-Proton Differential Cross-Section

[PDG, 2024]



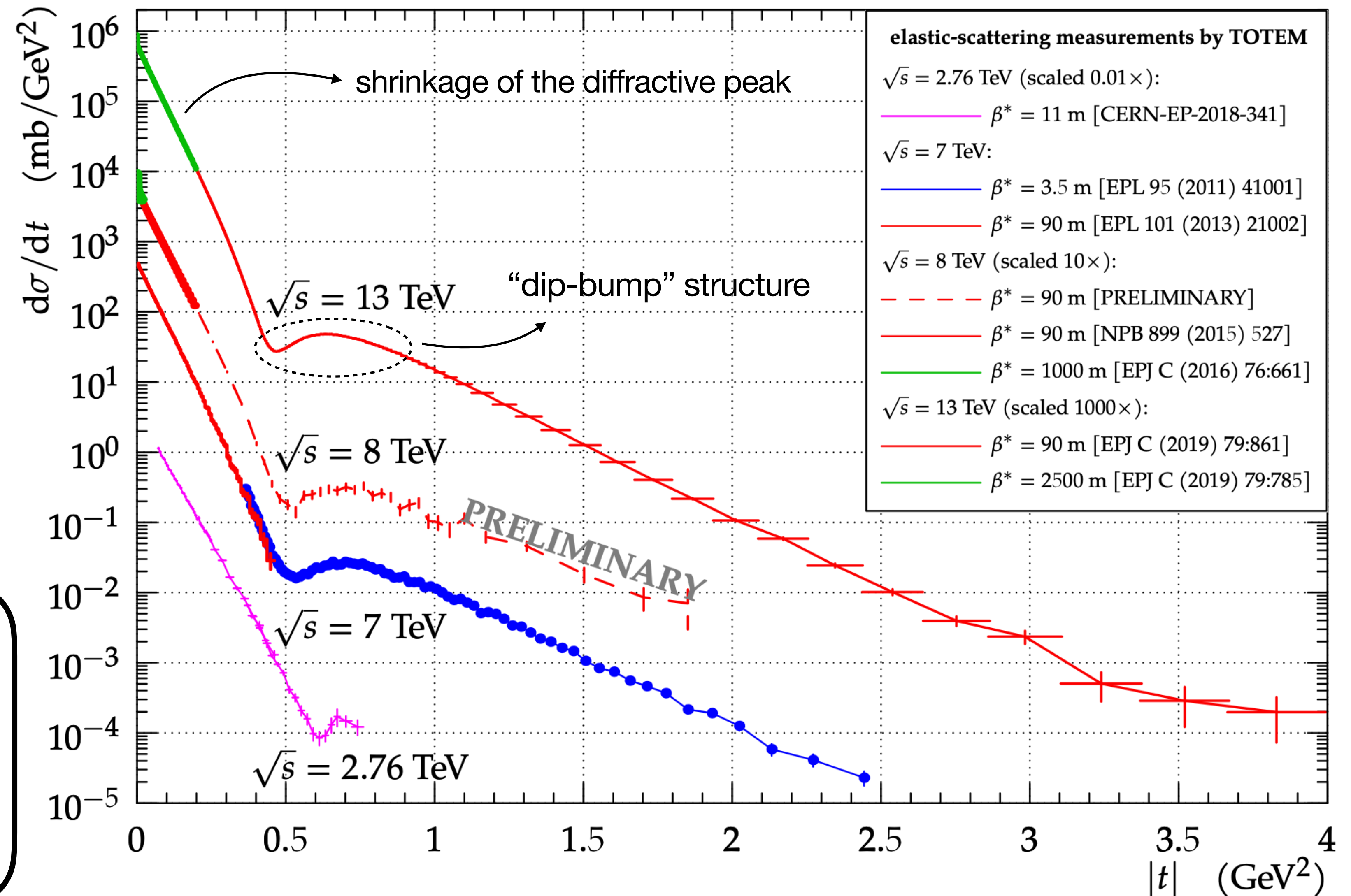
$$\frac{d\sigma_{el}}{d\Omega}(s, t) = ?$$

Why so difficult to describe?

$$s \gg 1 \text{ GeV}^2 \sim |t|$$

EFT, Lattice QCD
do not apply

Nonperturbative
(confinement)



Outline

- Overview of old results: Froissart bound, Regge theory and the Pomeron model.
- Applying the **modern S-matrix bootstrap** in the **high-energy soft regime**:
 1. Bound on total cross-section at finite energy.
 2. Study of the “strongest interacting” amplitude.

Froissart bound and Regge theory

- Assumptions:
- Mass gap $m > 0$
 - Higher-spin particles $J \geq 2$

$$\overline{\overline{\text{wavy line}}}_{m,J} = \frac{s^J}{t - m^2}$$

Froissart bound and Regge theory

- Assumptions:
- Mass gap $m > 0$
 - Higher-spin particles $J \geq 2$

$$\overbrace{\quad}^{m, J} = \frac{s^J}{t - m^2}$$

Froissart bound

$$\sigma_{tot}(s \rightarrow \infty) \leq \frac{\pi}{m^2} \log^2 s$$

[Froissart, 1961]

Froissart bound and Regge theory

- Assumptions:
- Mass gap $m > 0$
 - Higher-spin particles $J \geq 2$

$$\overbrace{\quad}^{m, J} = \frac{s^J}{t - m^2}$$

Froissart bound

$$\sigma_{tot}(s \rightarrow \infty) \leq \frac{\pi}{m^2} \log^2 s$$

[Froissart, 1961]

quick derivation: 1. $\sigma_{tot} \sim \pi R^2$

$$2. \quad R \overbrace{\quad}^{m, J} = s^{J-1} e^{-mR} \lesssim 1$$

↑
Unitarity

$$3. \quad R \lesssim \frac{\log s}{m} \quad (m > 0, J \geq 2)$$

Regge theory

$$T(s \rightarrow \infty, t) \sim s^{\alpha(t)}, \quad J = \alpha(t)$$

Froissart bound and Regge theory

- Assumptions:
- Mass gap $m > 0$
 - Higher-spin particles $J \geq 2$

$$\overline{\underbrace{\quad}_{m,J}} = \frac{s^J}{t - m^2}$$

Froissart bound

$$\sigma_{tot}(s \rightarrow \infty) \leq \frac{\pi}{m^2} \log^2 s$$

[Froissart, 1961]

quick derivation: 1. $\sigma_{tot} \sim \pi R^2$

$$2. \quad R \overline{\underbrace{\quad}_{m,J}} = s^{J-1} e^{-mR} \lesssim 1$$

↑
Unitarity

$$3. \quad R \lesssim \frac{\log s}{m} \quad (m > 0, J \geq 2)$$

Regge theory

$$T(s \rightarrow \infty, t) \sim s^{\alpha(t)}, \quad J = \alpha(t)$$

quick derivation: 1. Optical theorem $\sigma_{tot}(s) = \text{Im } T(s, 0)/s$

2. Froissart bound $T(s, 0) \lesssim s \log^2 s$

3. $\overline{\underbrace{\quad}_{m,J}} \sim s^J$ grows too fast!

4. Solution: $J = \alpha(t)$ such that $\alpha(0) \leq 1$

Regge phenomenology and the Pomeron

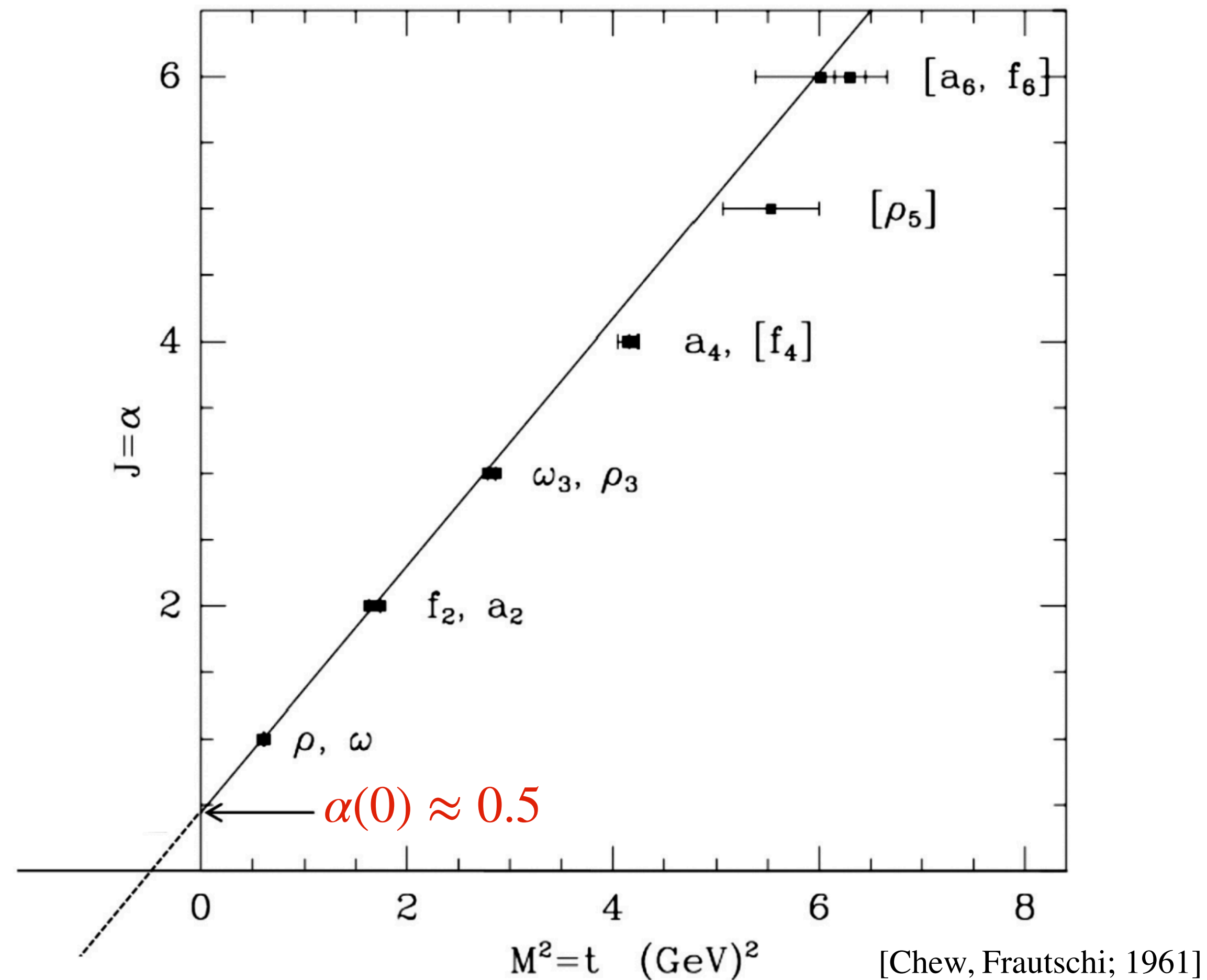
Two main consequences of Regge theory:

Regge phenomenology and the Pomeron

Two main consequences of Regge theory:

1. Higher-spin particles align along Regge trajectories

$$J = \alpha(t)$$

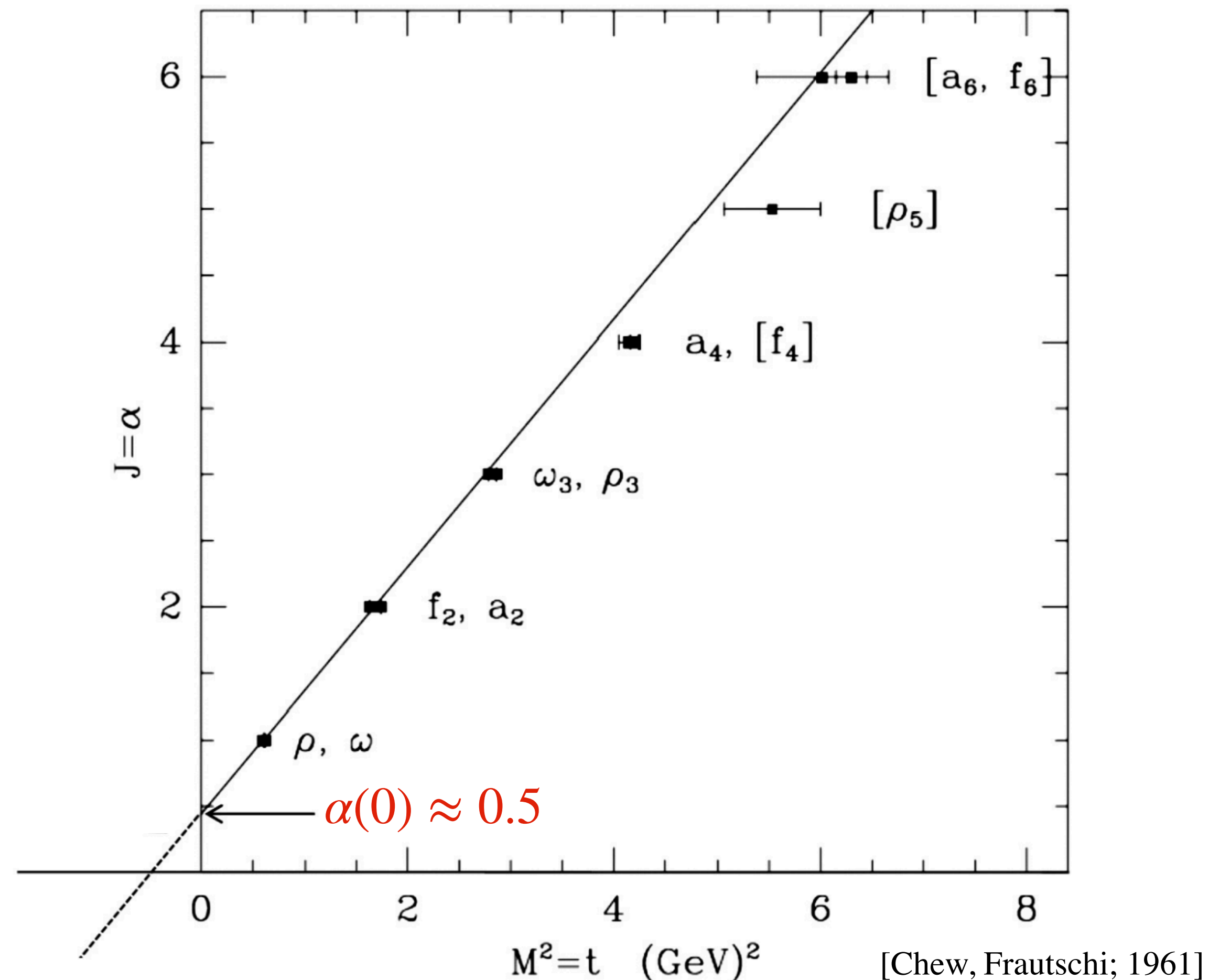


Regge phenomenology and the Pomeron

Two main consequences of Regge theory:

1. Higher-spin particles align along Regge trajectories

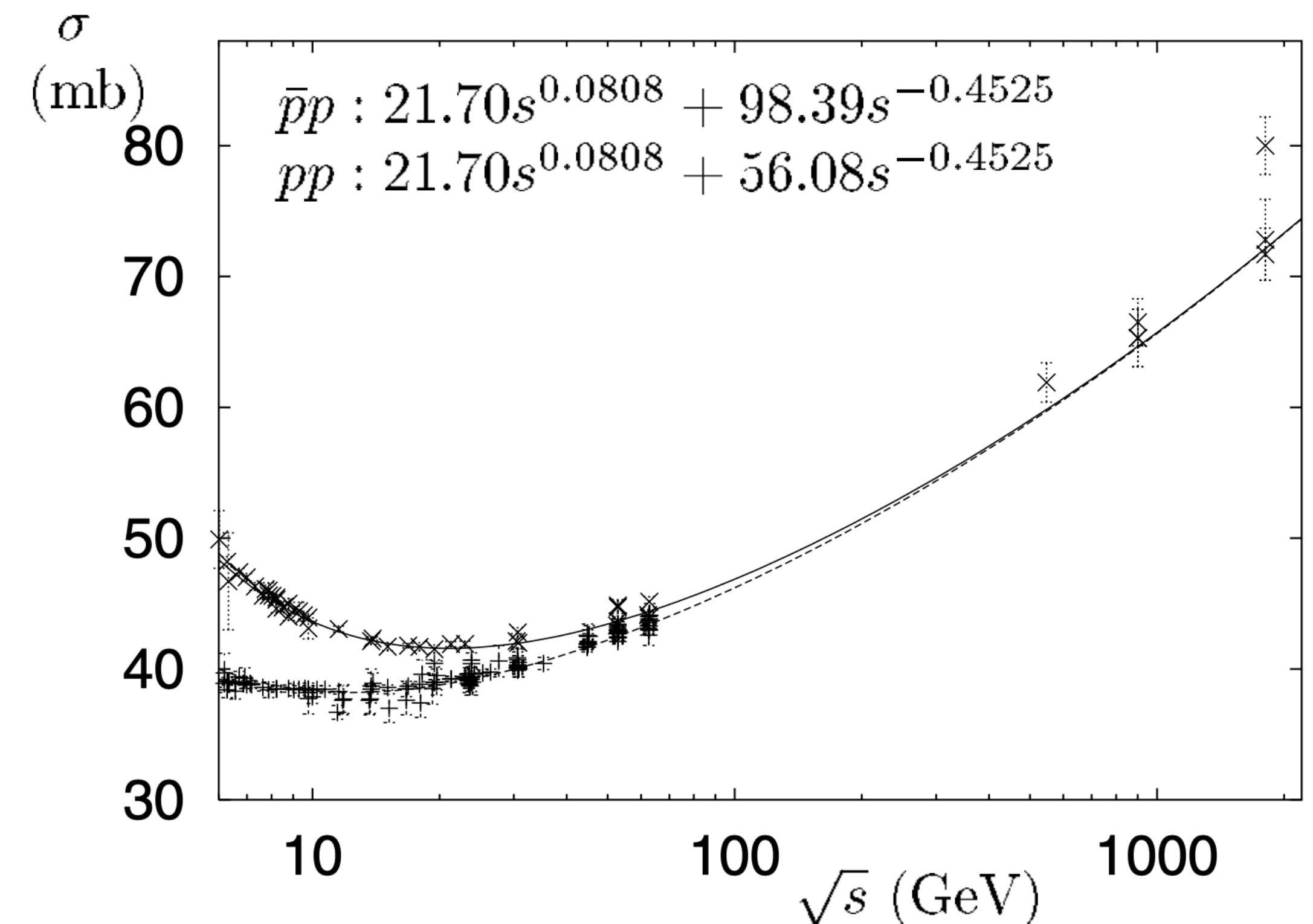
$$J = \alpha(t)$$



2. They determine the high-energy behavior.

$$T(s, t) \sim s^{\alpha(t)}$$

$$\sigma_{tot}(s \rightarrow \infty) \sim s^{\alpha(0)-1}$$



Regge phenomenology and the Pomeron

Two main consequences of Regge theory:

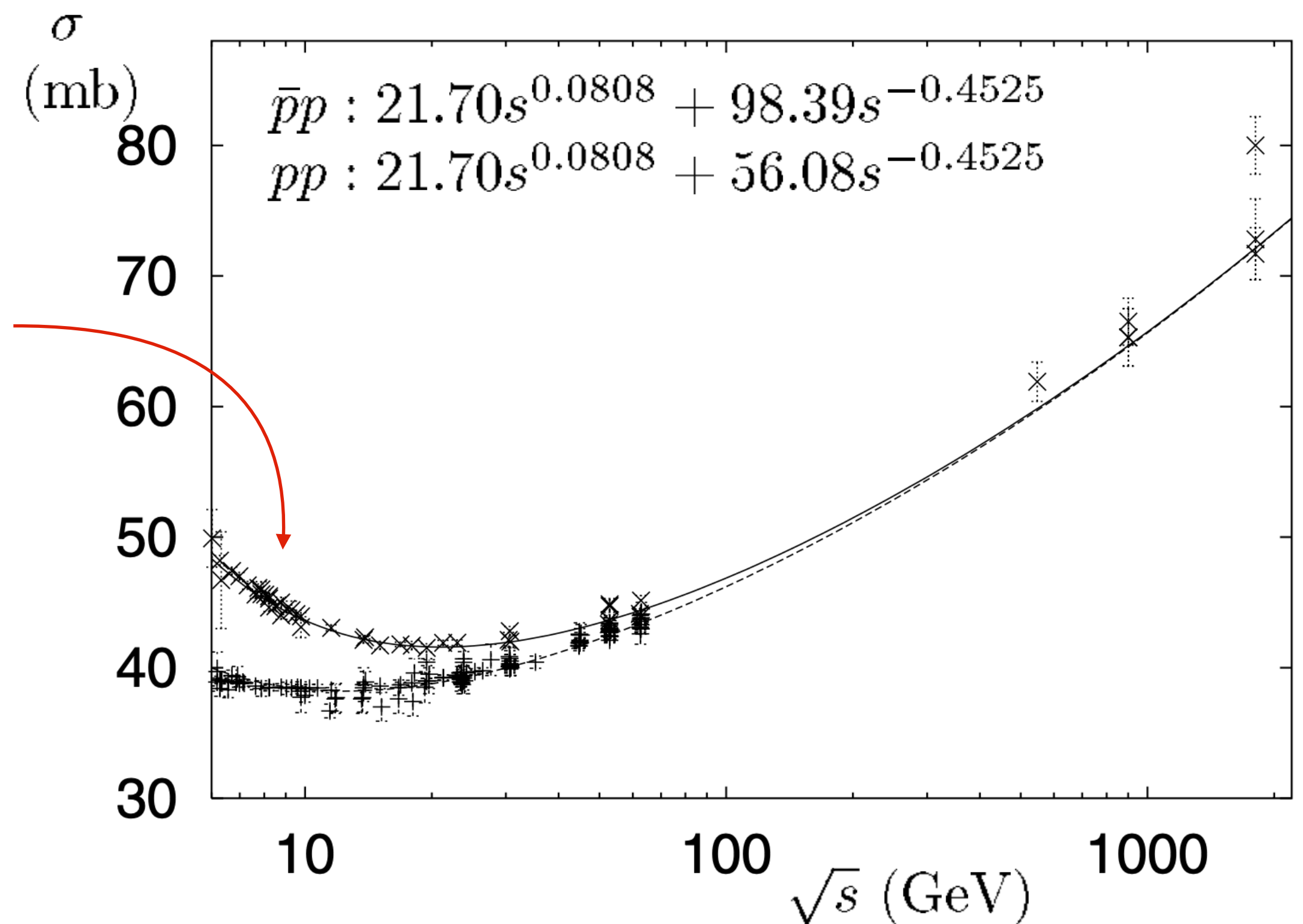
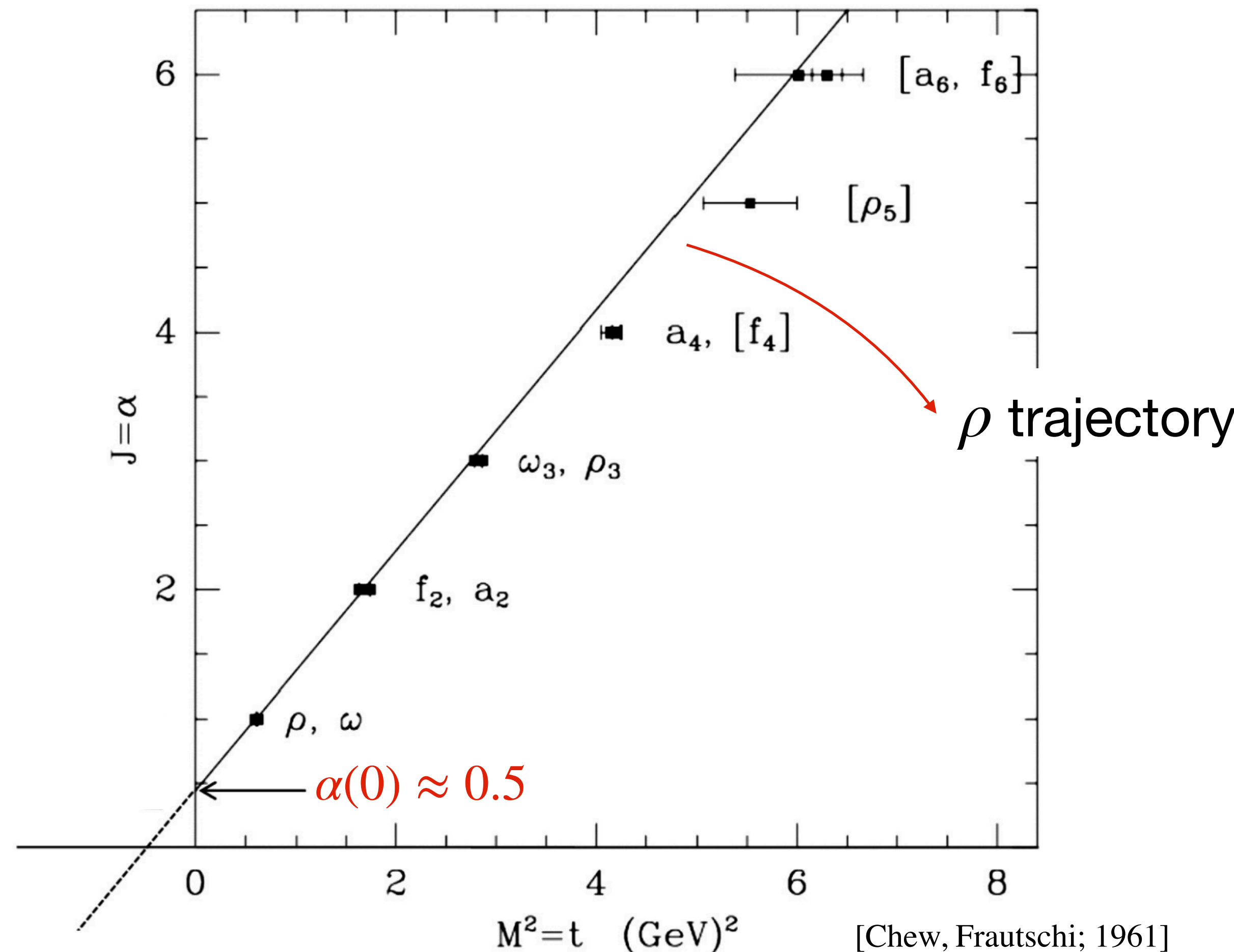
1. Higher-spin particles align along Regge trajectories

2. They determine the high-energy behavior.

$$J = \alpha(t)$$

$$T(s, t) \sim s^{\alpha(t)}$$

$$\sigma_{tot}(s \rightarrow \infty) \sim s^{\alpha(0)-1}$$



Regge phenomenology and the Pomeron

Two main consequences of Regge theory:

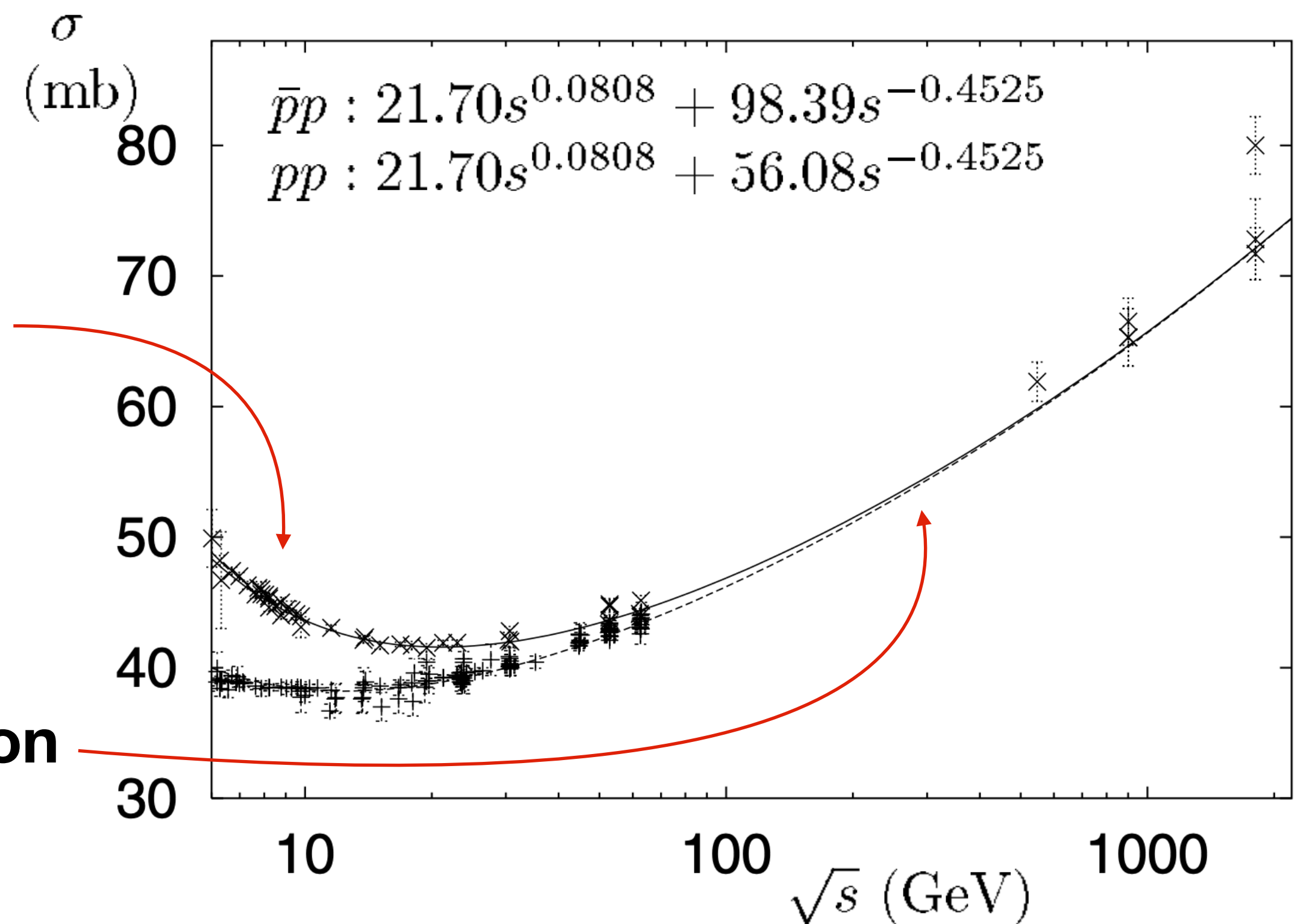
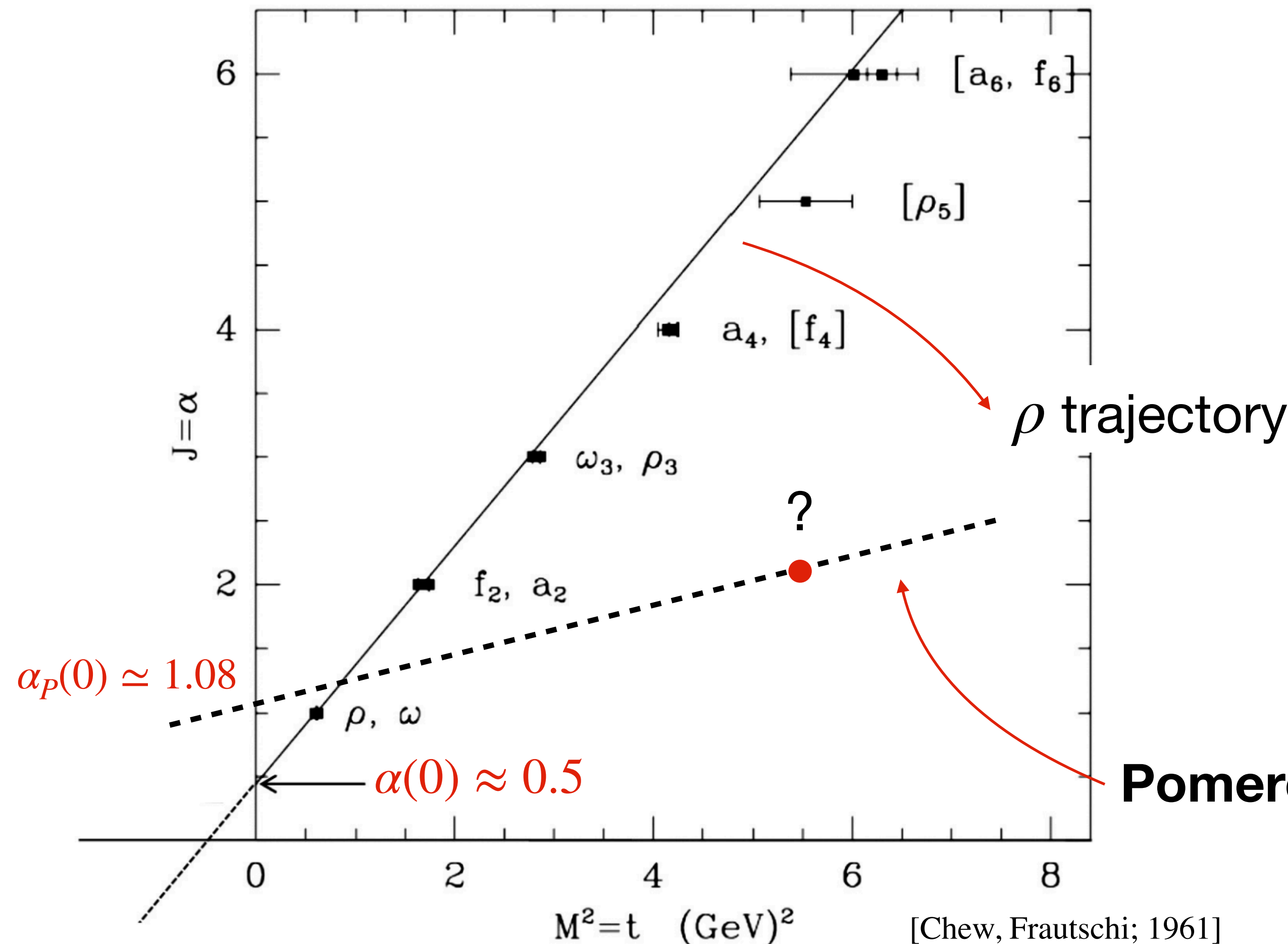
1. Higher-spin particles align along Regge trajectories

2. They determine the high-energy behavior.

$$J = \alpha(t)$$

$$T(s, t) \sim s^{\alpha(t)}$$

$$\sigma_{tot}(s \rightarrow \infty) \sim s^{\alpha(0)-1}$$



The Bootstrap program of the 1960s

The Pomeron: Family of particles (Regge trajectory) responsible for the universal growth of the hadronic cross-sections.

Status: **Unknown**

Froissart bound: $\sigma_{tot}(s) \lesssim \log^2 s$

The Bootstrap program of the 1960s

The Pomeron: Family of particles (Regge trajectory) responsible for the universal growth of the hadronic cross-sections.

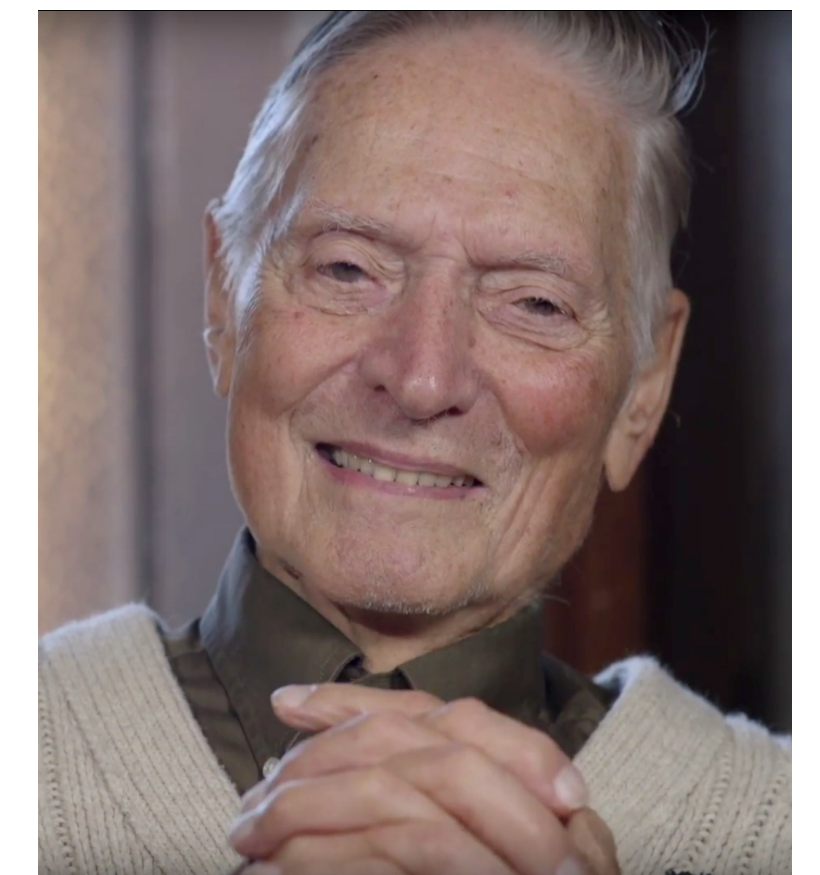
Status: **Unknown**

Froissart bound: $\sigma_{tot}(s) \lesssim \log^2 s$

Chew's Principle of Maximum Strength:

The strong interactions saturate the Froissart bound, and are thus fixed by bootstrap consistency alone.

[G. Chew, *The Analytic S-matrix*, 1966]



Geoffrey Chew, 2016

The Bootstrap program of the 1960s

The Pomeron: Family of particles (Regge trajectory) responsible for the universal growth of the hadronic cross-sections.

Status: **Unknown**

Froissart bound: $\sigma_{tot}(s) \lesssim \log^2 s$

Chew's Principle of Maximum Strength:

The strong interactions saturate the Froissart bound, and are thus fixed by bootstrap consistency alone.

[G. Chew, *The Analytic S-matrix*, 1966]



Geoffrey Chew, 2016

Growing Cross-Section



Analyticity, Crossing, Unitarity.

The Bootstrap program of the 1960s

The Pomeron: Family of particles (Regge trajectory) responsible for the universal growth of the hadronic cross-sections.

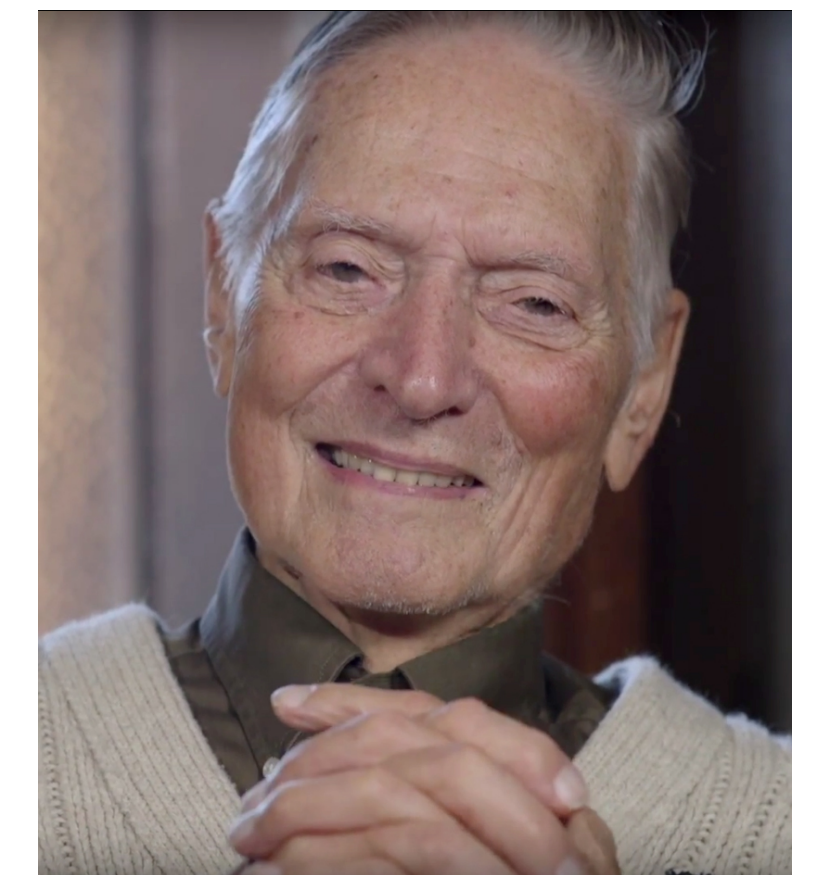
Status: **Unknown**

Froissart bound: $\sigma_{tot}(s) \lesssim \log^2 s$

Chew's Principle of Maximum Strength:

The strong interactions saturate the Froissart bound, and are thus fixed by bootstrap consistency alone.

[G. Chew, *The Analytic S-matrix*, 1966]



Geoffrey Chew, 2016

Growing Cross-Section



Analyticity, Crossing, Unitarity.

Concrete first target: **Bounding the cross-section at finite energy**

Tool we use: Modern S-matrix Bootstrap

INPUT:

Analyticity →

Crossing Symmetry →

Unitarity →

**Primal
S-matrix
Bootstrap**

[Paulos, Penedones, Toledo, van Rees, Vieira; 2016]

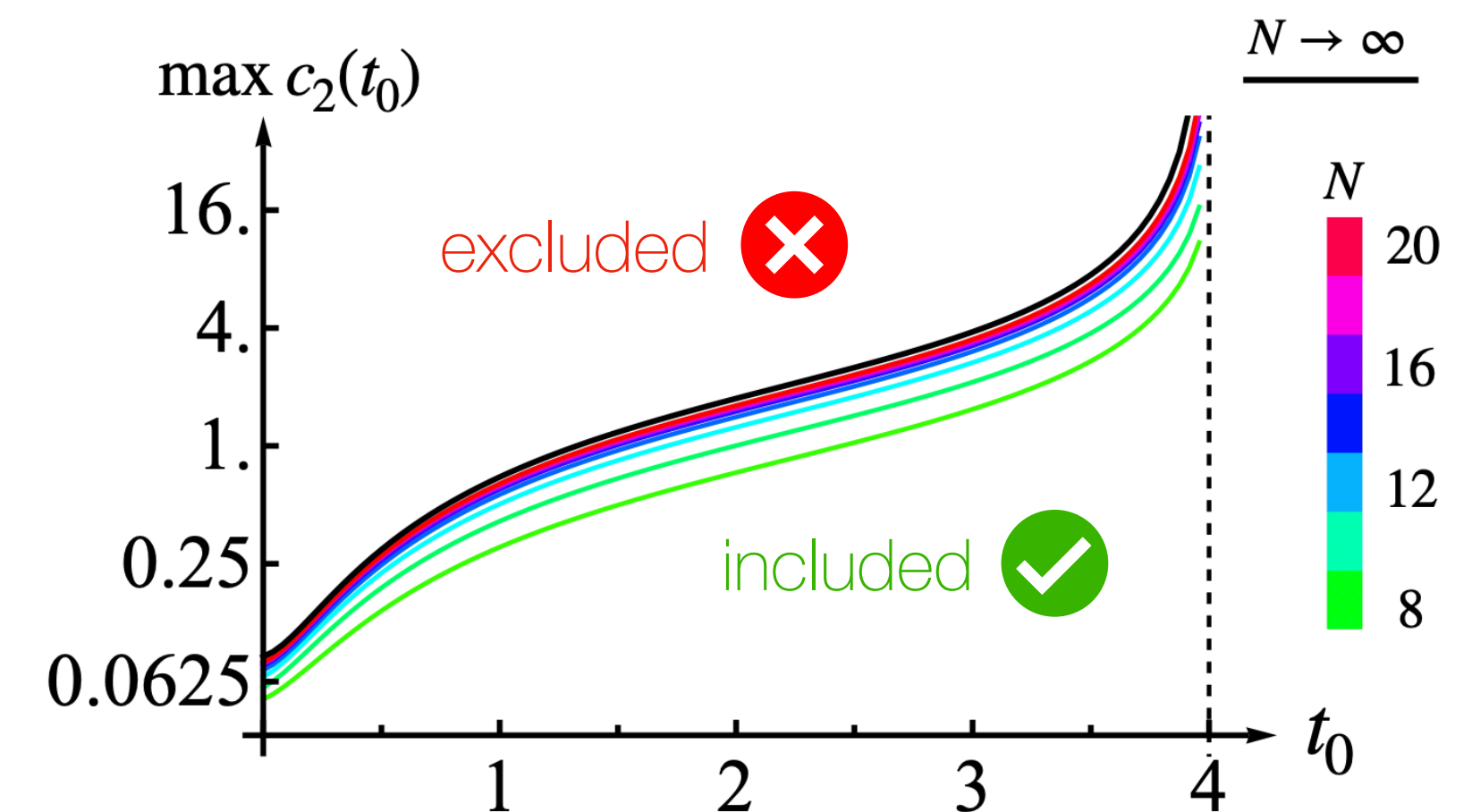
• Cordova, MC, Elias Miró, Gümus, **Karateev**,
• Homrich, **He**, Kruczenski, Hebbar, **Zhou**...

[Guerrieri, Häring, **Su**; 2024]

$N, L \rightarrow \infty$

OUTPUT:

→ Bounds on low-energy data



→ Consistent Extremal Amplitude

$$T(s, t) = T_{max}(s, t)$$

Bounding the Cross-Section **at Finite Energy**

Bound on Integrated Total Cross-Section

Scattering of identical scalar bosons of mass m

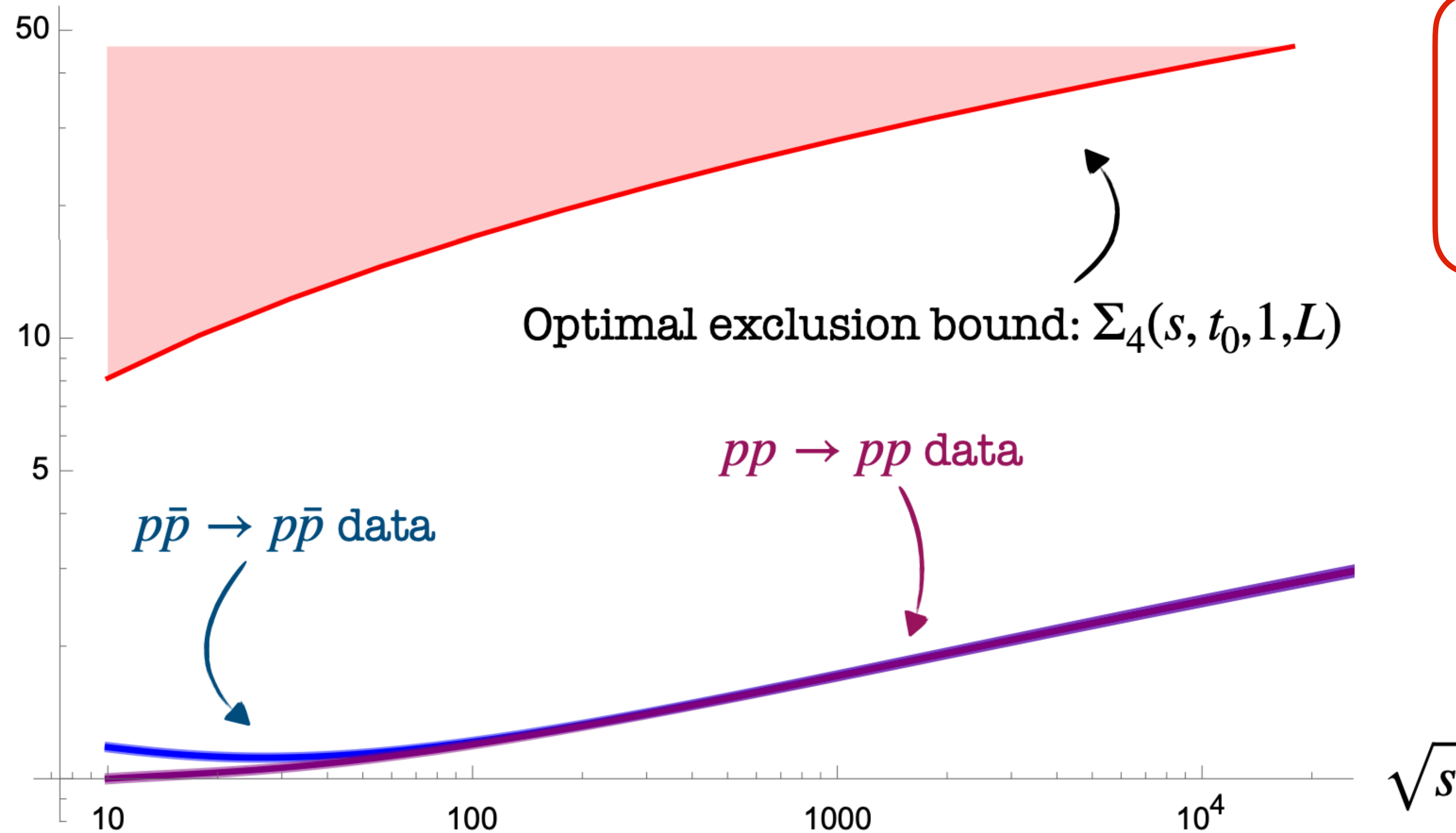
$$\bar{\sigma}_{tot}(s) \equiv \frac{1}{16\pi} \int_{4m^2}^s \frac{s' - 4m^2}{s - 4m^2} \sigma_{tot}(s') ds'$$

[Yndurain, 1970]

Bound on Integrated Total Cross-Section

Scattering of identical scalar bosons of mass $m = 1$ GeV

$\bar{\sigma}_{tot}(s)/s$



$$\bar{\sigma}_{tot}(s) \equiv \frac{1}{16\pi} \int_{4m^2}^s \frac{s' - 4m^2}{s - 4m^2} \sigma_{tot}(s') ds'$$

[Yndurain, 1970]

Strategy of the derivation

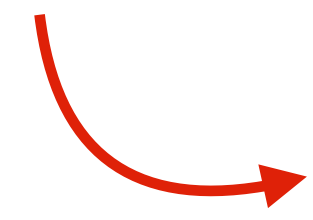
$$\bar{\sigma}_{tot}(s) \equiv \frac{1}{16\pi} \int_{4m^2}^s \frac{s' - 4m^2}{s - 4m^2} \sigma_{tot}(s') ds'$$

- 1) Analytical: Bound $\bar{\sigma}_{tot}(s)$ in terms low energy coefficient $c_2(t_0) \equiv \partial_s^2 T(s, t_0) |_{s \rightarrow 2 - \frac{t_0}{2}}$
- 2) Numerical: Bound $c_2(t_0)$ via the **modern S-matrix Bootstrap**.

Strategy of the derivation

$$\bar{\sigma}_{tot}(s) \equiv \frac{1}{16\pi} \int_{4m^2}^s \frac{s' - 4m^2}{s - 4m^2} \sigma_{tot}(s') ds'$$

1) Analytical: Bound $\bar{\sigma}_{tot}(s)$ in terms low energy coefficient $c_2(t_0) \equiv \partial_s^2 T(s, t_0) |_{s \rightarrow 2 - \frac{t_0}{2}}$



Key idea: Decompose $\bar{\sigma}_{tot}(s) =$ Low spins + High spins

bound by **unitarity**

relate to **low-energy data**

2) Numerical: Bound $c_2(t_0)$ via the **modern S-matrix Bootstrap**.

$$\bar{\sigma}_{tot}(s) = \int_4^s \frac{s' - 4}{s - 4} \sigma_{tot}(s') ds' = \frac{1}{s - 4} \int_4^s ds' \left[\sum_{\ell=0}^{L-2} + \sum_{\ell=L}^{\infty} \right] (2\ell + 1) \text{Im} f_{\ell}(s')$$

$$\bar{\sigma}_{tot}(s) = \int_4^s \frac{s' - 4}{s - 4} \sigma_{tot}(s') ds' = \frac{1}{s - 4} \int_4^s ds' \left[\sum_{\ell=0}^{L-2} + \sum_{\ell=L}^{\infty} \right] (2\ell + 1) \text{Im} f_{\ell}(s')$$

Unitarity: $\text{Im} f_{\ell}(s) \leq 2$

Bound in terms of $c_2(t_0)$:

$$\bar{\sigma}_{tot}(s) = \int_4^s \frac{s' - 4}{s - 4} \sigma_{tot}(s') ds' = \frac{1}{s - 4} \int_4^s ds' \left[\sum_{\ell=0}^{L-2} + \sum_{\ell=L}^{\infty} \right] (2\ell + 1) \text{Im} f_{\ell}(s')$$

Unitarity: $\text{Im} f_{\ell}(s) \leq 2$

Bound in terms of $c_2(t_0)$:

$$c_2(t_0) = \int_4^{\infty} \frac{\text{Im} T(s', t_0)}{\left(s' - 2 + \frac{t_0}{2}\right)^3} ds' = \int_4^{\infty} ds' \sum_{\ell=0}^{\infty} \frac{(2\ell + 1) P_{\ell}\left(1 + \frac{2t_0}{s' - 4}\right)}{\left(s' - 2 + \frac{t_0}{2}\right)^3} \text{Im} f_{\ell}(s')$$

$$\geq \frac{P_L\left(1 + \frac{2t_0}{s - 4}\right)}{\left(s - 2 + \frac{t_0}{2}\right)^3} \int_4^s ds' \sum_{\ell=L}^{\infty} (2\ell + 1) \text{Im} f_{\ell}(s')$$

$$\bar{\sigma}_{tot}(s) = \int_4^s \frac{s' - 4}{s - 4} \sigma_{tot}(s') ds' = \frac{1}{s - 4} \int_4^s ds' \left[\sum_{\ell=0}^{L-2} + \sum_{\ell=L}^{\infty} \right] (2\ell + 1) \text{Im} f_{\ell}(s')$$

Unitarity: $\text{Im} f_{\ell}(s) \leq 2$

Bound in terms of $c_2(t_0)$:

$$c_2(t_0) = \int_4^{\infty} \frac{\text{Im} T(s', t_0)}{\left(s' - 2 + \frac{t_0}{2}\right)^3} ds' = \int_4^{\infty} ds' \sum_{\ell=0}^{\infty} \frac{(2\ell + 1) P_{\ell}\left(1 + \frac{2t_0}{s' - 4}\right)}{\left(s' - 2 + \frac{t_0}{2}\right)^3} \text{Im} f_{\ell}(s')$$

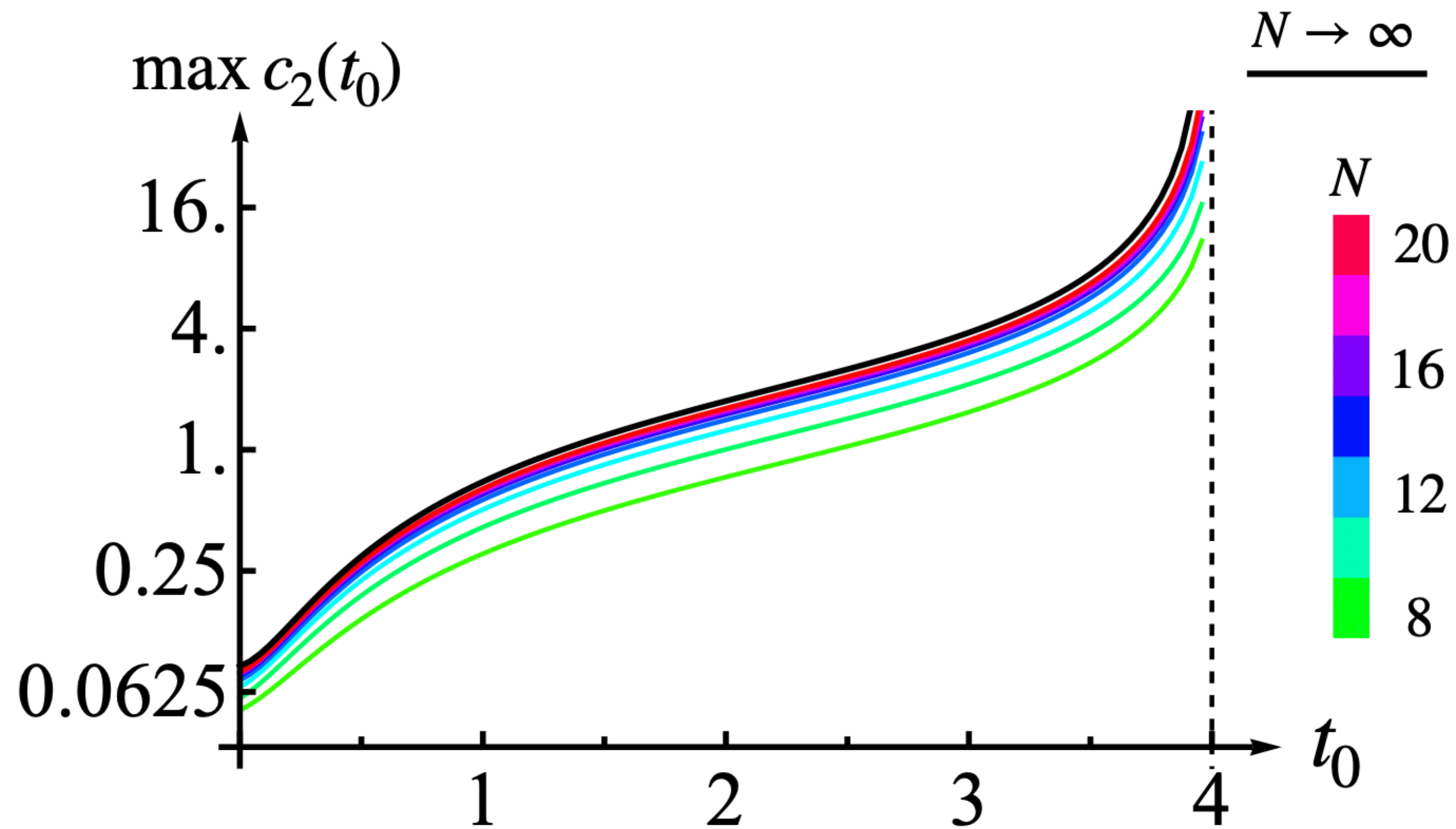
$$\geq \frac{P_L\left(1 + \frac{2t_0}{s - 4}\right)}{\left(s - 2 + \frac{t_0}{2}\right)^3} \int_4^s ds' \sum_{\ell=L}^{\infty} (2\ell + 1) \text{Im} f_{\ell}(s')$$

$$\bar{\sigma}_{tot}(s) \leq L(L - 1) + \frac{2\pi c_2(t_0) \left(s - 2 + \frac{t_0}{2}\right)^3}{\sqrt{s(s - 4)} P_L\left(1 + \frac{2t_0}{s - 4}\right)}$$

, valid for any even L and $t_0 \in (0, 4)$.

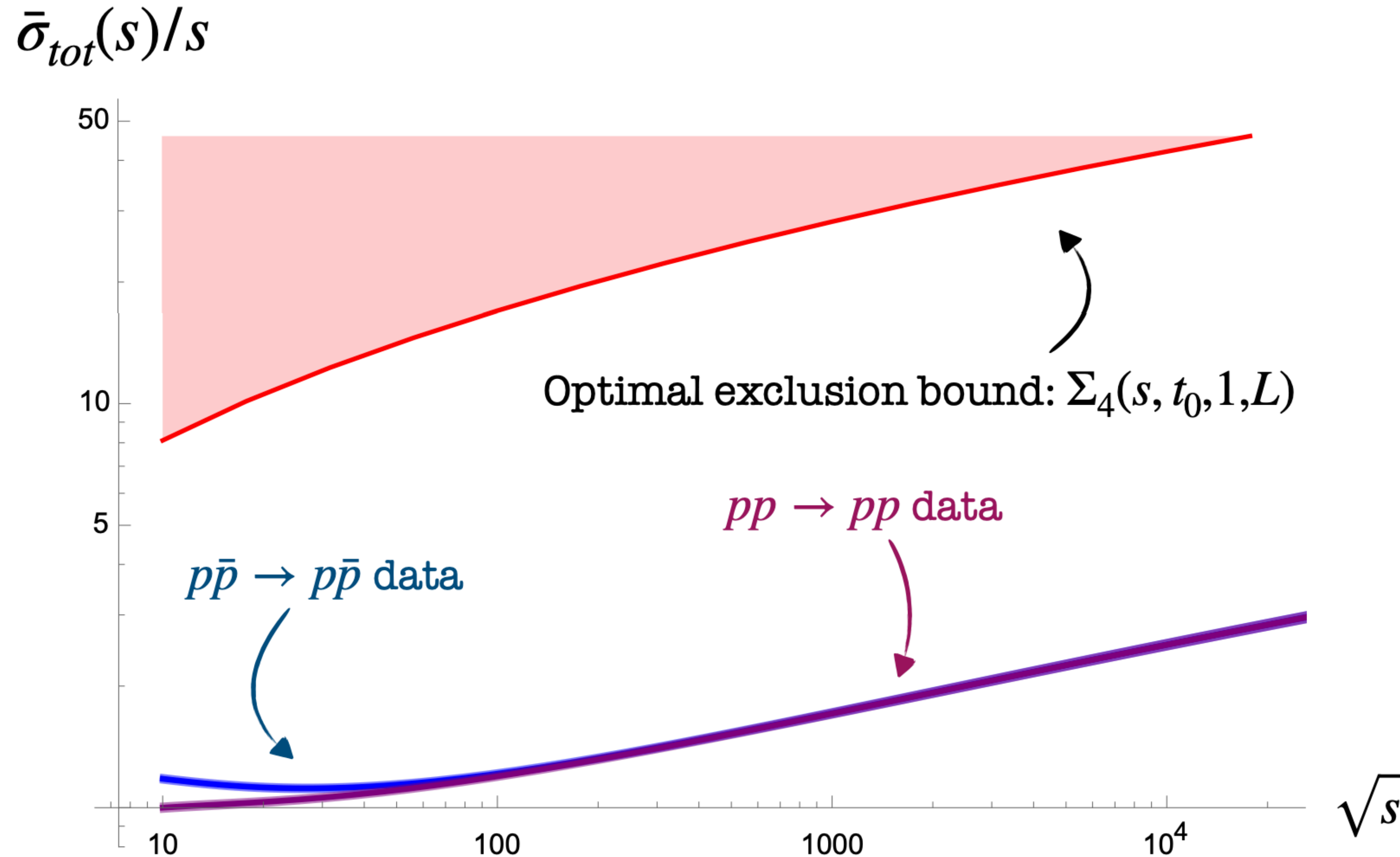
Optimize over L and t_0 !

2) **Bound on $c_2(t_0) \propto \partial_s^2 T(s, t_0) |_{s \rightarrow 2 + \frac{t_0}{2}}$**

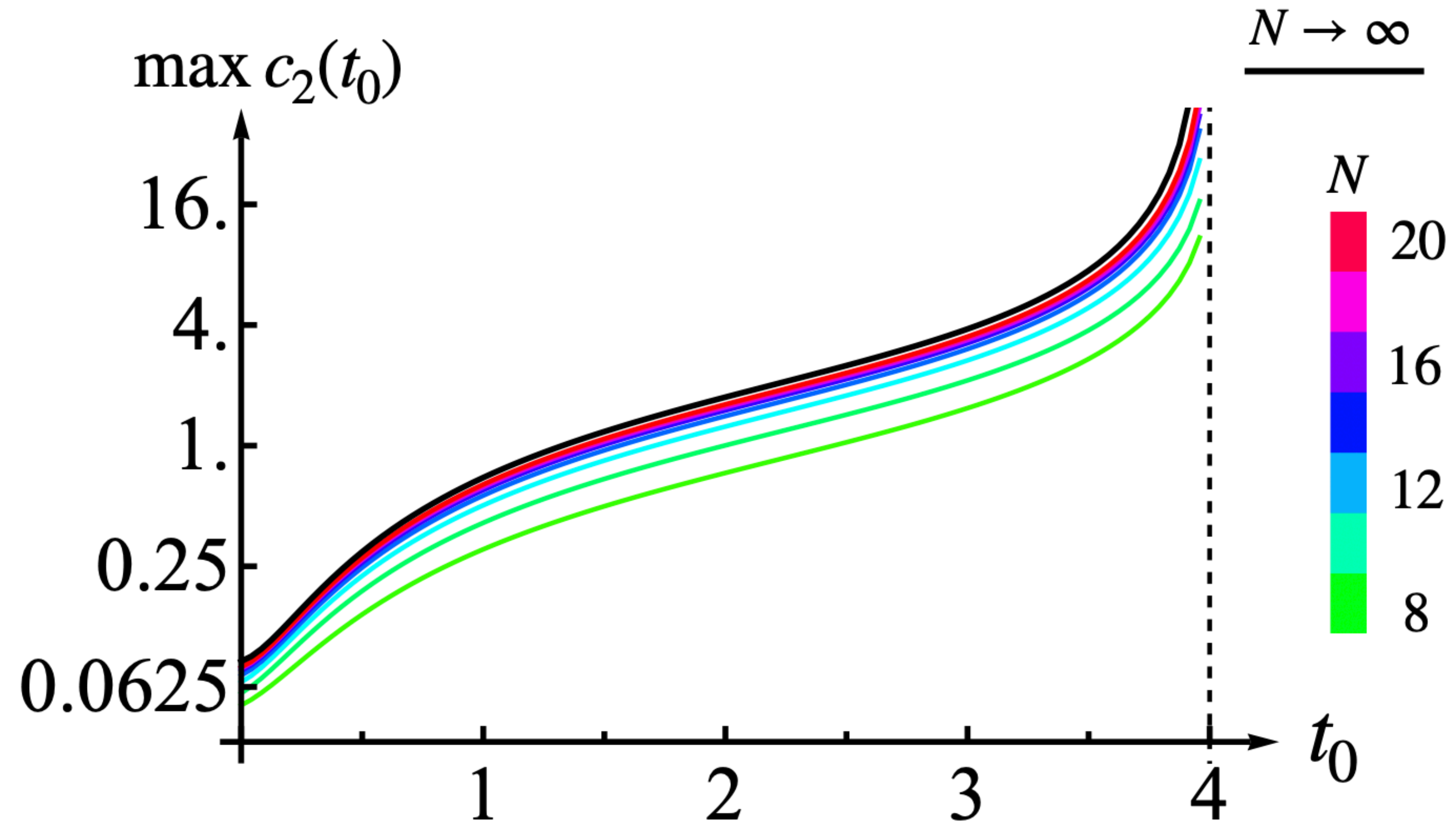


Computed using numerical S-matrix Bootstrap

Bound on Total Cross-Section at finite energy



What is the Amplitude that maximizes this coupling?



Tool we use: Modern S-matrix Bootstrap

INPUT:

Analyticity →

Crossing
Symmetry →

Unitarity →

**Primal
S-matrix
Bootstrap**

[Paulos, Penedones, Toledo, van Rees, Vieira; 2016]

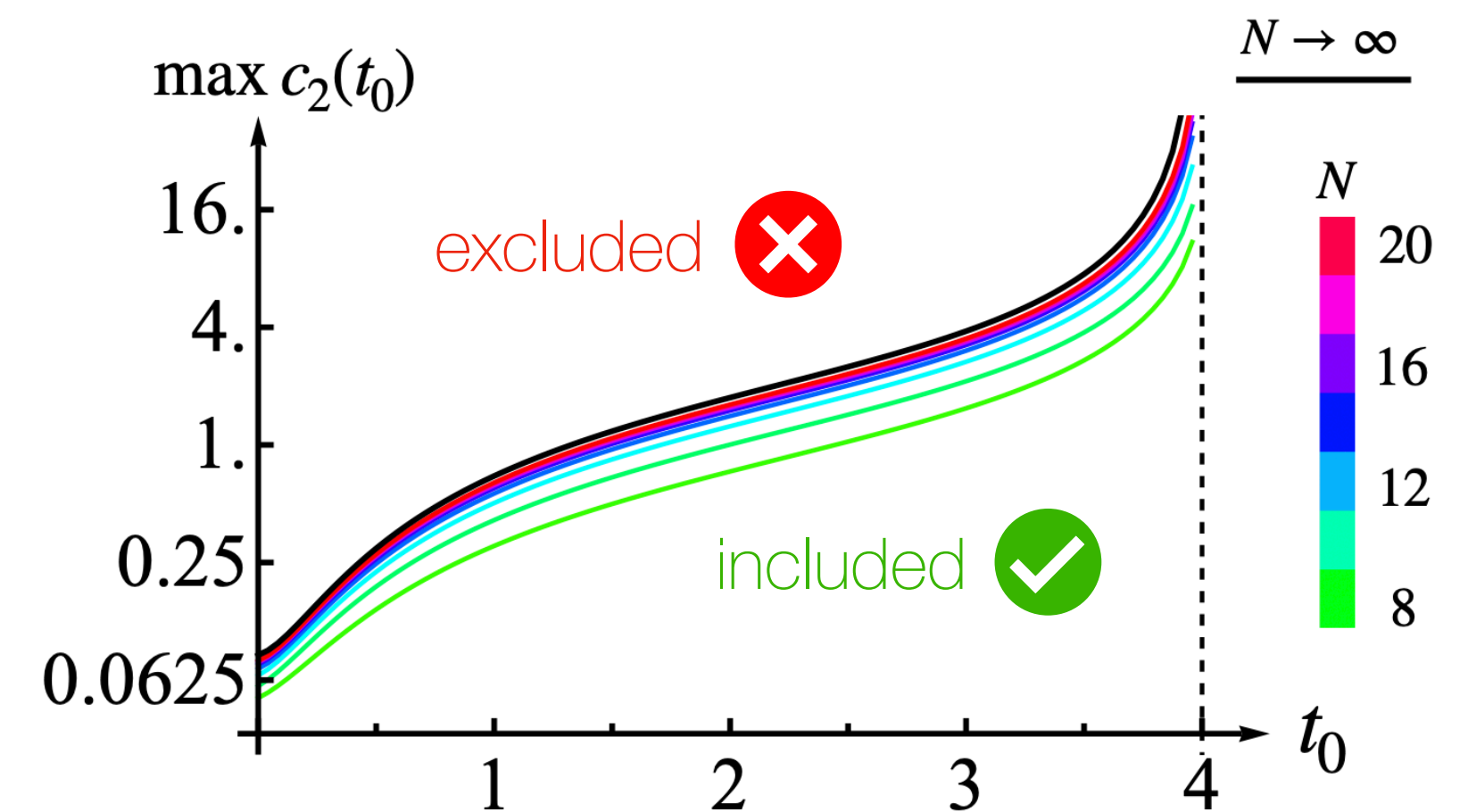
• Cordova, MC, Elias Miró, Gümus, Karateev,
• Homrich, Vuignier, Sever, Tourkine, Zhiboedov, ...

[Guerrieri, Häring, Su; 2024]

$N, L \rightarrow \infty$

OUTPUT:

→ Bounds on low-energy data



→ Consistent Extremal Amplitude

$$T(s, t) = T_{max}(s, t)$$

The “Froissart” Amplitude:

strongest interacting amplitude in $2 \rightarrow 2$ sector

The “Froissart” Amplitude:

strongest interacting amplitude in $2 \rightarrow 2$ sector

- Maximizes all dispersive low-energy coefficients $c_n > 0$
- Maximizes growth of cross-section at high-energies

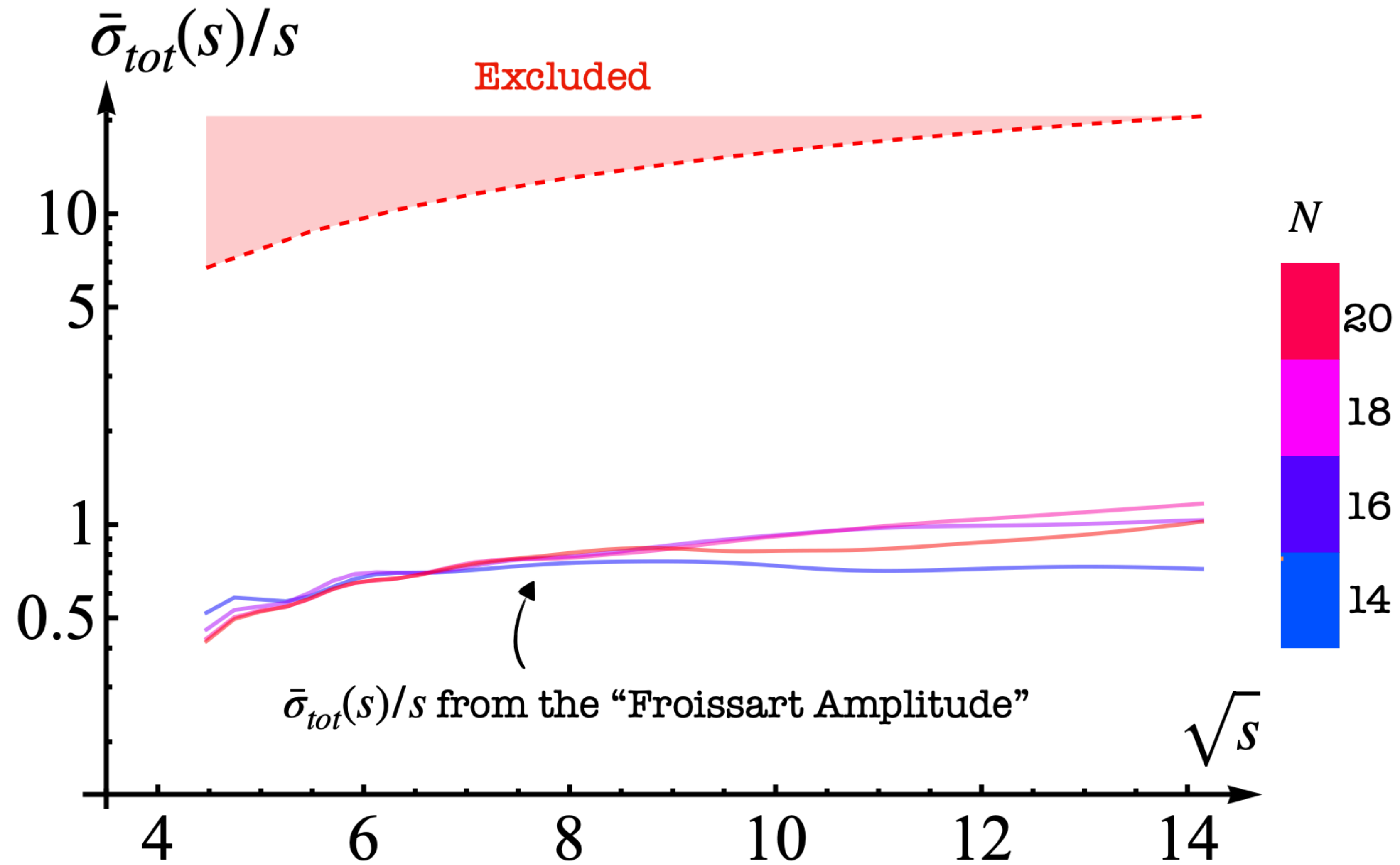
The “Froissart” Amplitude:

strongest interacting amplitude in $2 \rightarrow 2$ sector

- Maximizes all dispersive low-energy coefficients $c_n > 0$
- Maximizes growth of cross-section at high-energies

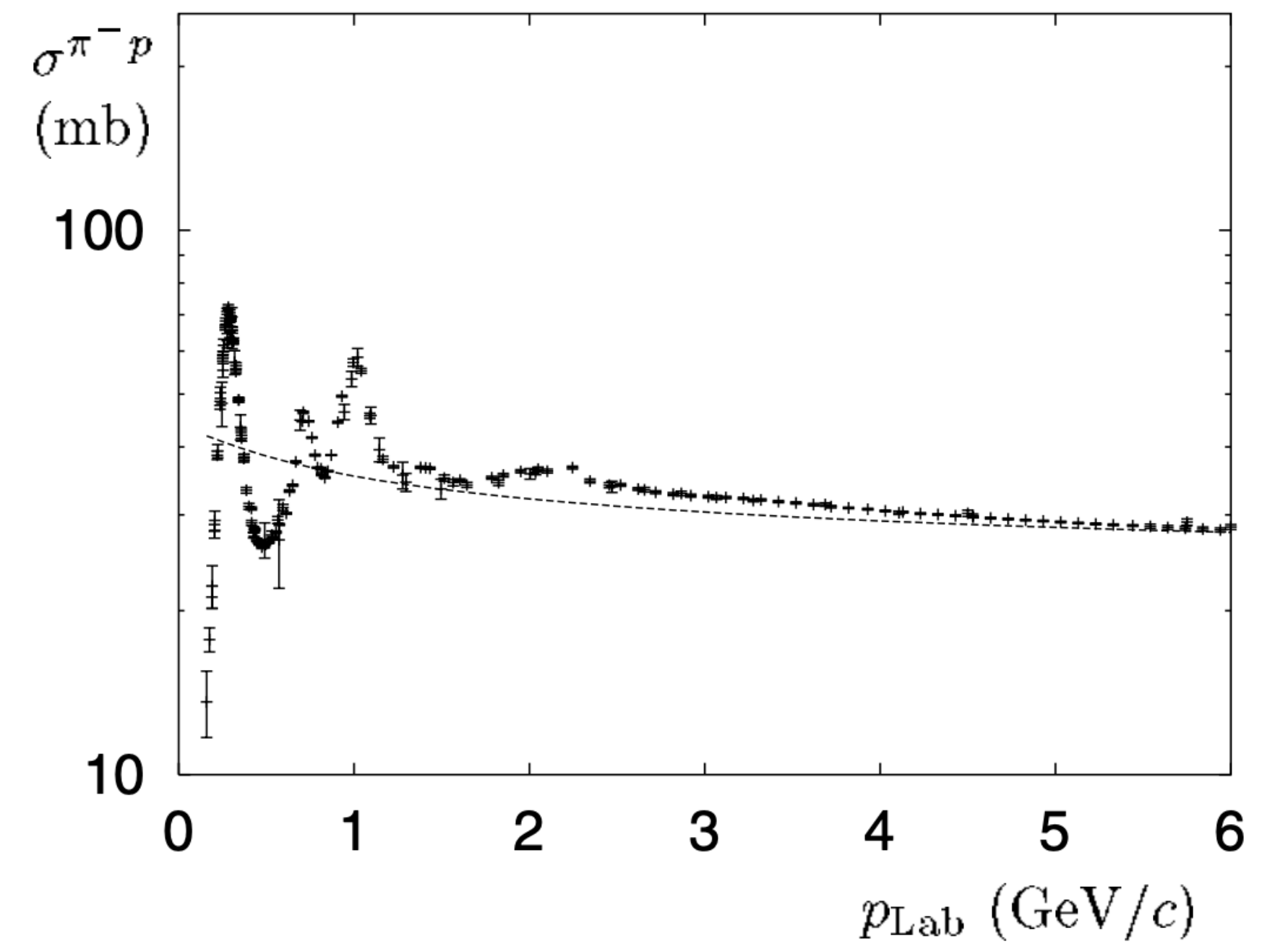
Amplitude with a growing cross-section compatible with all the principles.

Integrated cross-section



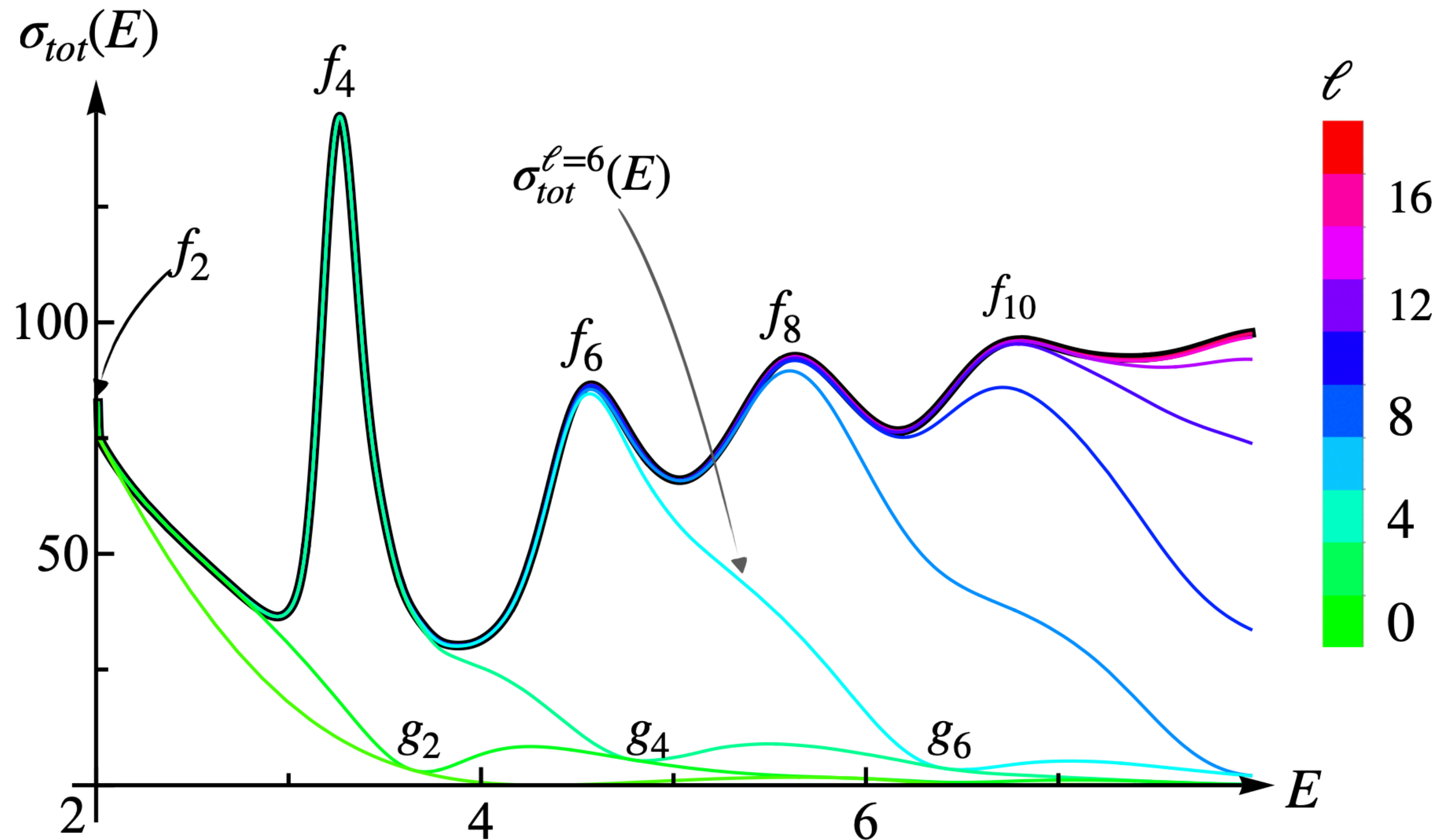
Total cross-section and resonance peaks

Hadronic cross-section

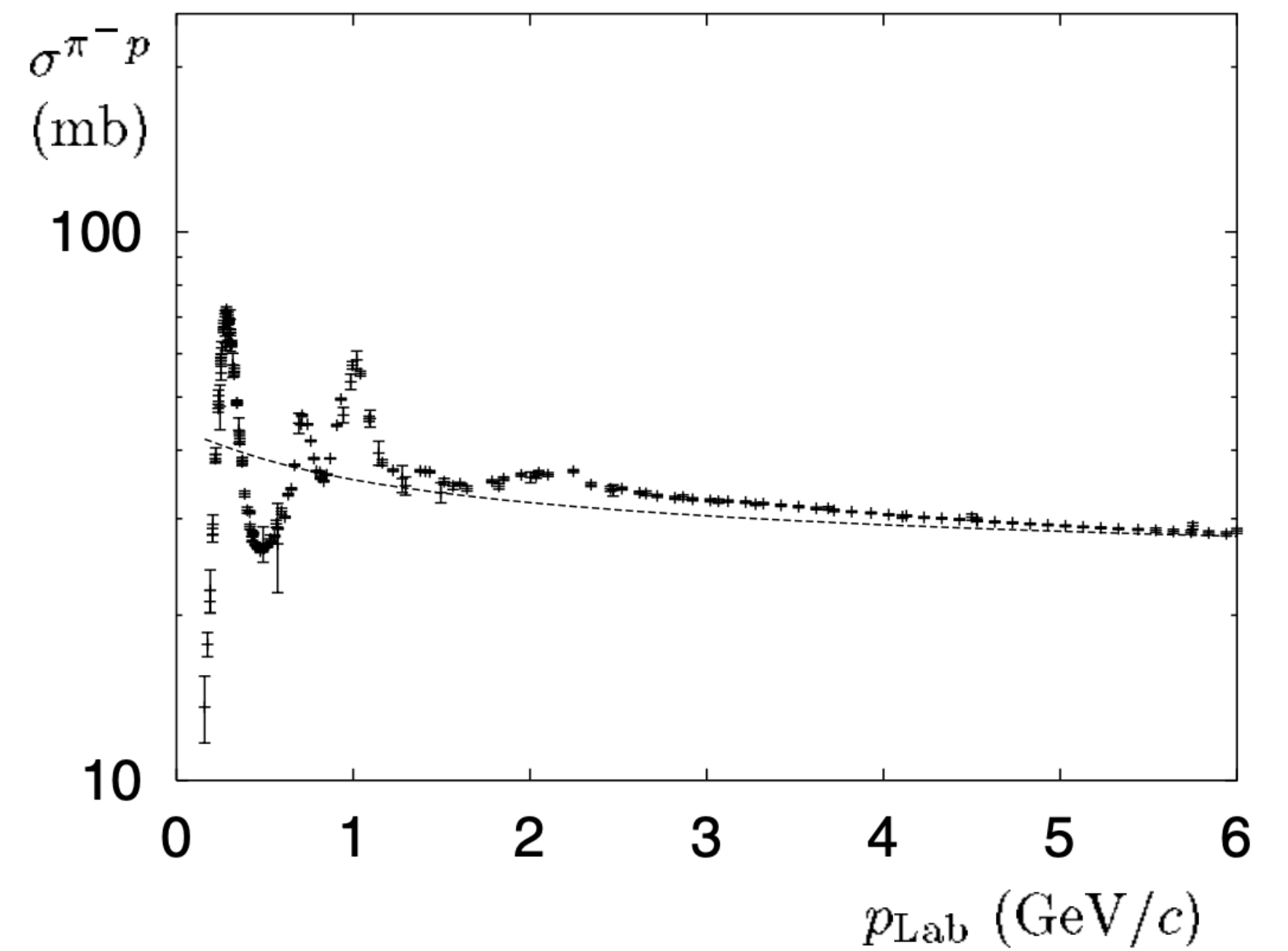


Total cross-section and resonance peaks

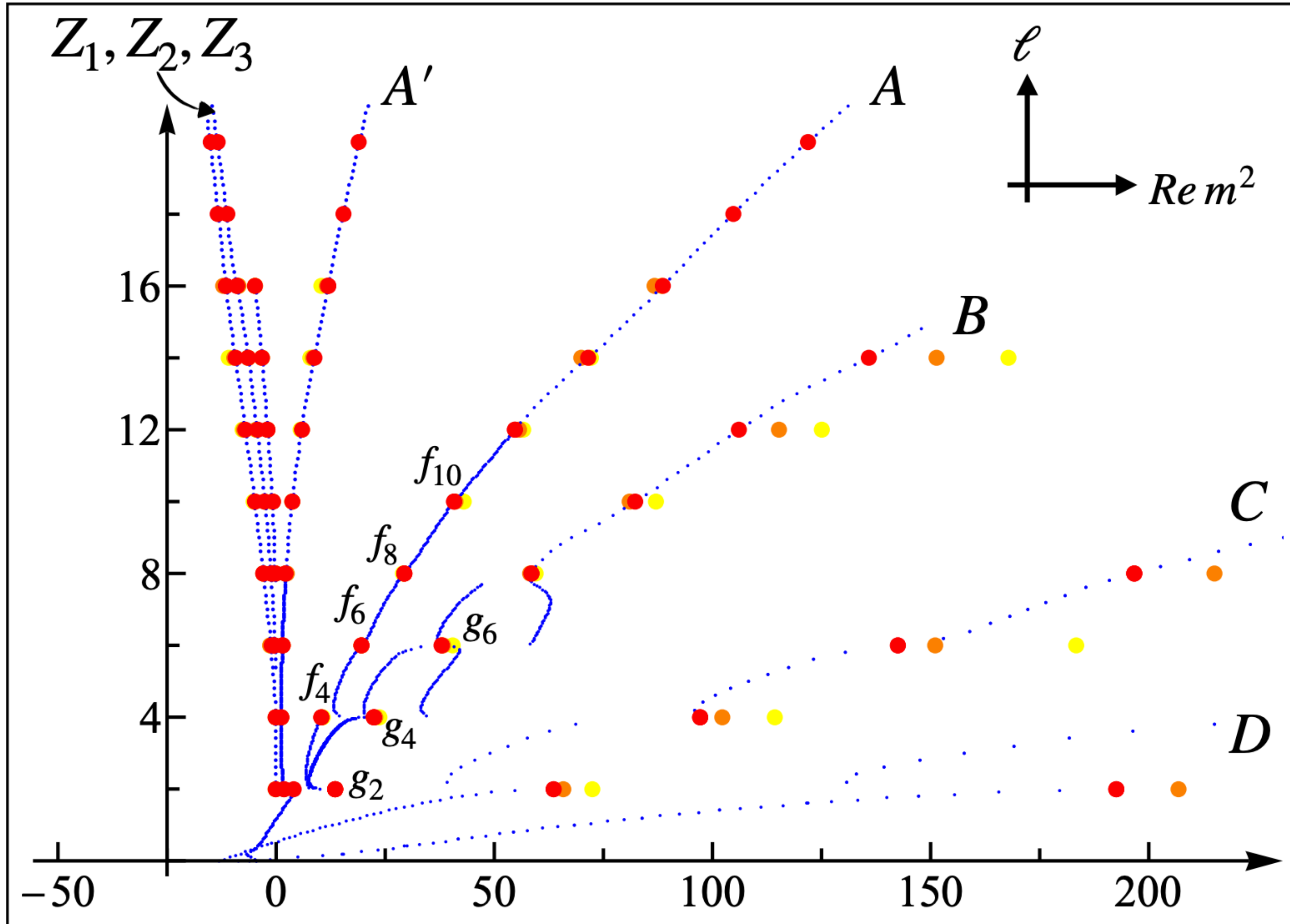
Froissart amplitude (bootstrap)



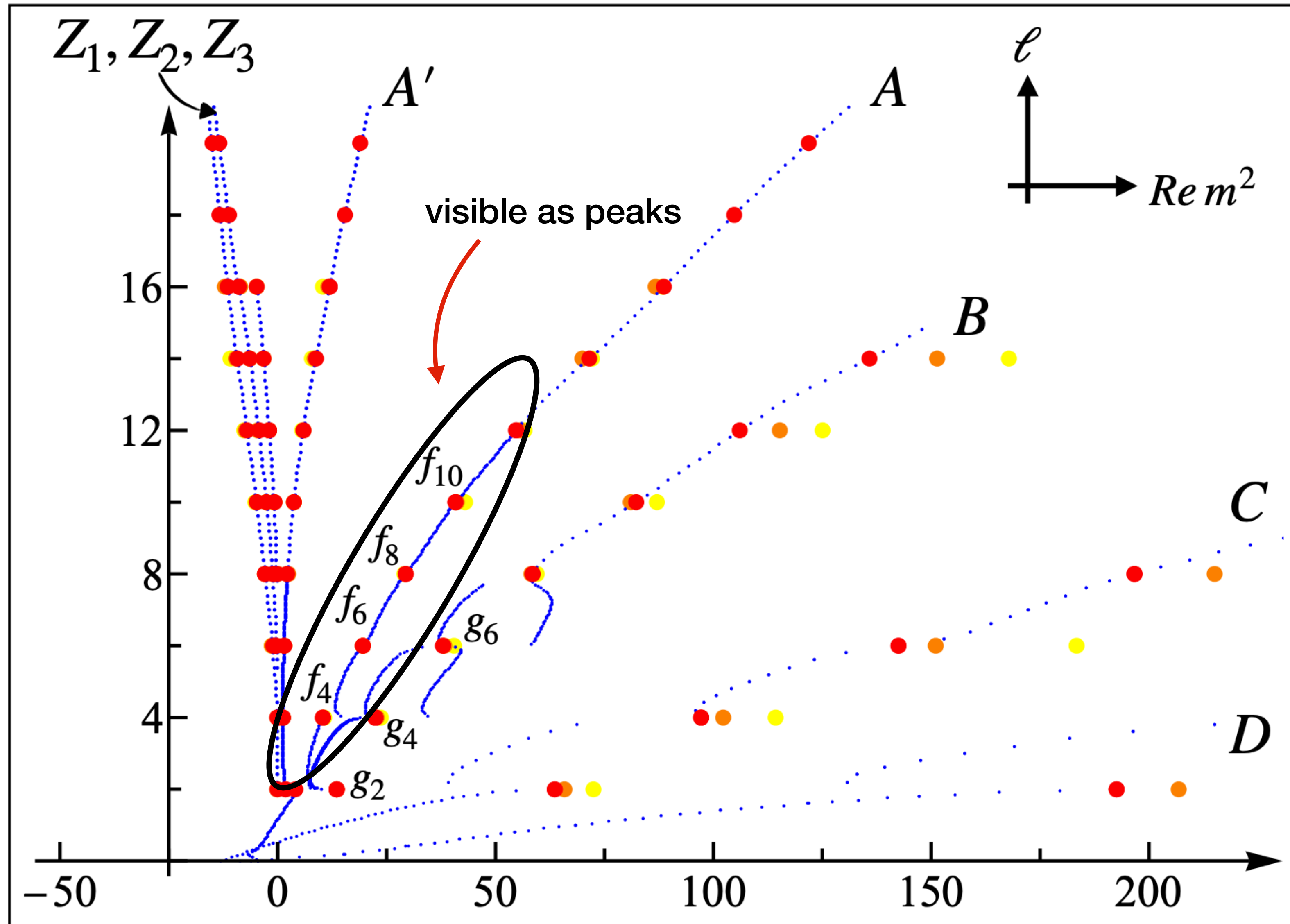
Hadronic cross-section



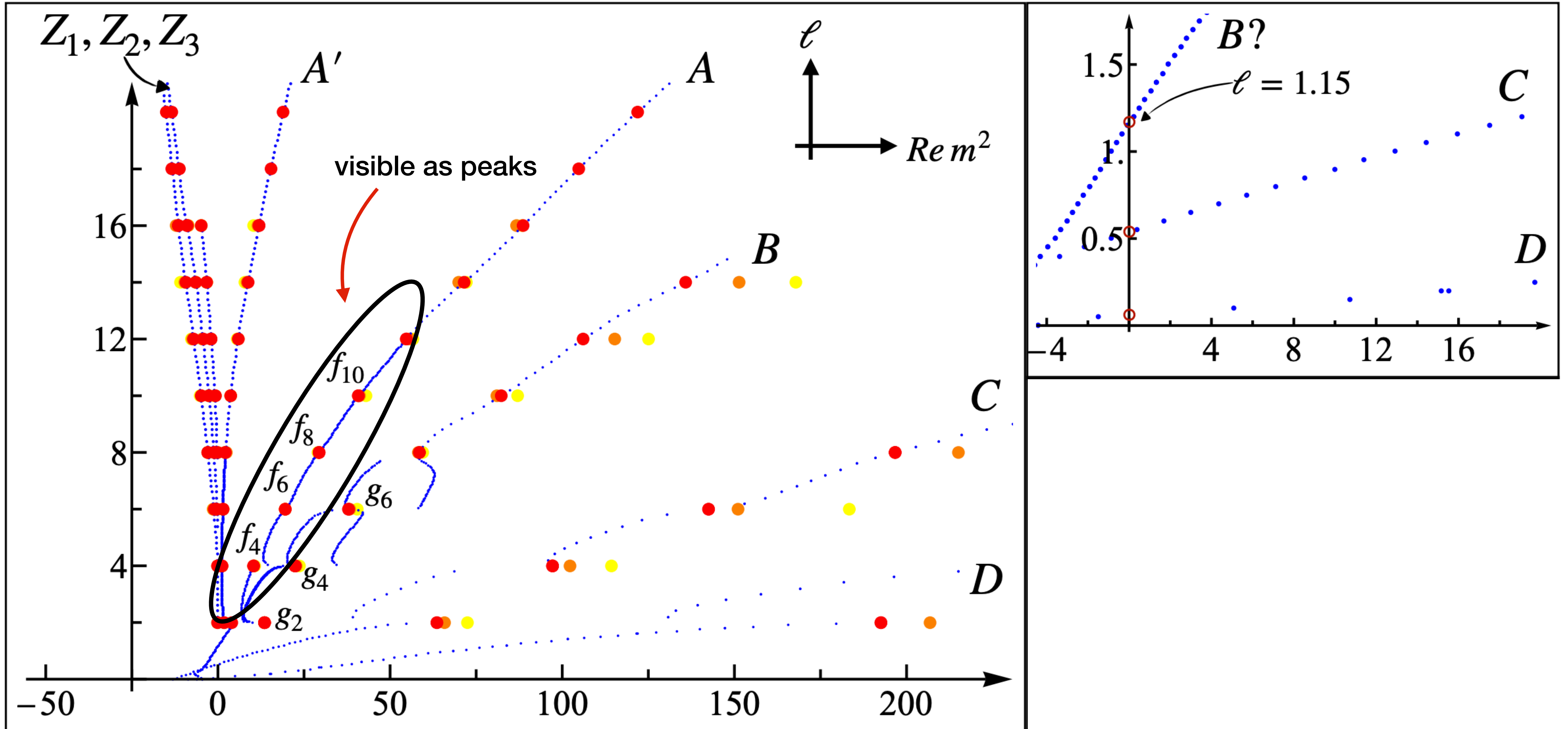
Chew-Frautschi plot of “Froissart amplitude”



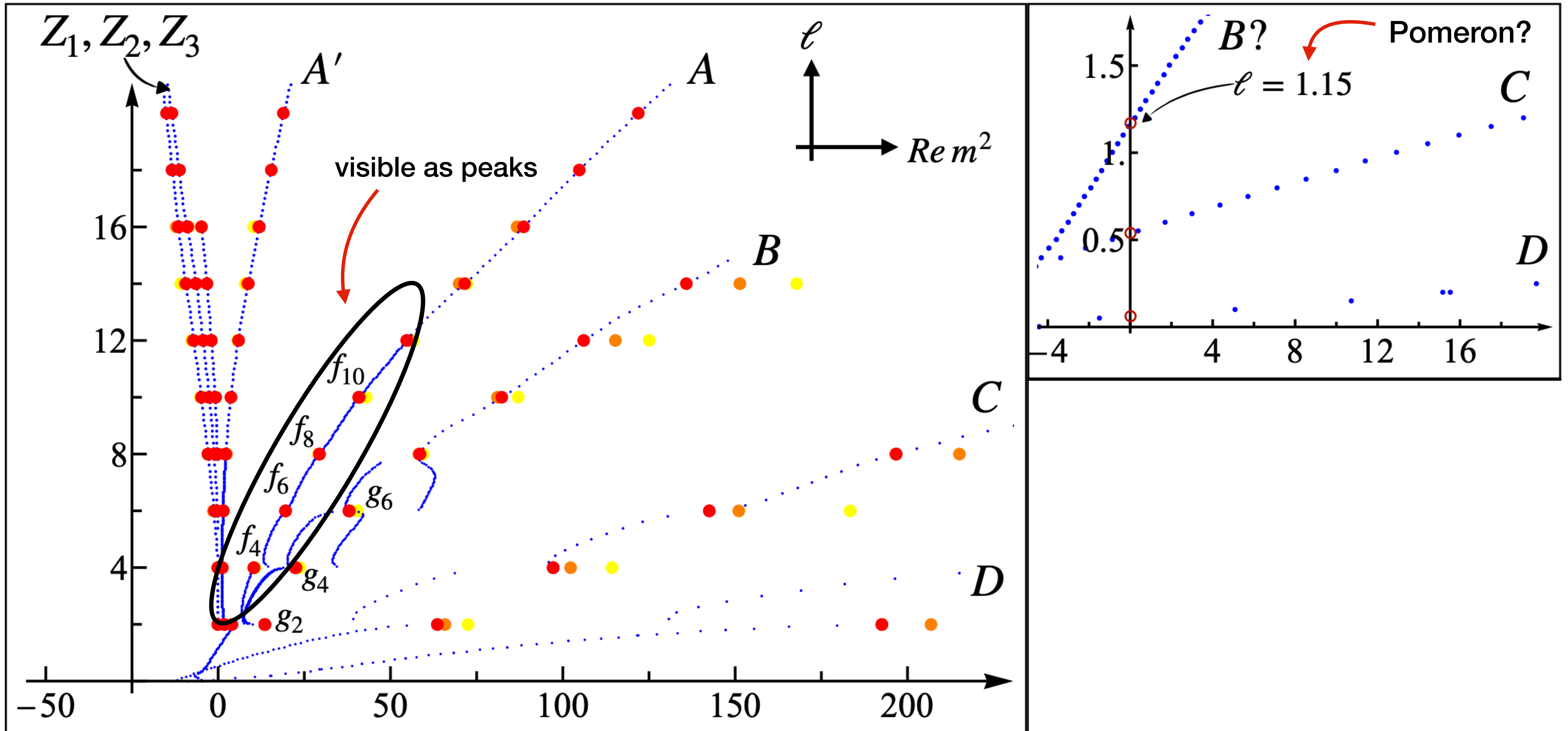
Chew-Frautschi plot of “Froissart amplitude”



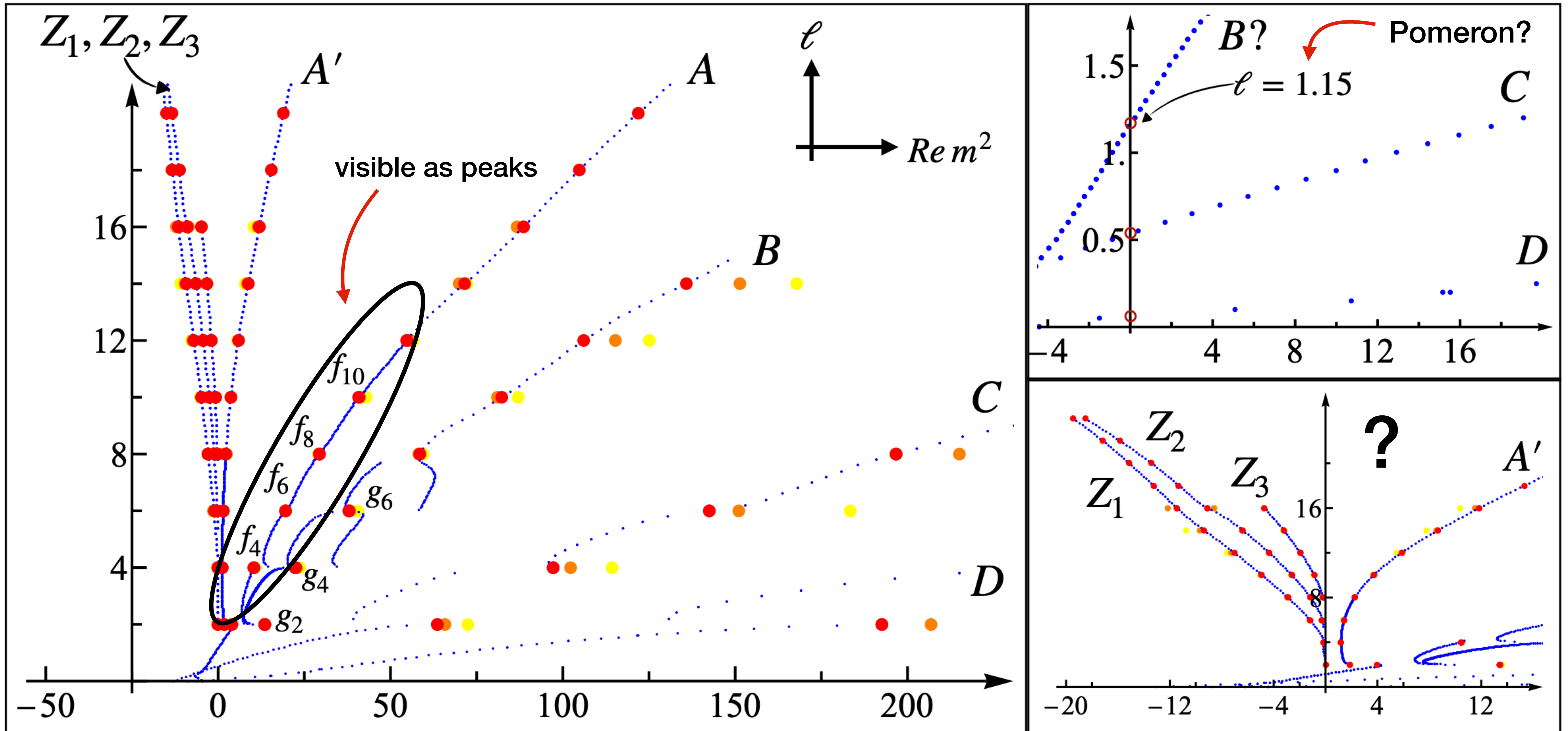
Chew-Frautschi plot of “Froissart amplitude”



Chew-Frautschi plot of “Froissart amplitude”



Chew-Frautschi plot of “Froissart amplitude”



Recap: Observables in Soft QCD

Total Cross-Section

$$\sigma_{tot}(s) = \frac{\text{Im } T(s,0)}{s}$$

Resonances and
Regge trajectories

$$\ell = \alpha(t)$$

Recap: Observables in Soft QCD

Total Cross-Section

$$\sigma_{tot}(s) = \frac{\text{Im } T(s,0)}{s}$$

$$\sigma_{tot}(s) \sim s^{\alpha(0)-1}$$

Resonances and
Regge trajectories

$$\ell = \alpha(t)$$

$$T(s, t) \sim s^{\alpha(t)}$$

$$\alpha(t) = \alpha(0) + \alpha' t$$



Recap: Observables in Soft QCD

Total Cross-Section

$$\sigma_{tot}(s) = \frac{\text{Im } T(s,0)}{s}$$

$$\sigma_{tot}(s) \sim s^{\alpha(0)-1}$$

Resonances and
Regge trajectories

$$\ell = \alpha(t)$$

$$T(s, t) \sim s^{\alpha(t)}$$

$$\alpha(t) = \alpha(0) + \alpha' t$$

Elastic Differential
Cross-Section

$$\frac{d\sigma_{el}}{dt} = \frac{|T(s, t)|^2}{s^2}$$

Recap: Observables in Soft QCD

Total Cross-Section

$$\sigma_{tot}(s) = \frac{\text{Im } T(s,0)}{s}$$

$$\sigma_{tot}(s) \sim s^{\alpha(0)-1}$$

Resonances and
Regge trajectories

$$\ell = \alpha(t)$$

$$T(s, t) \sim s^{\alpha(t)}$$

$$\alpha(t) = \alpha(0) + \alpha' t$$

Elastic Differential
Cross-Section

$$\frac{d\sigma_{el}}{dt} = \frac{|T(s, t)|^2}{s^2}$$

$$\frac{d\sigma_{el}}{dt} \sim s^{2(\alpha(0)-1)} s^{2\alpha' t}$$

$$t \leq 0$$

Recap: Observables in Soft QCD

Total Cross-Section

$$\sigma_{tot}(s) = \frac{\text{Im } T(s,0)}{s}$$

$$\sigma_{tot}(s) \sim s^{\alpha(0)-1}$$

Resonances and
Regge trajectories

$$\ell = \alpha(t)$$

$$T(s, t) \sim s^{\alpha(t)}$$

$$\alpha(t) = \alpha(0) + \alpha' t$$

Elastic Differential
Cross-Section

$$\frac{d\sigma_{el}}{dt} = \frac{|T(s, t)|^2}{s^2}$$

$$\frac{d\sigma_{el}}{dt} \sim s^{2(\alpha(0)-1)} s^{2\alpha' t}$$

$$t \leq 0$$

Elastic Differential Cross-Section:

“Shrinking of the Diffractive Cone”

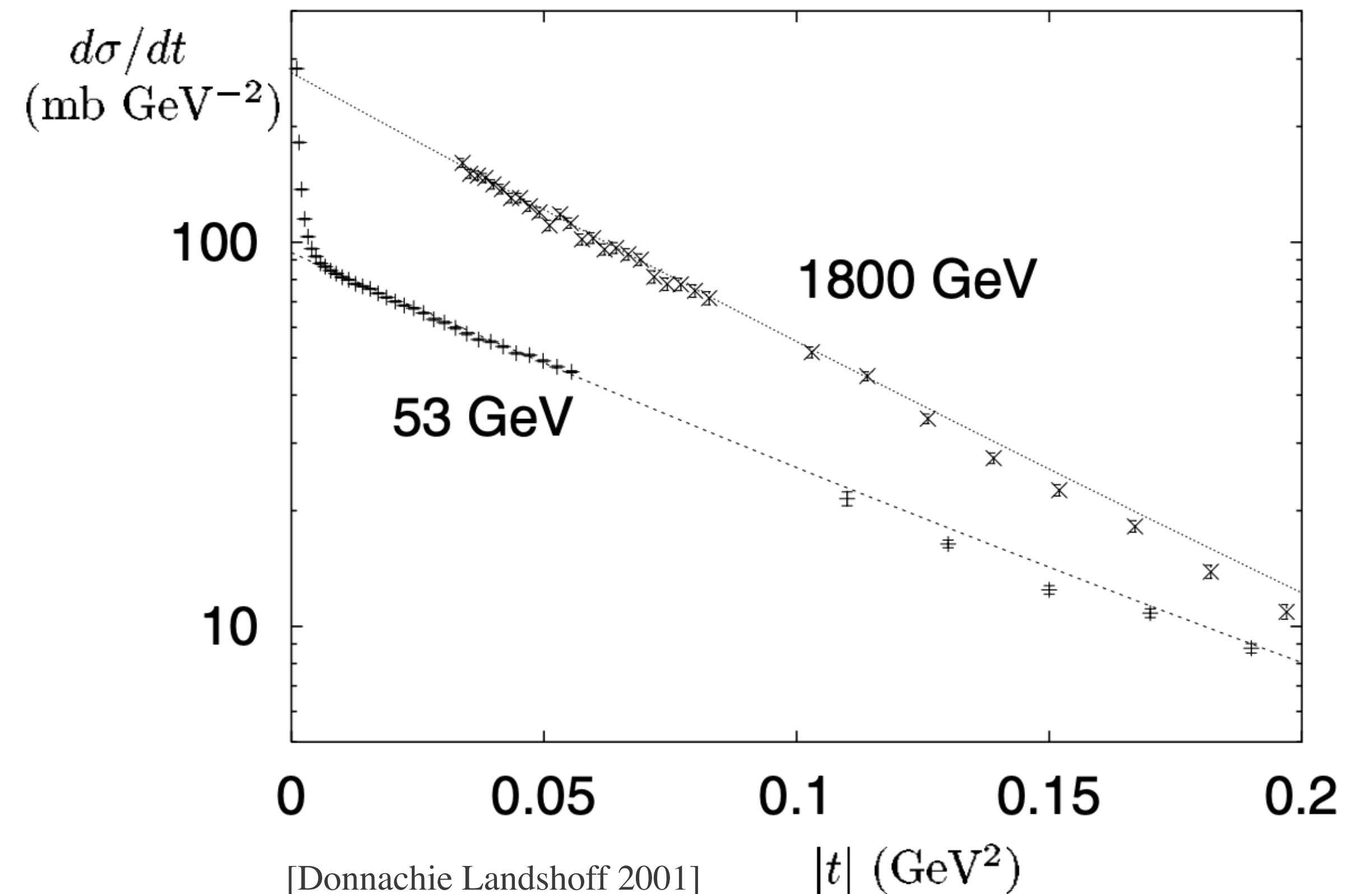
$$\frac{d\sigma_{el}}{dt} \sim s^{2(\alpha(0)-1)} e^{-(2\alpha' \log s) |t|}$$

Elastic Differential Cross-Section:

“Shrinking of the Diffractive Cone”

$$\frac{d\sigma_{el}}{dt} \sim s^{2(\alpha(0)-1)} e^{-(2\alpha' \log s) |t|}$$

Proton-proton (experiment)

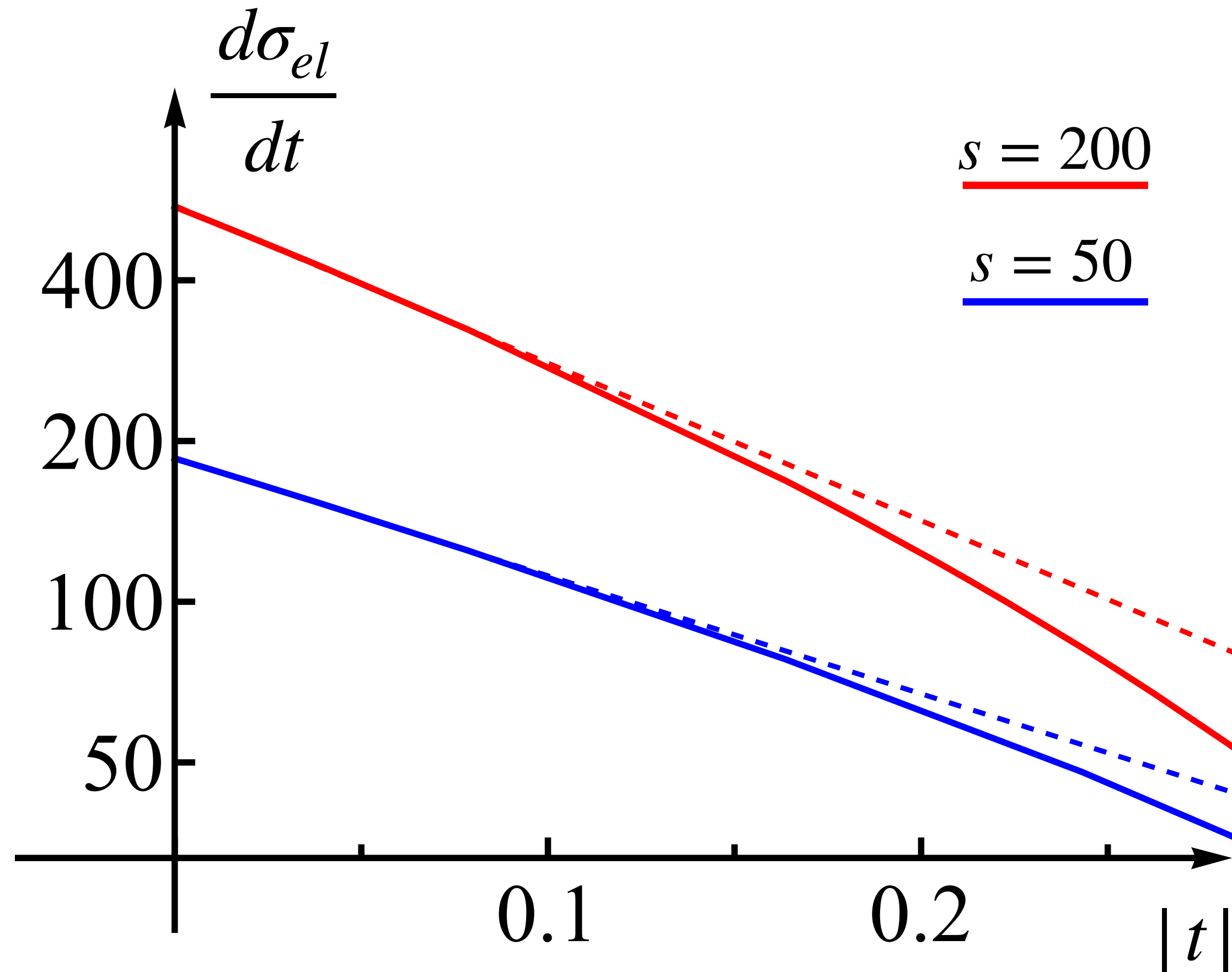


Elastic Differential Cross-Section:

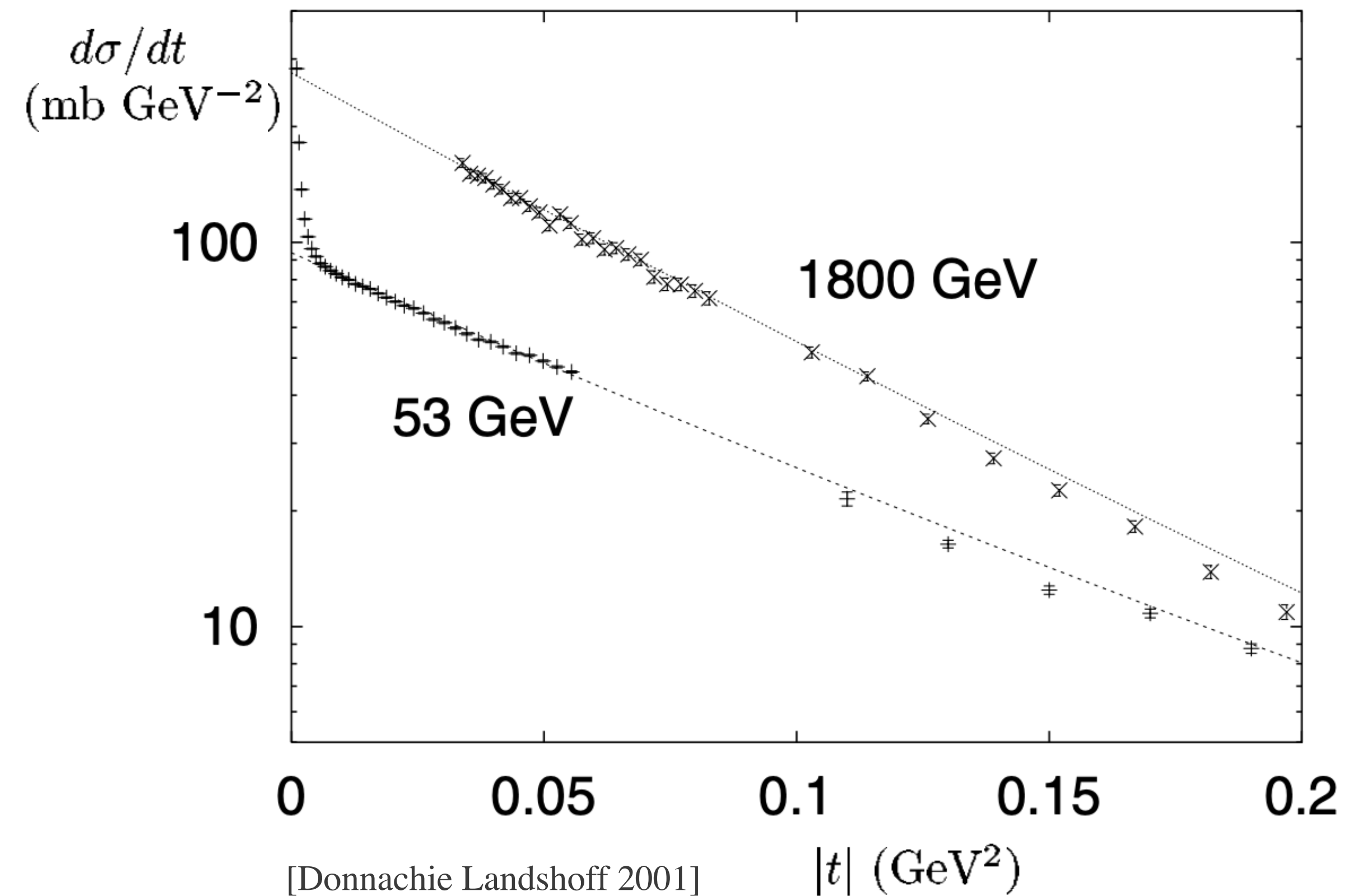
“Shrinking of the Diffractive Cone”

$$\frac{d\sigma_{el}}{dt} \sim s^{2(\alpha(0)-1)} e^{-(2\alpha' \log s) |t|}$$

Froissart amplitude (bootstrap)

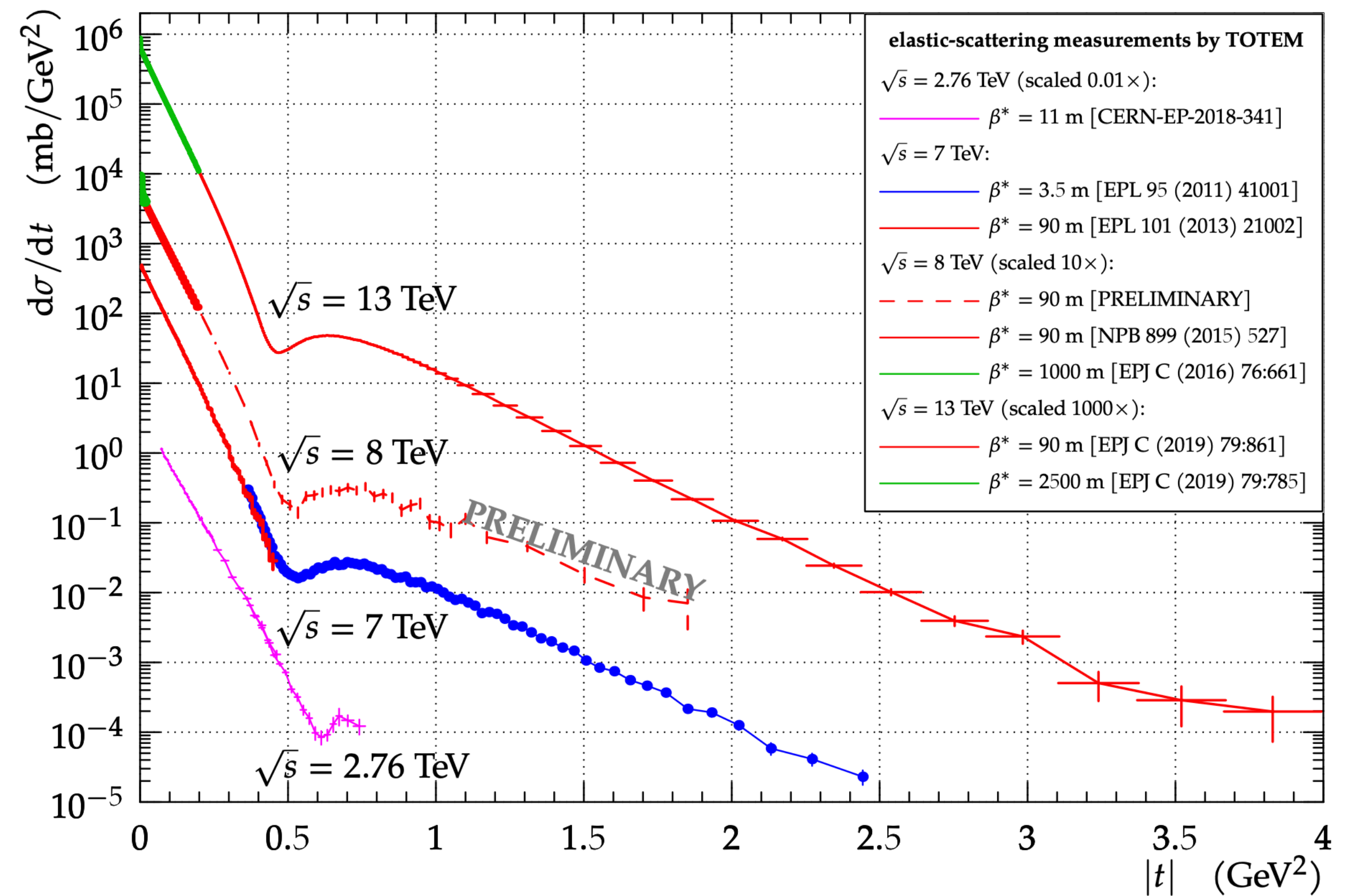


Proton-proton (experiment)



Elastic Differential Cross-Section: Larger $|t|$

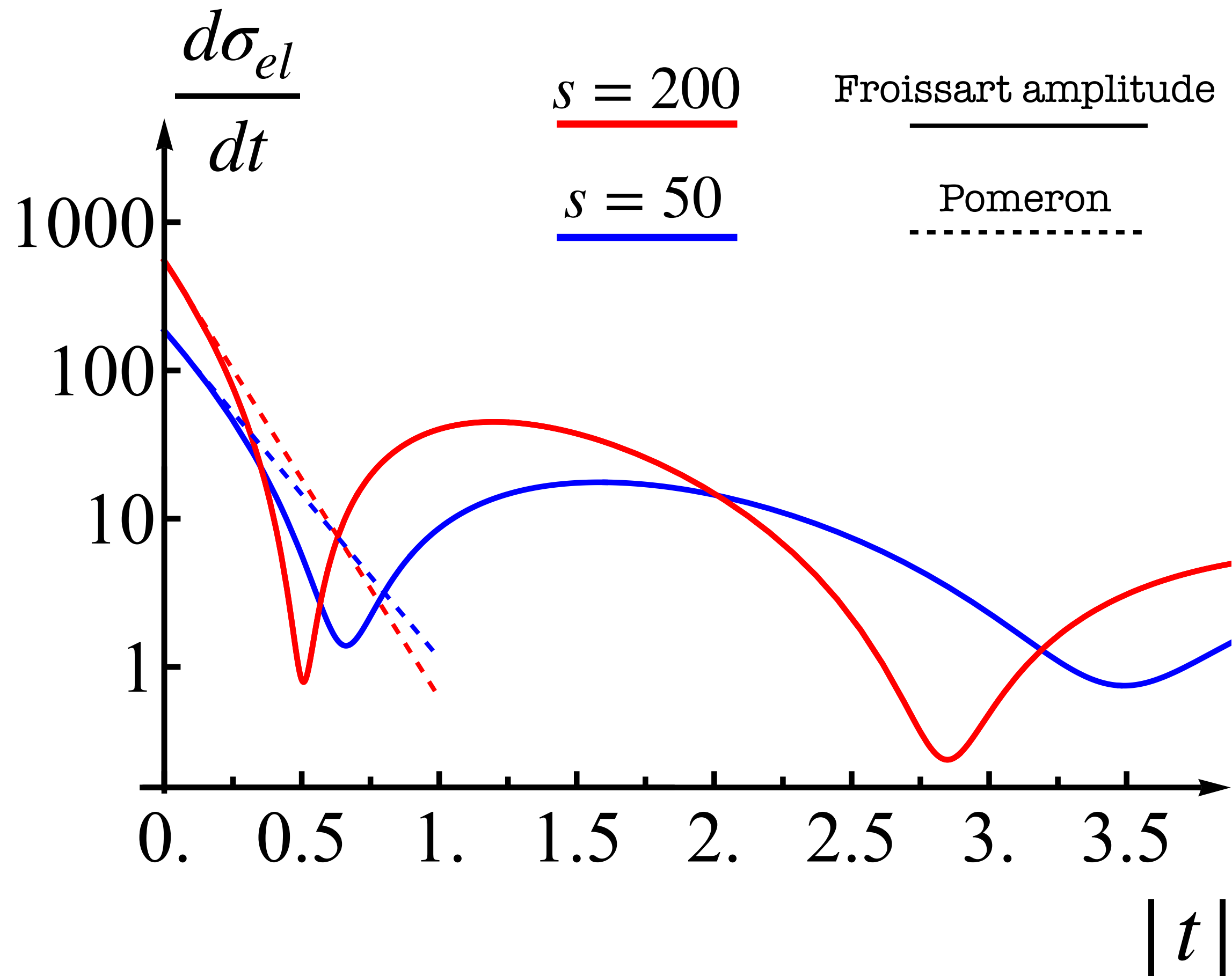
Proton-proton (LHC)



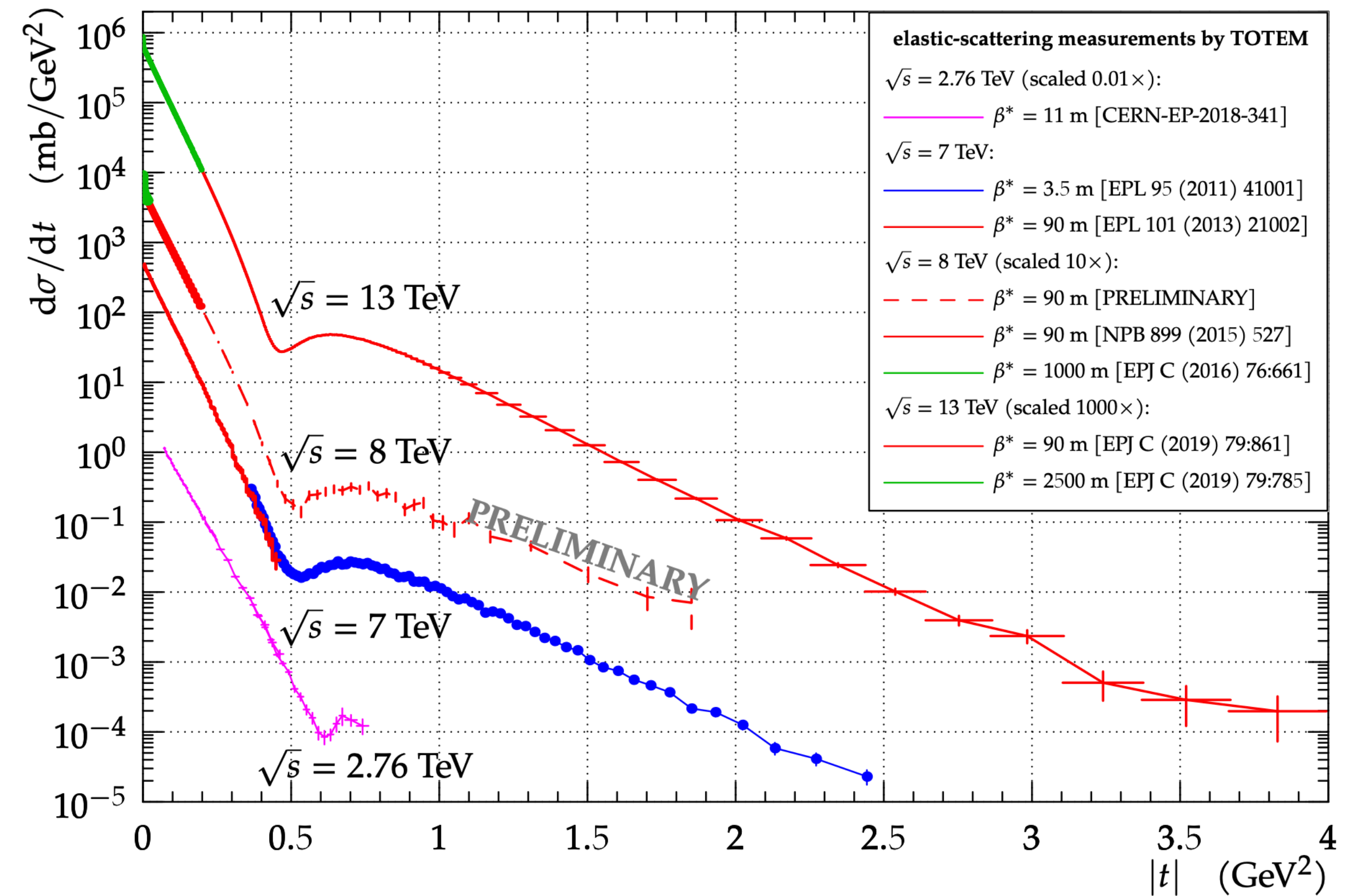
[TOTEM collaboration, 2018]

Elastic Differential Cross-Section: Larger $|t|$

Froissart amplitude (bootstrap)



Proton-proton (LHC)



[TOTEM collaboration, 2018]

Conclusion

- Bounded the cross-section at finite energy;
- Explored the Froissart amplitude and compared with proton-proton data;

Conclusion

- Bounded the cross-section at finite energy;
- Explored the Froissart amplitude and compared with proton-proton data;

Future directions

Phenomenological

The Pomeron puzzle in QCD

INPUT: High-energy cross-section data (TeV)

Primal
S-matrix
Bootstrap

OUTPUT: Resonances & Regge trajectories (GeV)

Precision era of Regge phenomenology?

Conclusion

- Bounded the cross-section at finite energy;
- Explored the Froissart amplitude and compared with proton-proton data;

Future directions

Phenomenological

The Pomeron puzzle in QCD

INPUT: High-energy cross-section data (TeV)

Primal
S-matrix
Bootstrap

OUTPUT: Resonances & Regge trajectories (GeV)

Precision era of Regge phenomenology?

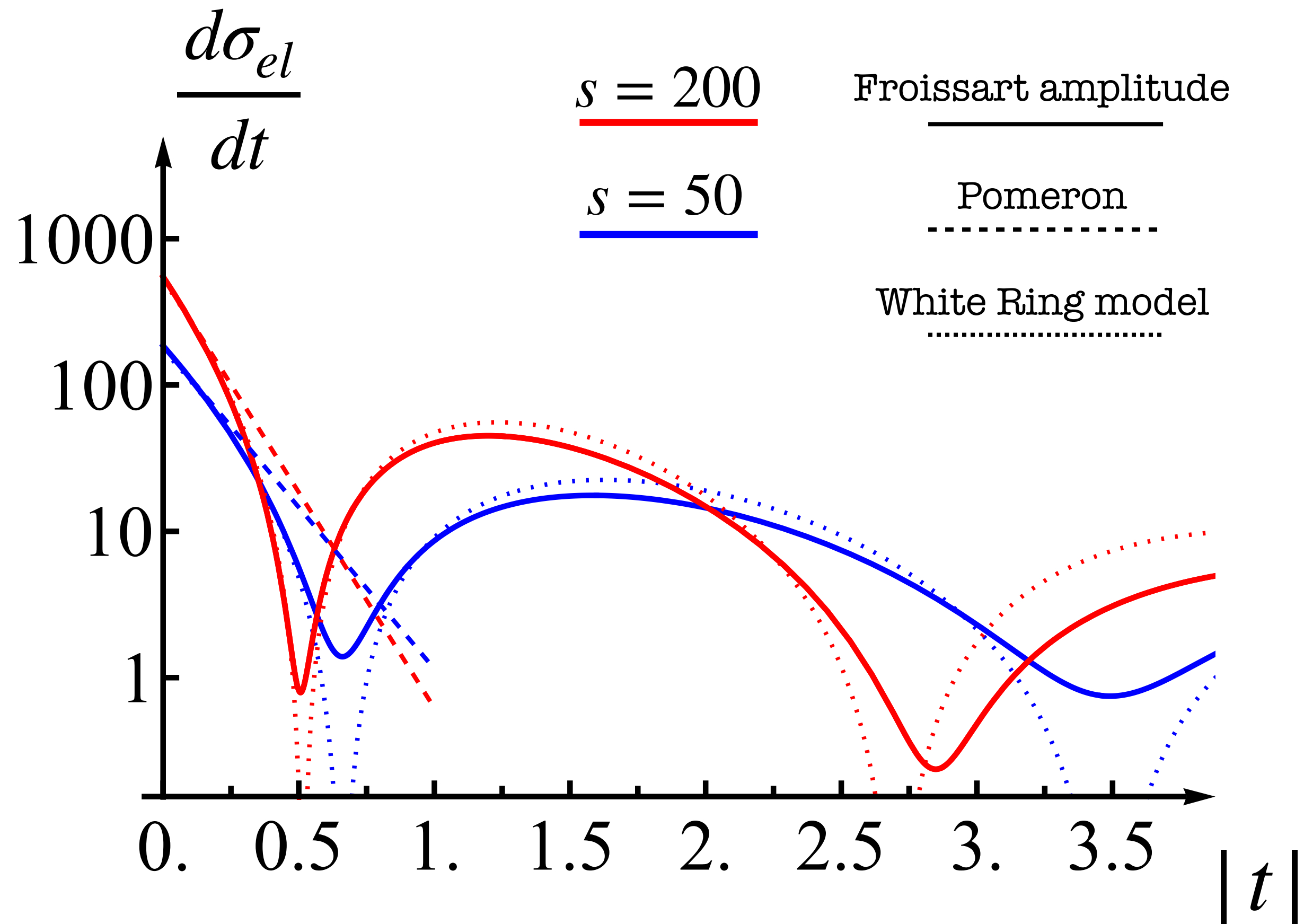
Theoretical

How constraining are growing cross-sections?

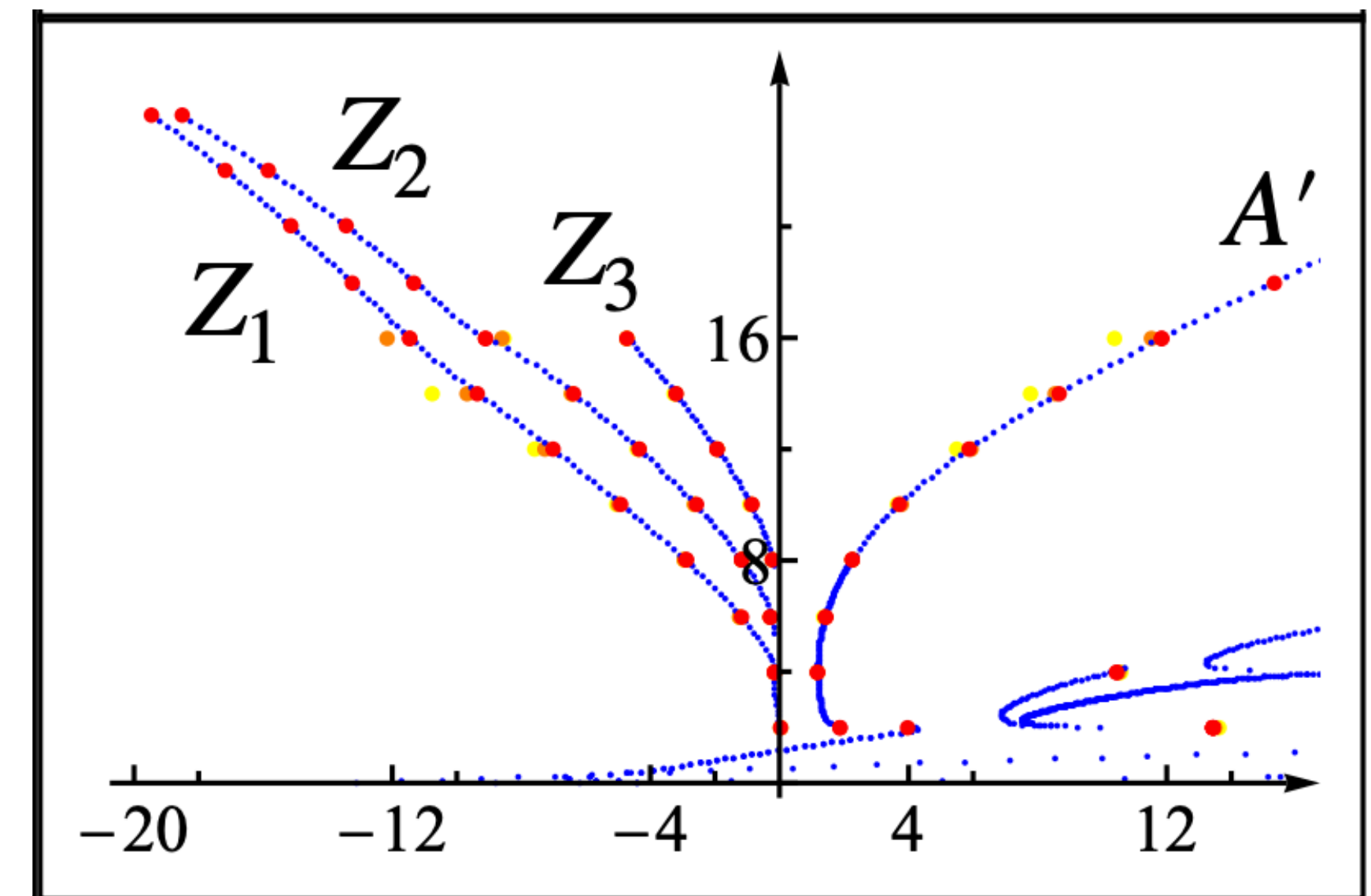
- ➔ Shrinking diffractive cone
- ➔ Presence of dip-bump structures
- ➔ Very rich Regge spectrum

S-matrix bootstrap as a tool to understand high-energy soft QCD

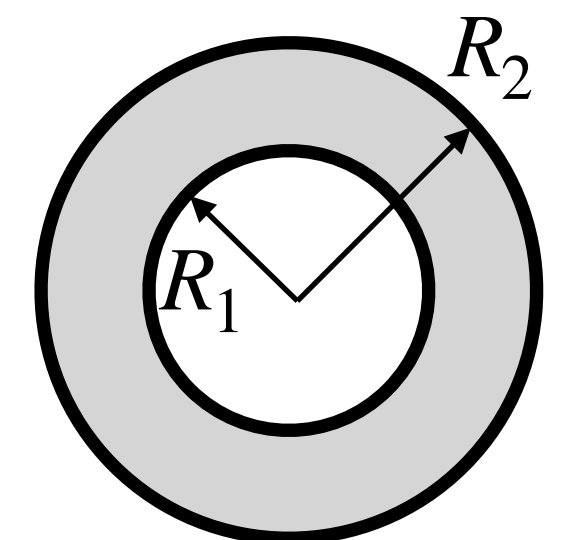
Are these minima consistent with Regge theory?



Could these weird trajectories be the culprit?



White ring model:
$$T_{WR}(s, t) = \frac{8\pi i s}{\sqrt{-t}} \left[R_2 J_1(R_2 \sqrt{-t}) - R_1 J_1(R_1 \sqrt{-t}) \right]$$

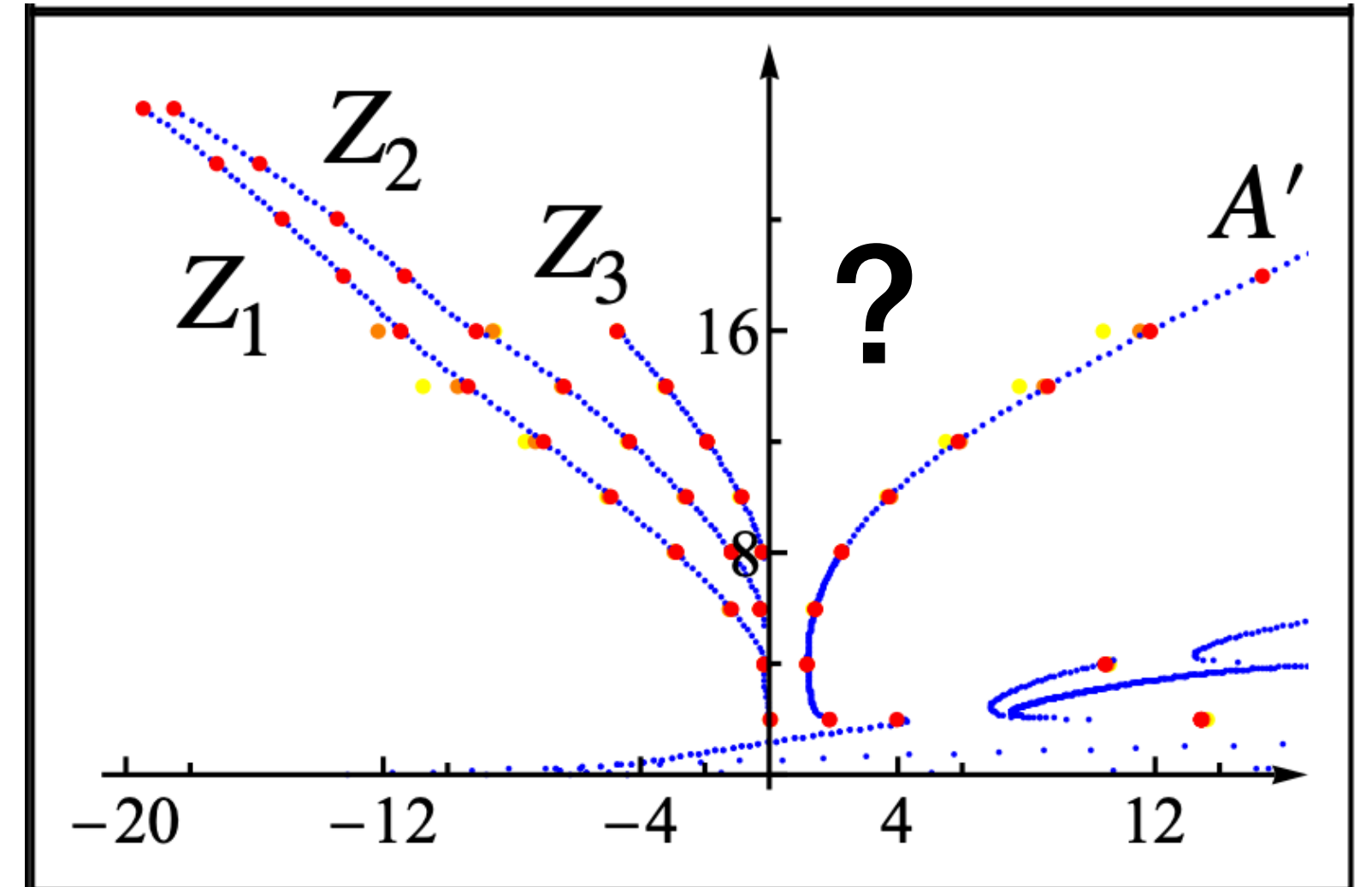


White Ring analytical model

$$T_{WR}(s, t) = \frac{8\pi i s}{\sqrt{-t}} \left[R_2 J_1(R_2 \sqrt{-t}) - R_1 J_1(R_1 \sqrt{-t}) \right]$$

Is this model consistent with **analyticity in spin**?

Yes! for $R_2 \sim r_0 \log s$, compatible with our numerics.



Sommerfeld-Watson transform:

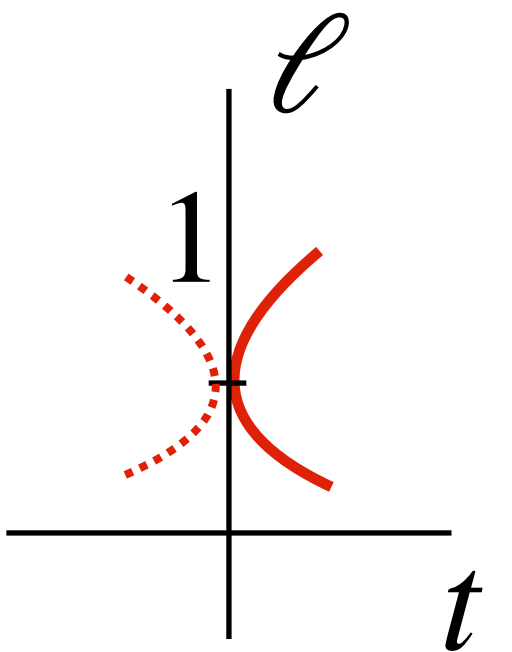
$$T(s \rightarrow \infty, t) \simeq \frac{1}{2\pi i} \oint_C s^\ell f_\ell(t) d\ell$$

t-channel partial wave:

$$f_\ell(t) = \frac{1}{((\ell - 1)^2 - r_0^2 t)^{3/2}}$$

Regge cut with branch-points:

$$\ell_{\pm} = 1 \pm r_0 \sqrt{t}$$



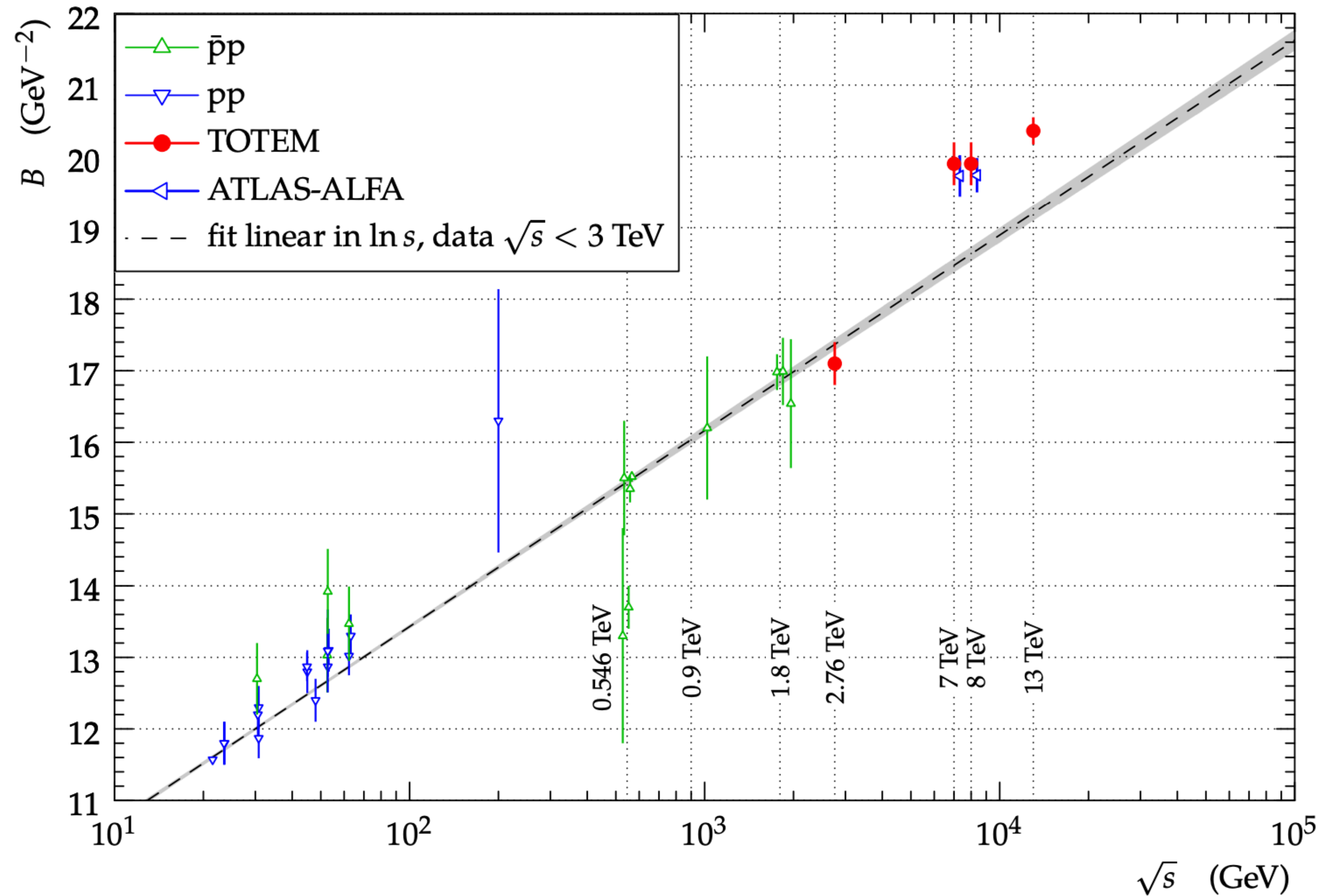
Unusual Possibilities for the Pomeron*

JOHN H. SCHWARZ

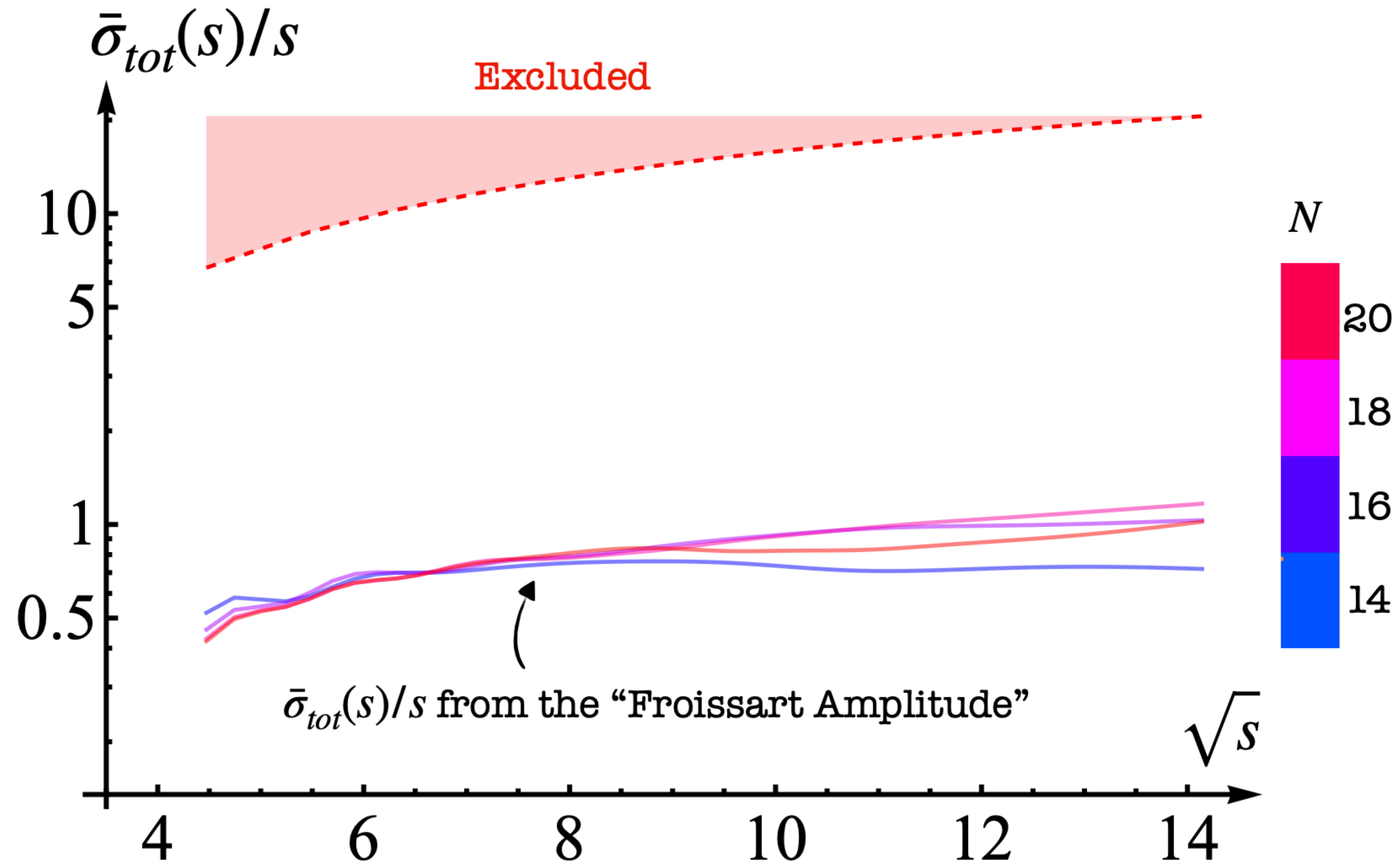
Palmer Physical Laboratory, Princeton University, Princeton, New Jersey

(Received 6 November 1967)

Slope of cone at the LHC



Integrated cross-section



Location in space of low-energy coefficients

Conjecture:

$$\max \bar{\sigma}_{tot}(s \rightarrow \infty) \Leftrightarrow (\max c_2, \min c_0)$$

$$c_0 \equiv T\left(\frac{4}{3}, \frac{4}{3}\right)$$

non-dispersive!

$$c_2 \equiv c_2\left(\frac{4}{3}\right) = \partial_s^2 T\left(\frac{4}{3}, \frac{4}{3}\right) > 0$$

dispersive

The Bootstrap Almond

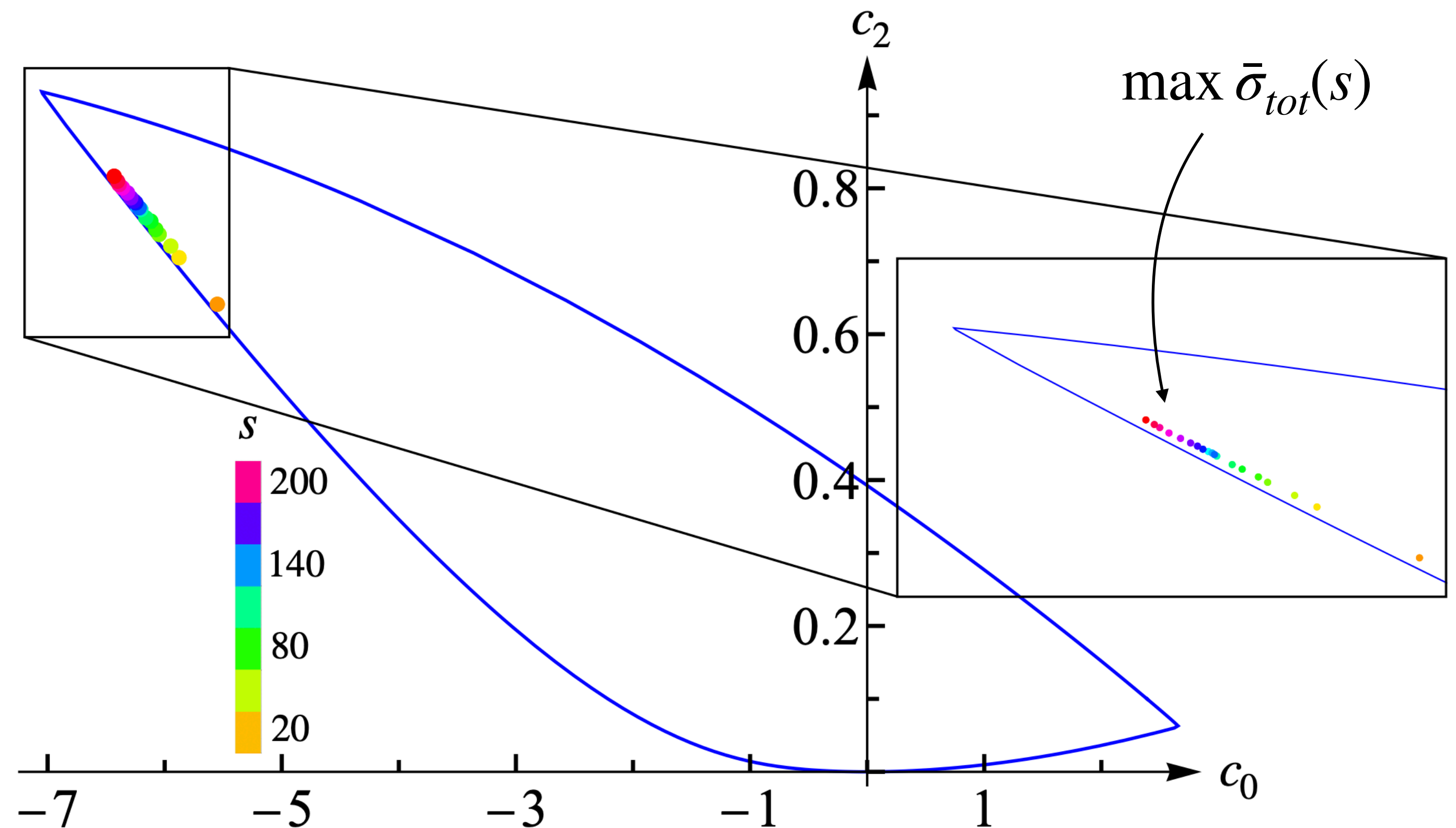
[Paulos, Penedones, Toledo, van Rees, Vieira]

[He, Kruczenski]

[Chen, Fitzpatrick, Karateev]

[Miró, Gümüs, Guerrieri]

[Gümüs, Leflot, Tourkine, Zhiboedov]



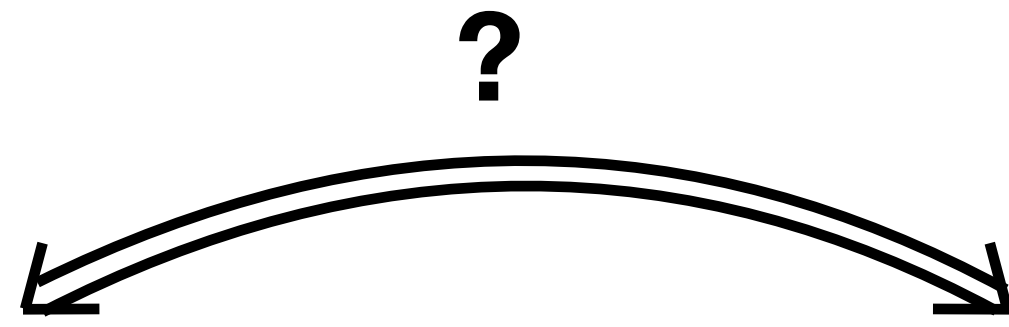
A universal amplitude?

Minimum quartic coupling
($\min c_0$)

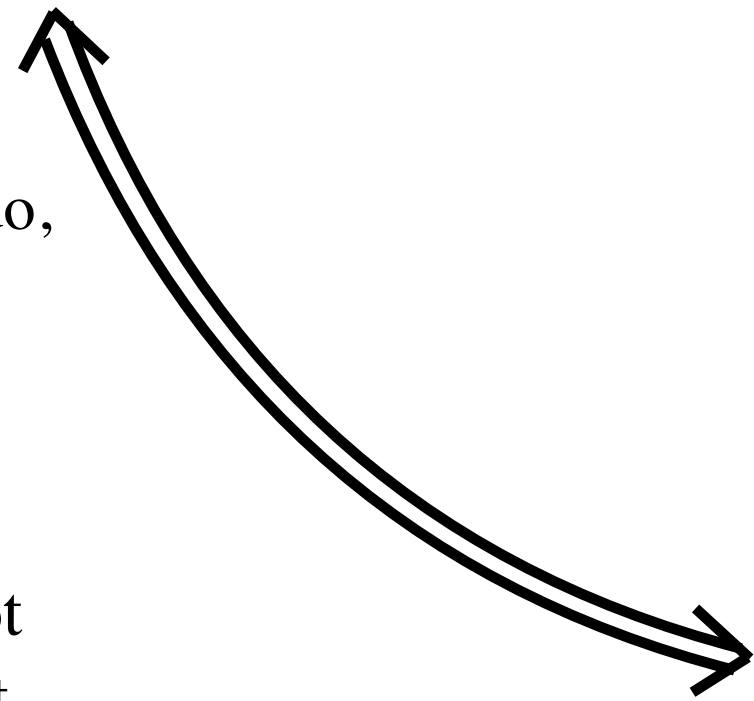
[M. Paulos, J. Penedones, J. Toledo,
B. van Rees, P. Vieira - 2016]

$$-7.8 \lesssim c_0 < 2.6613$$

“Unfortunately we were not able to identify the relevant singularity in this case and thus were not able to improve the slow convergence.”



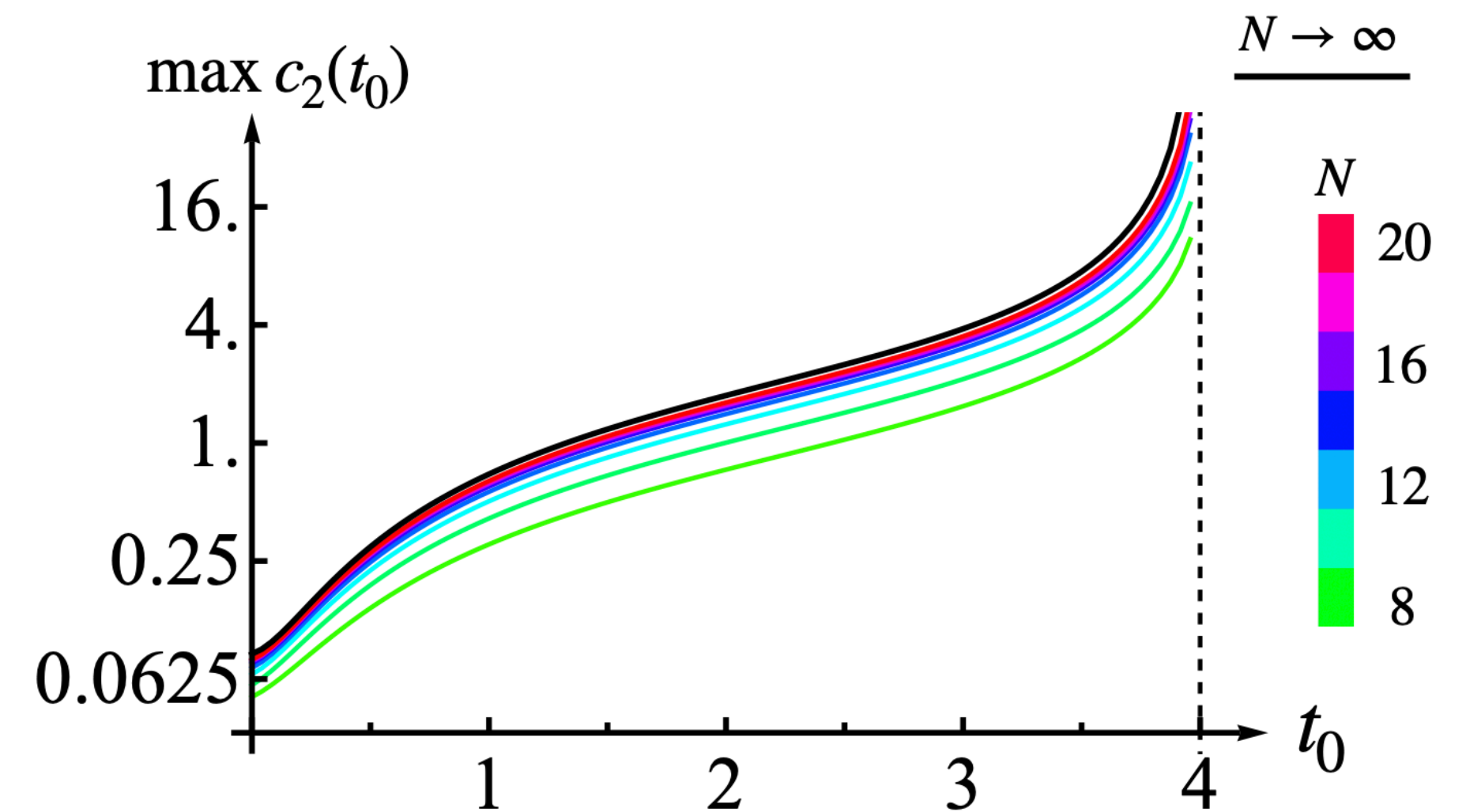
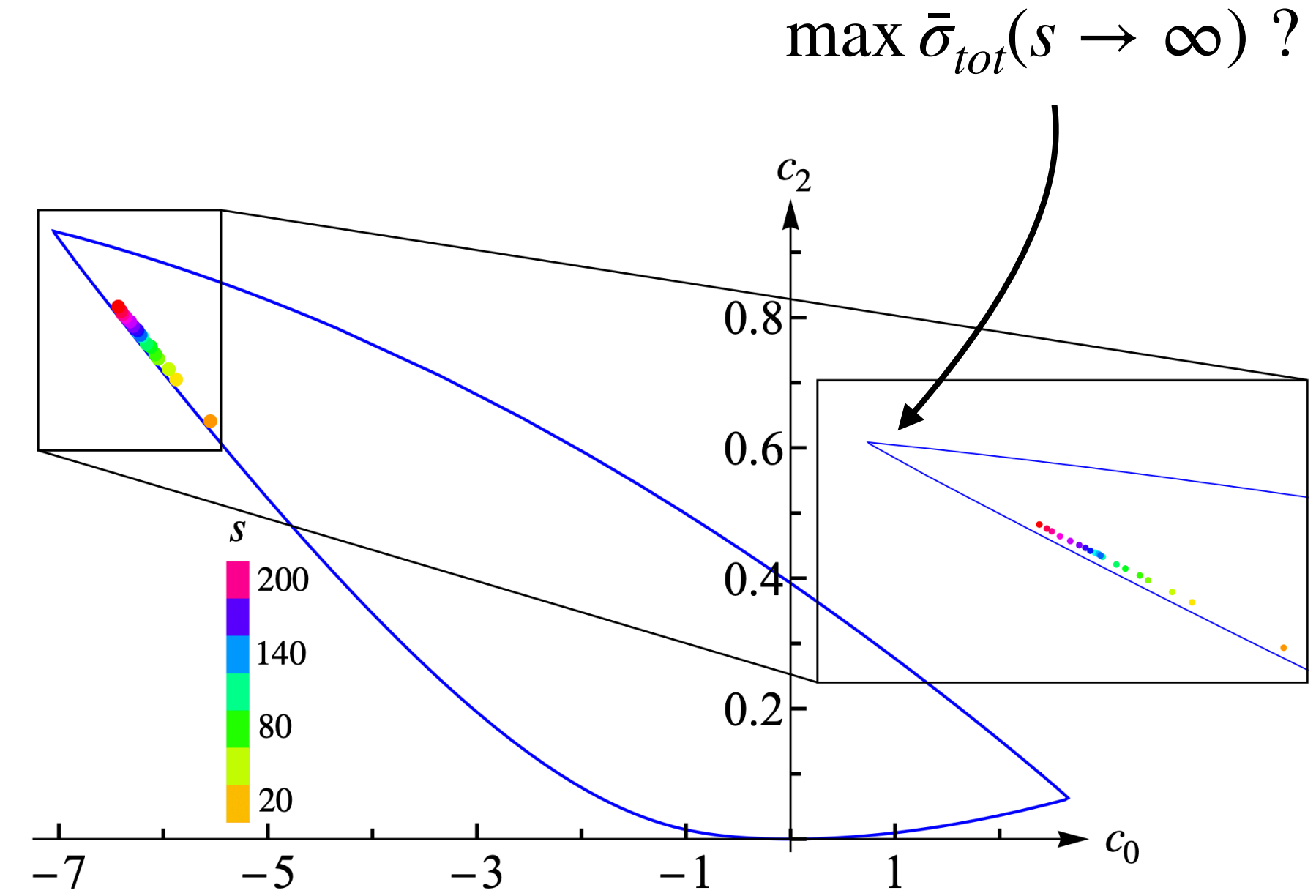
Maximum growth
("Saturation of Froissart")



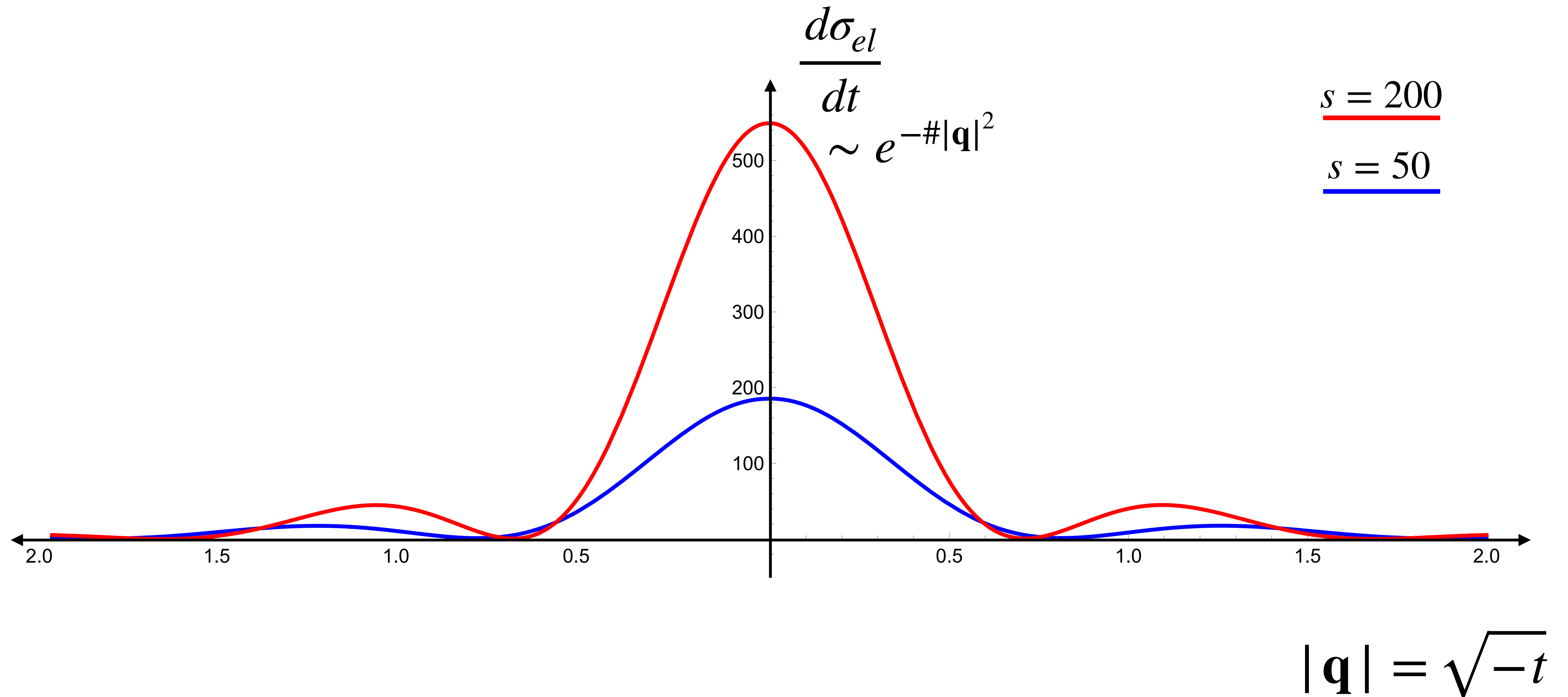
Spin-2 resonance at threshold
($a_2^t \rightarrow \infty$)

It has to Reggeize!

Regge trajectory responsible for Froissart growth?



Elastic differential cross-section (larger $|t| = |\mathbf{q}|^2$)

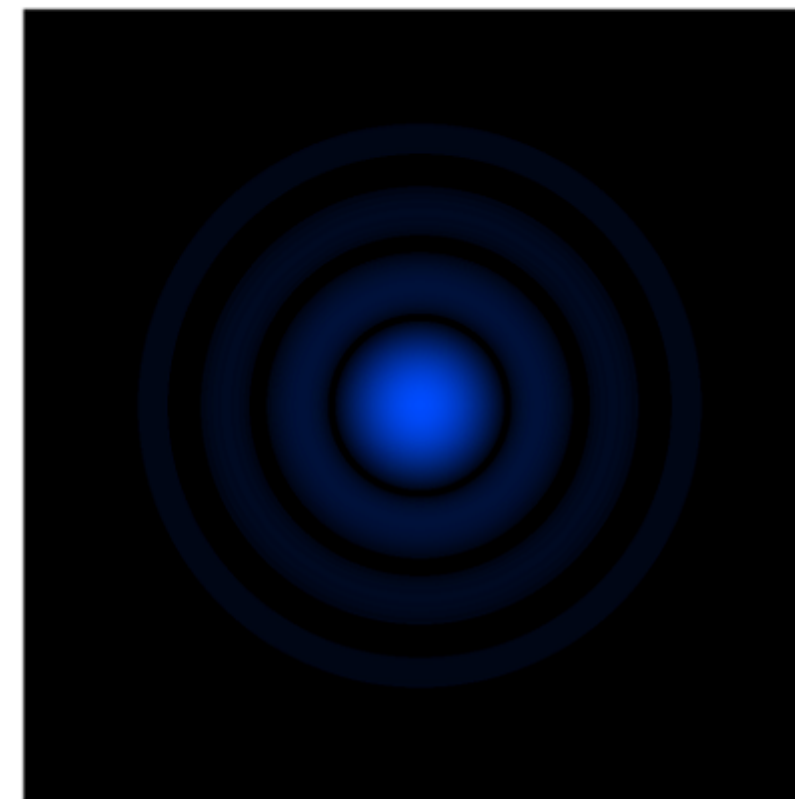


Fraunhofer diffraction and Airy disk

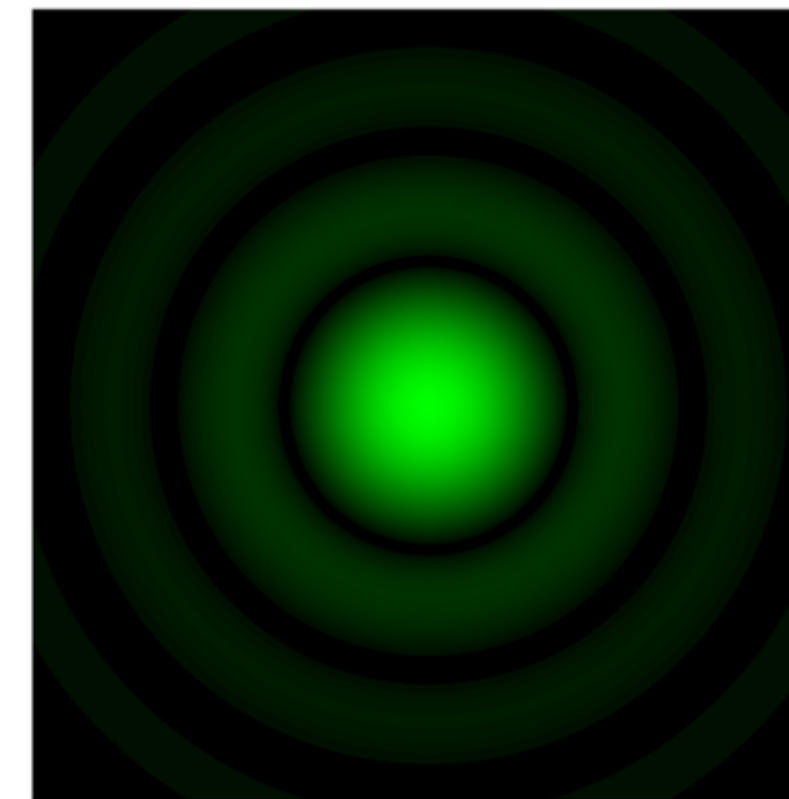
Airy Disk:

“Diffraction pattern produced by light passing through a circular aperture”.

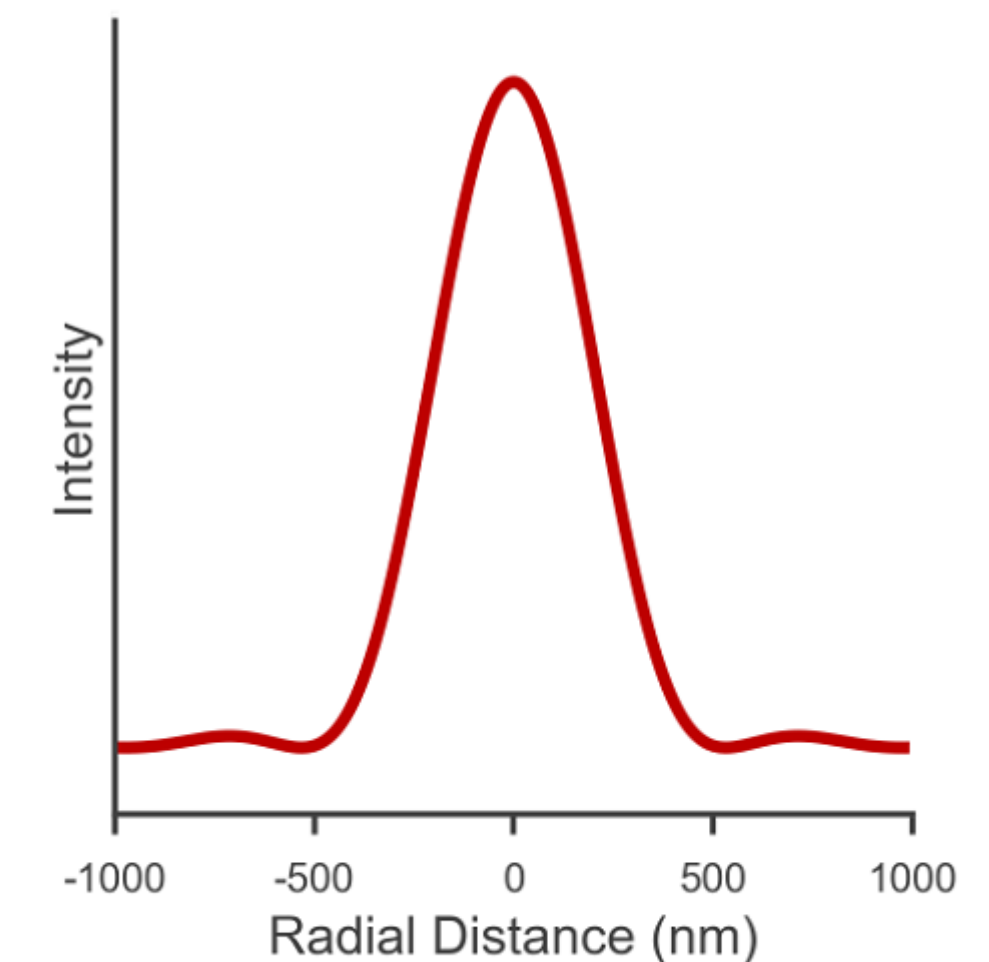
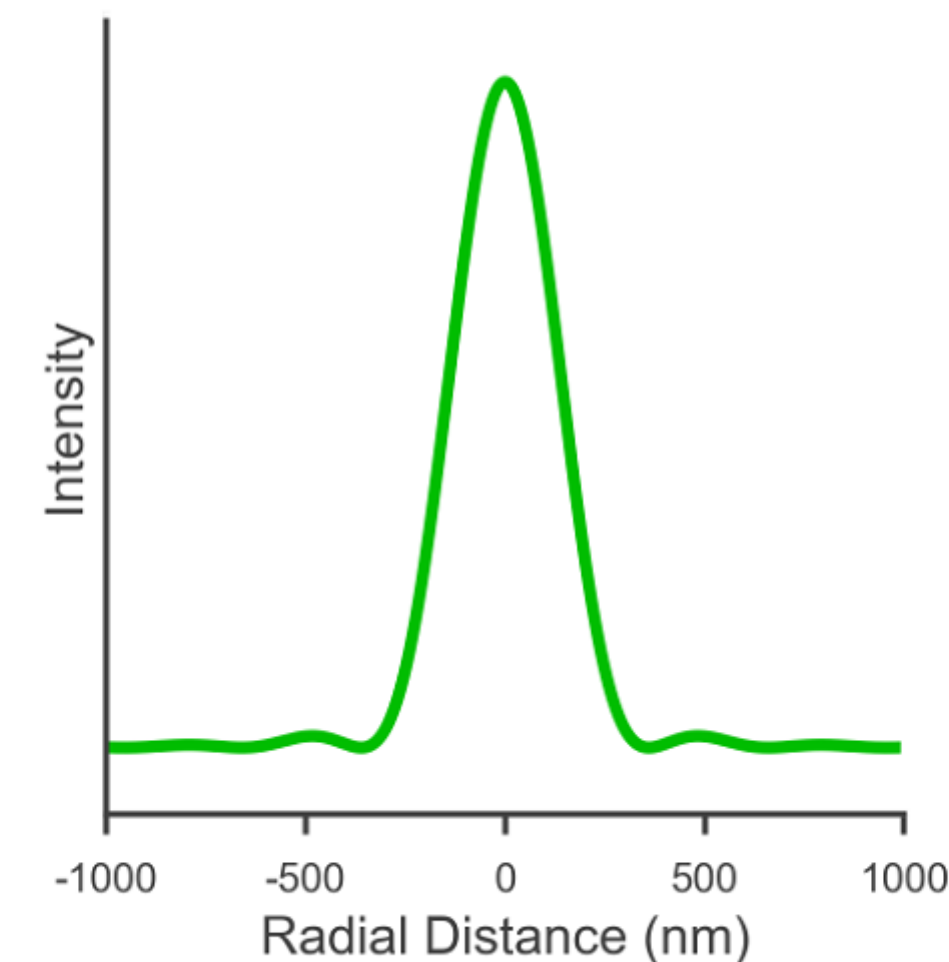
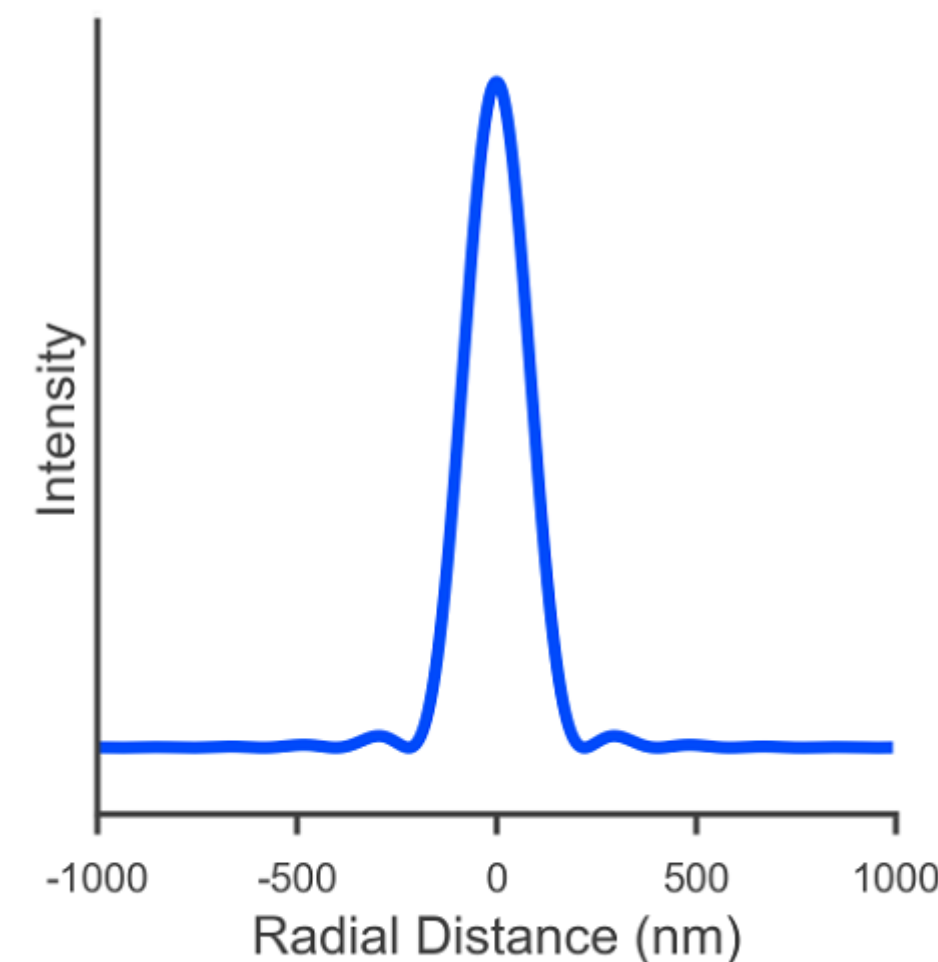
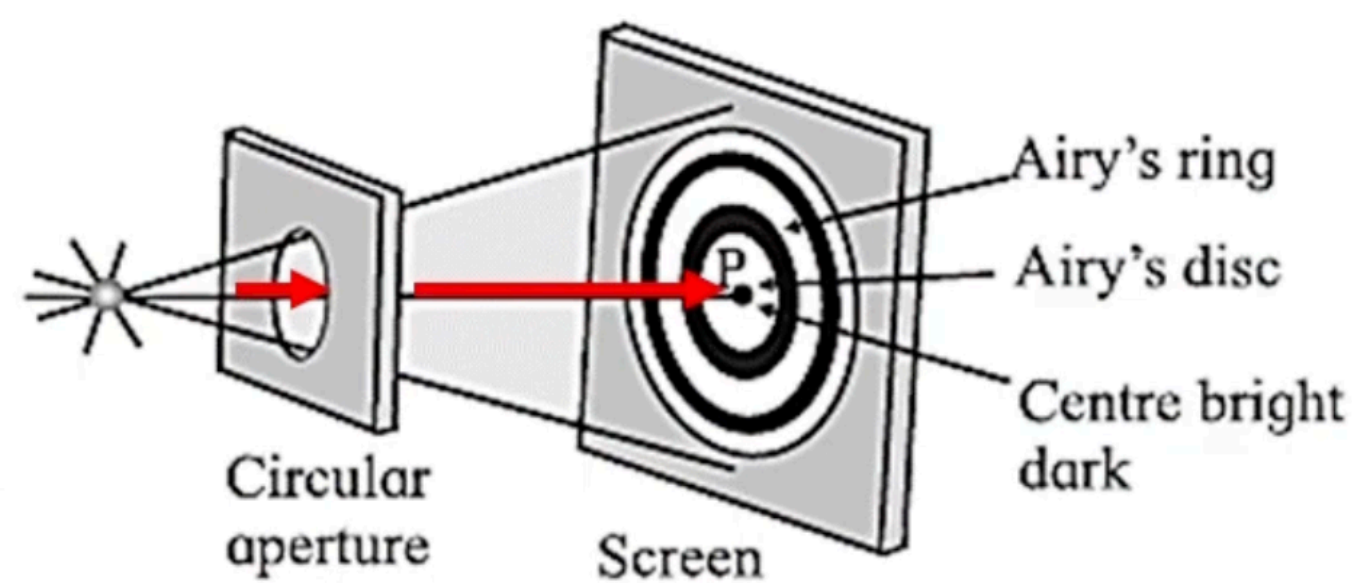
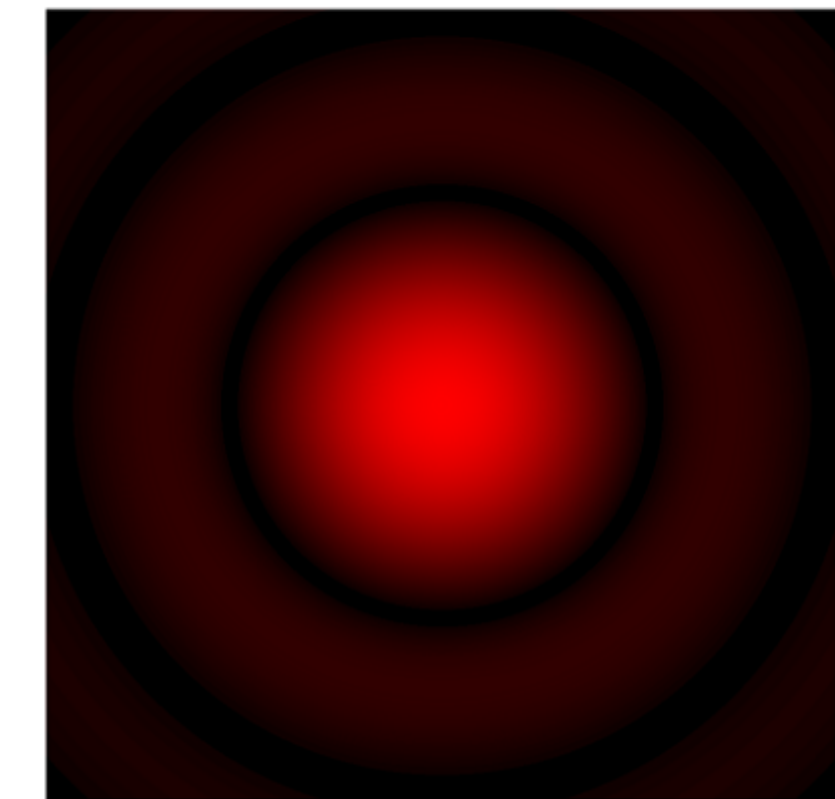
$\lambda = 325 \text{ nm}$
Airy Disc Diameter = 440 nm



$\lambda = 532 \text{ nm}$
Airy Disc Diameter = 720 nm

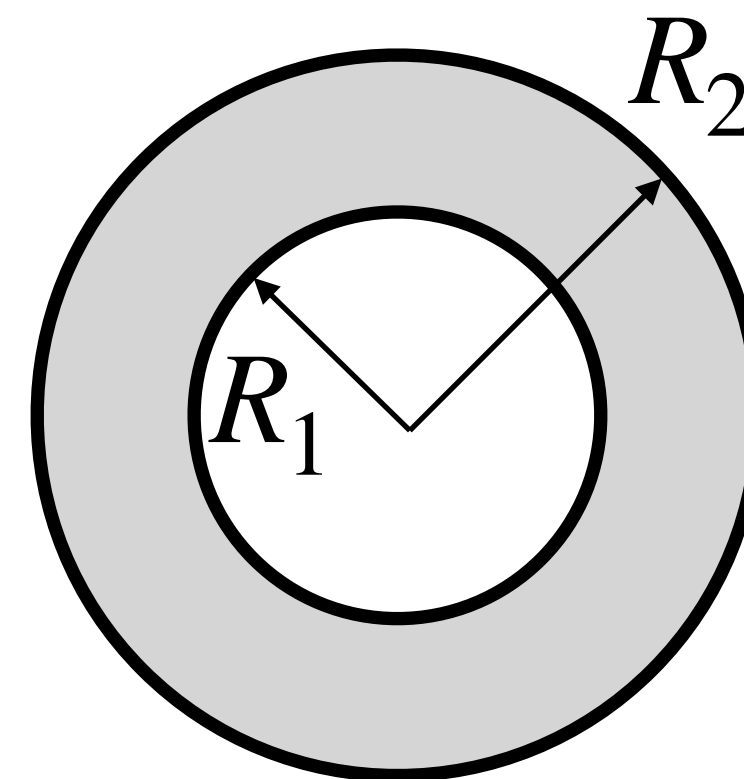
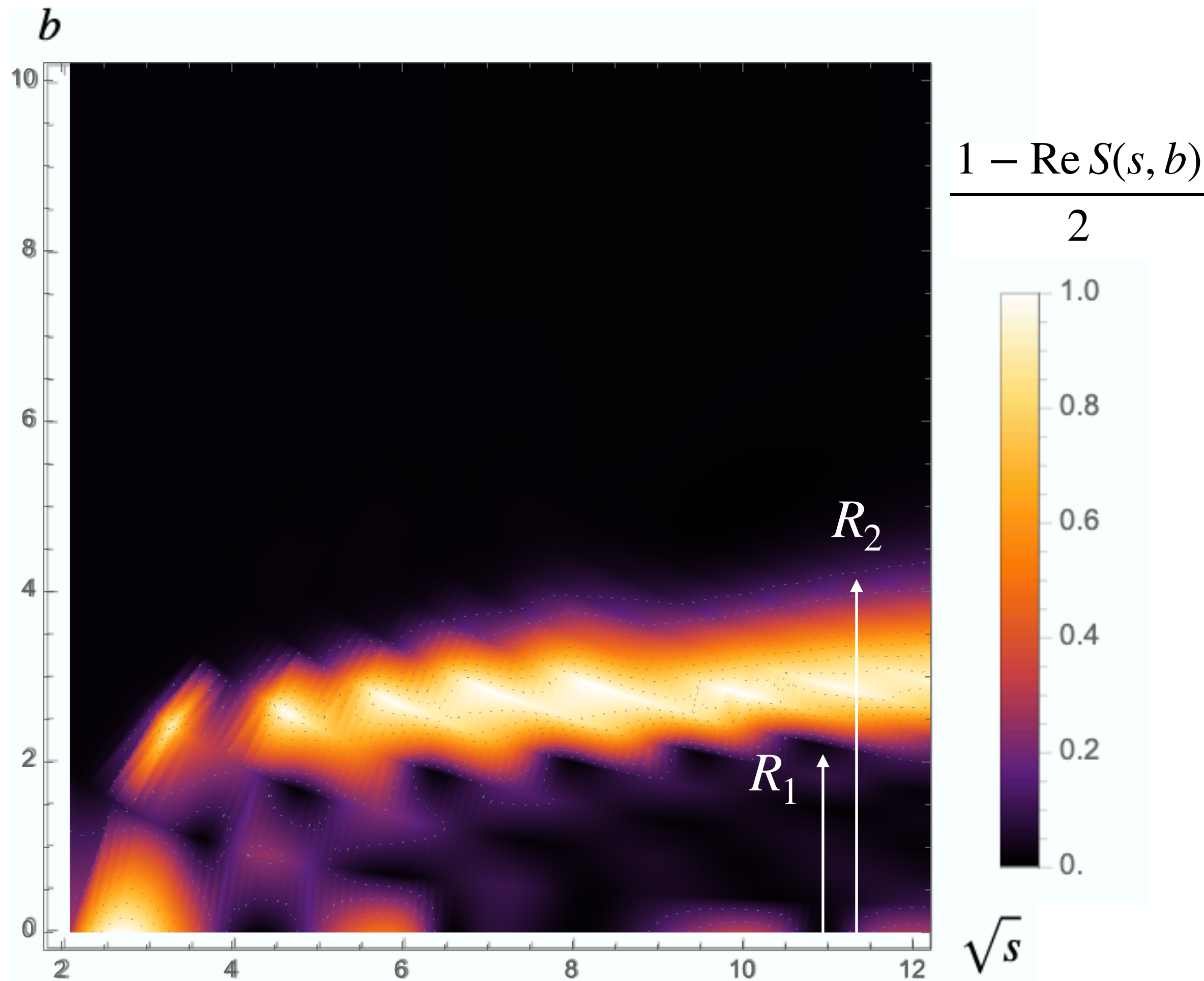


$\lambda = 785 \text{ nm}$
Airy Disc Diameter = 1064 nm



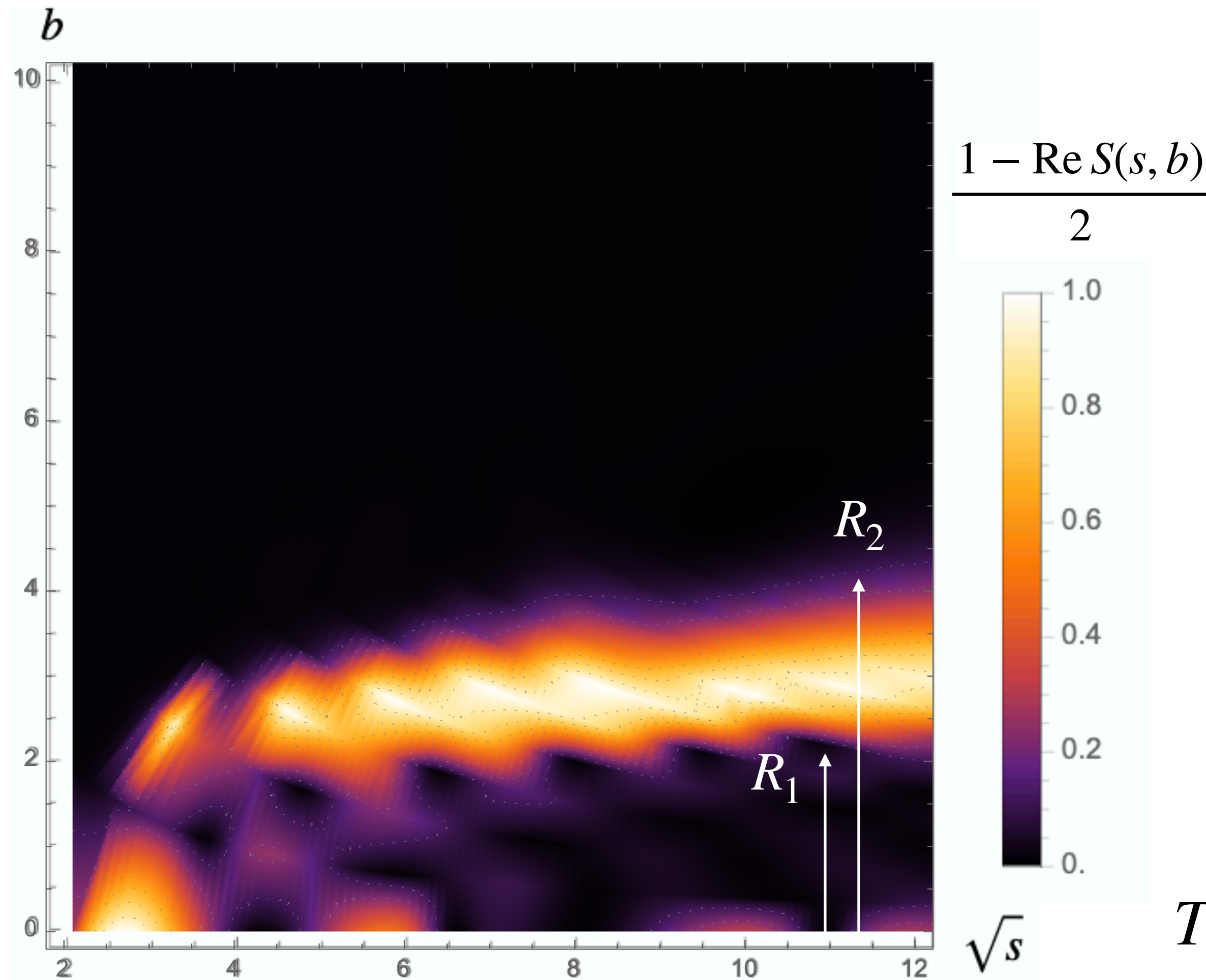
Eikonal representation and white ring model

$$T(s, t) \simeq 2is \int d^{d-2} \mathbf{b} e^{-i\mathbf{q} \cdot \mathbf{b}} (1 - S(s, b))$$

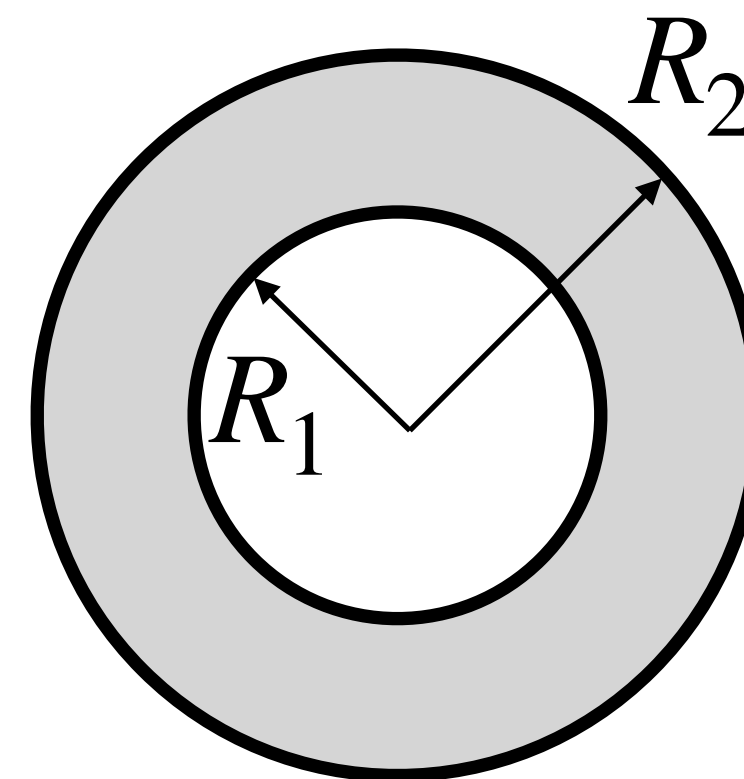


Eikonal representation (bootstrap)

Eikonal representation and white ring model



$$T(s, t) \simeq 2is \int d^{d-2} \mathbf{b} e^{-i\mathbf{q} \cdot \mathbf{b}} (1 - S(s, b))$$



white ring model:

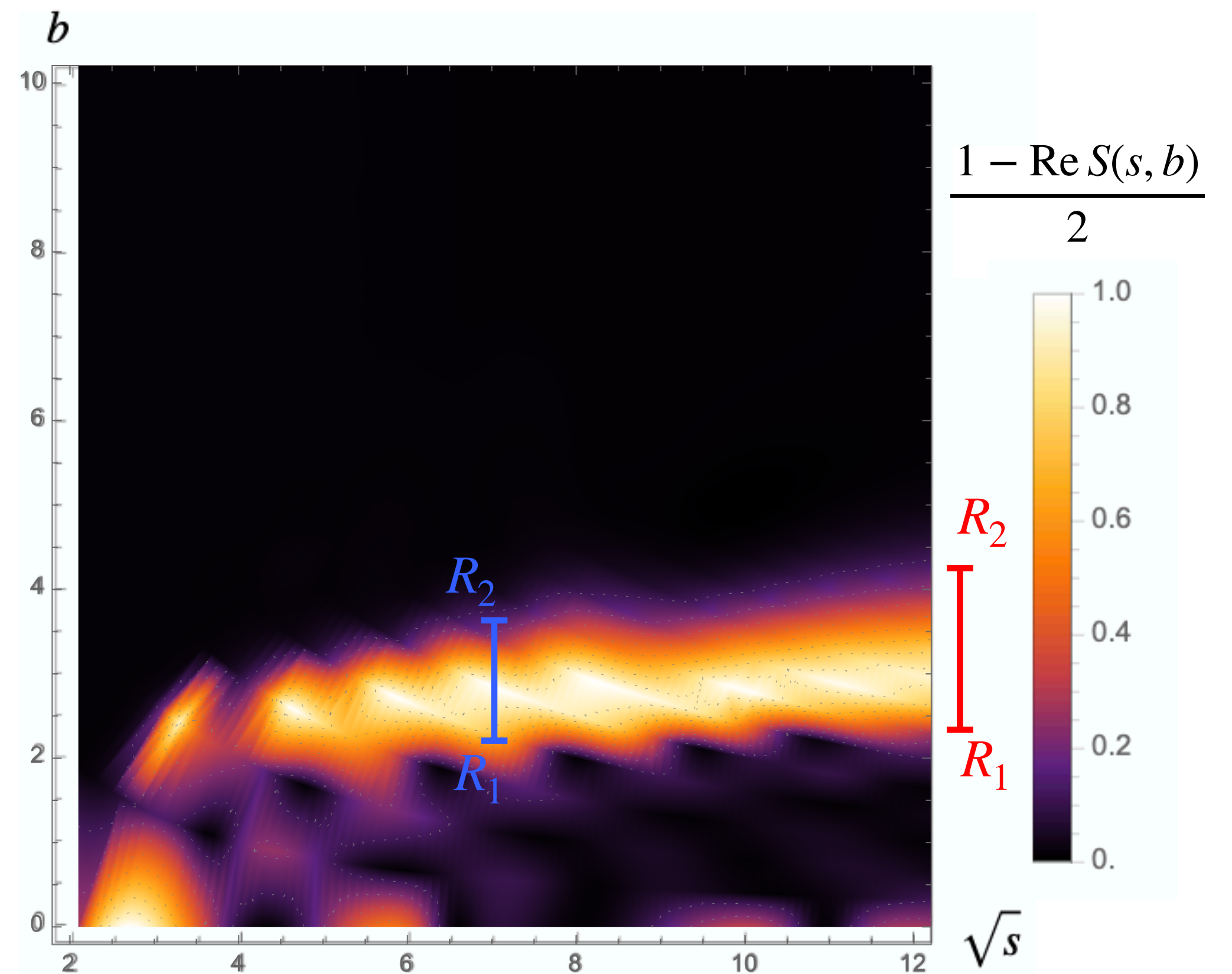
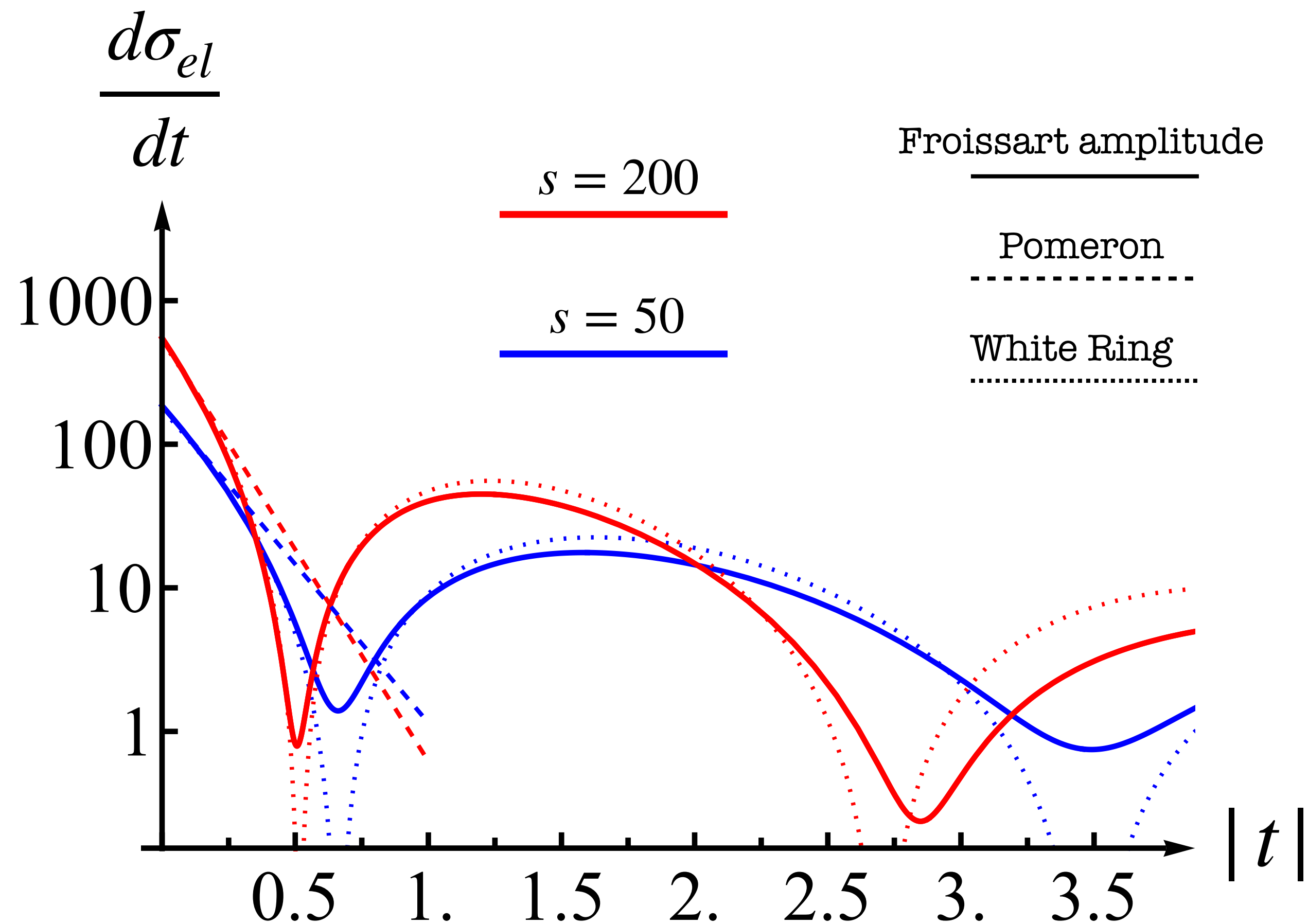
$$S(s, b) = \begin{cases} +1 & \text{if } b < R_1 \\ -1 & \text{if } R_1 \leq b \leq R_2 \\ +1 & \text{if } b > R_2 \end{cases}$$

$$T_{WR}(s, t) = \frac{8\pi is}{\sqrt{-t}} [R_2 J_1(R_2 \sqrt{-t}) - R_1 J_1(R_1 \sqrt{-t})]$$

Eikonal representation (bootstrap)

Elastic differential cross-section

$$T_{WR}(s, t) = \frac{8\pi i s}{\sqrt{-t}} \left[R_2 J_1(R_2 \sqrt{-t}) - R_1 J_1(R_1 \sqrt{-t}) \right]$$



Kupsch

Saturation of the Froissart Bound by Crossing Symmetric and Unitary Amplitudes.

J. KUPSCH

*Fachberich Physik, Universität Kaiserslautern - Kaiserslautern
CERN - Geneva*

(ricevuto il 19 Aprile 1982)

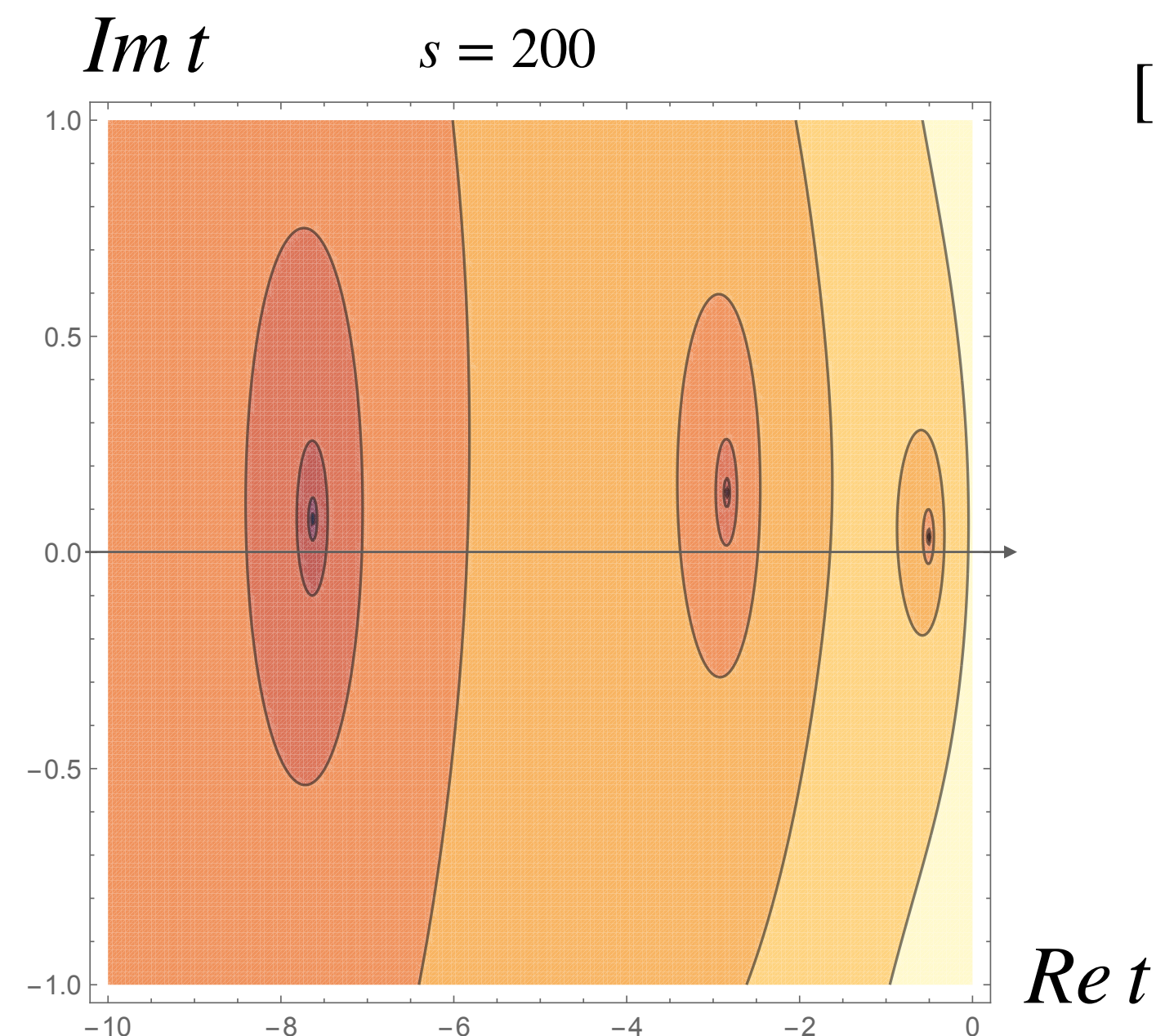
The pomeron of the constructed amplitudes is determined by the function (2.25) $F(s, u)$. Characterized as a singularity in the angular momentum plane, it consists of two branch cuts

$$\mathcal{Q}^{\pm}(t) = \{l = 1 + \lambda\gamma(\pm\sqrt{t}), \lambda_1 \leq \lambda \leq \lambda_2\},$$

where $\gamma(\xi)$ is given in eq. (2.15). For $t = 0$ these branch cuts degenerate to a pole of third order at the coincidence point $l = 1 + \gamma(0) = 1$.

“Forgotten treasures” on Froissart-Regge growth

- Froissart growth requires 3rd order Regge pole at intercept.
- Froissart growth is incompatible with linear trajectory: Requires shrinking of cone with $\log^2 s$ slope (versus $\log s$ slope provided by linear trajectory). [R. Oehme - 1972]
- Froissart growth requires infinitely many zeros near physical region $t \leq 0$ as $s \rightarrow \infty$.



[G. Auberson, T. Kinoshita, A. Martin - 1971]

“Froissart amplitude”

“Black ring” effect

Energy evolution of the overlap functions:
increasing ratio of $\sigma_{el}(s)/\sigma_{tot}(s)$ and black ring
emergence [2022]

S.M. Troshin, N.E. Tyurin

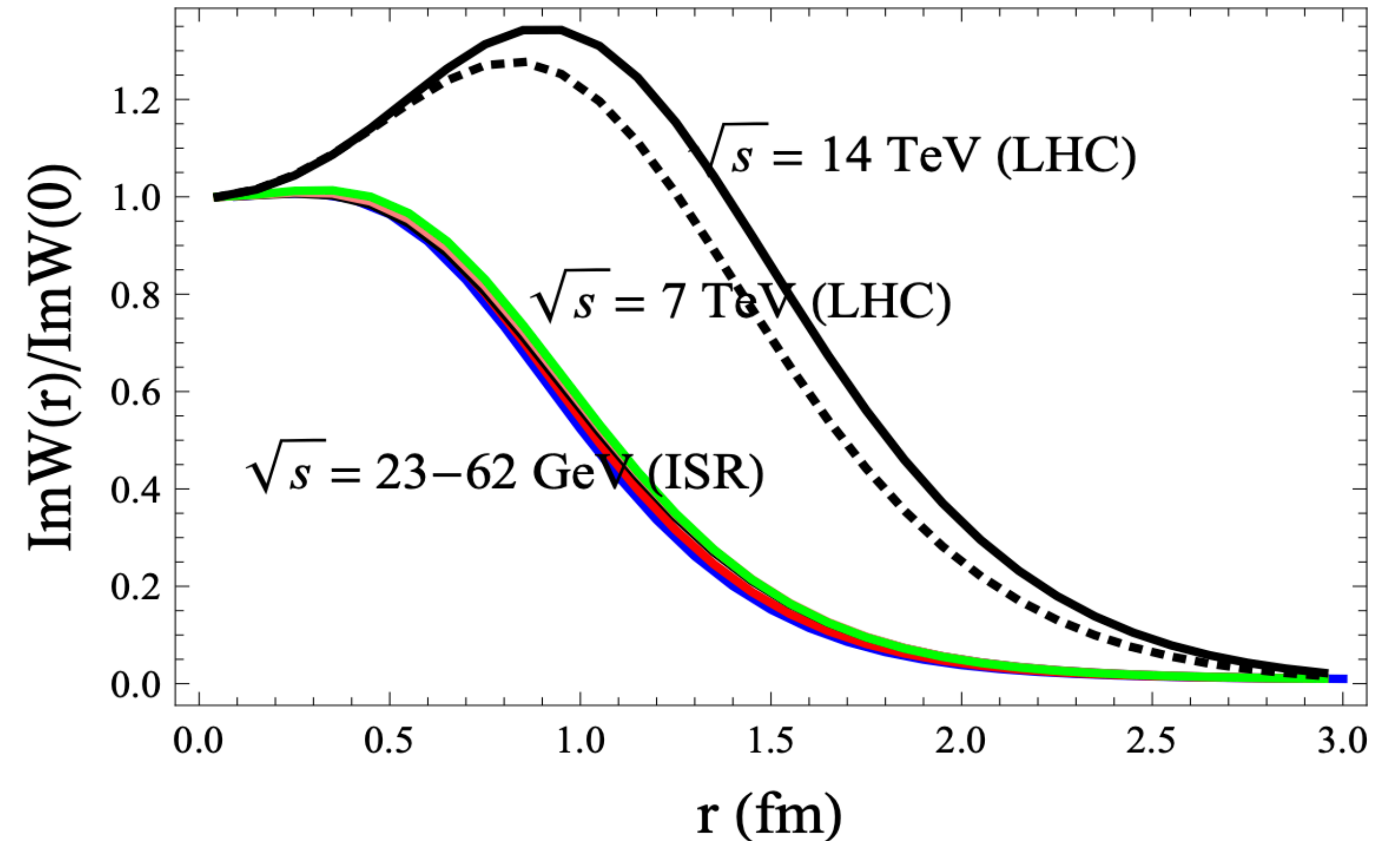
NRC “Kurchatov Institute”–IHEP
Protvino, 142281, Russia

Abstract

We consider two possible options of the energy dependency of the elastic and inelastic overlap functions. Those correspond to saturation of the black disk limit (BEL effect) and to the unitarity saturation (REL effect) at $s \rightarrow \infty$. Relation of the REL effect to increase of the ratio $\sigma_{el}(s)/\sigma_{tot}(s)$ and emergence of black ring picture at the LHC is underlined.

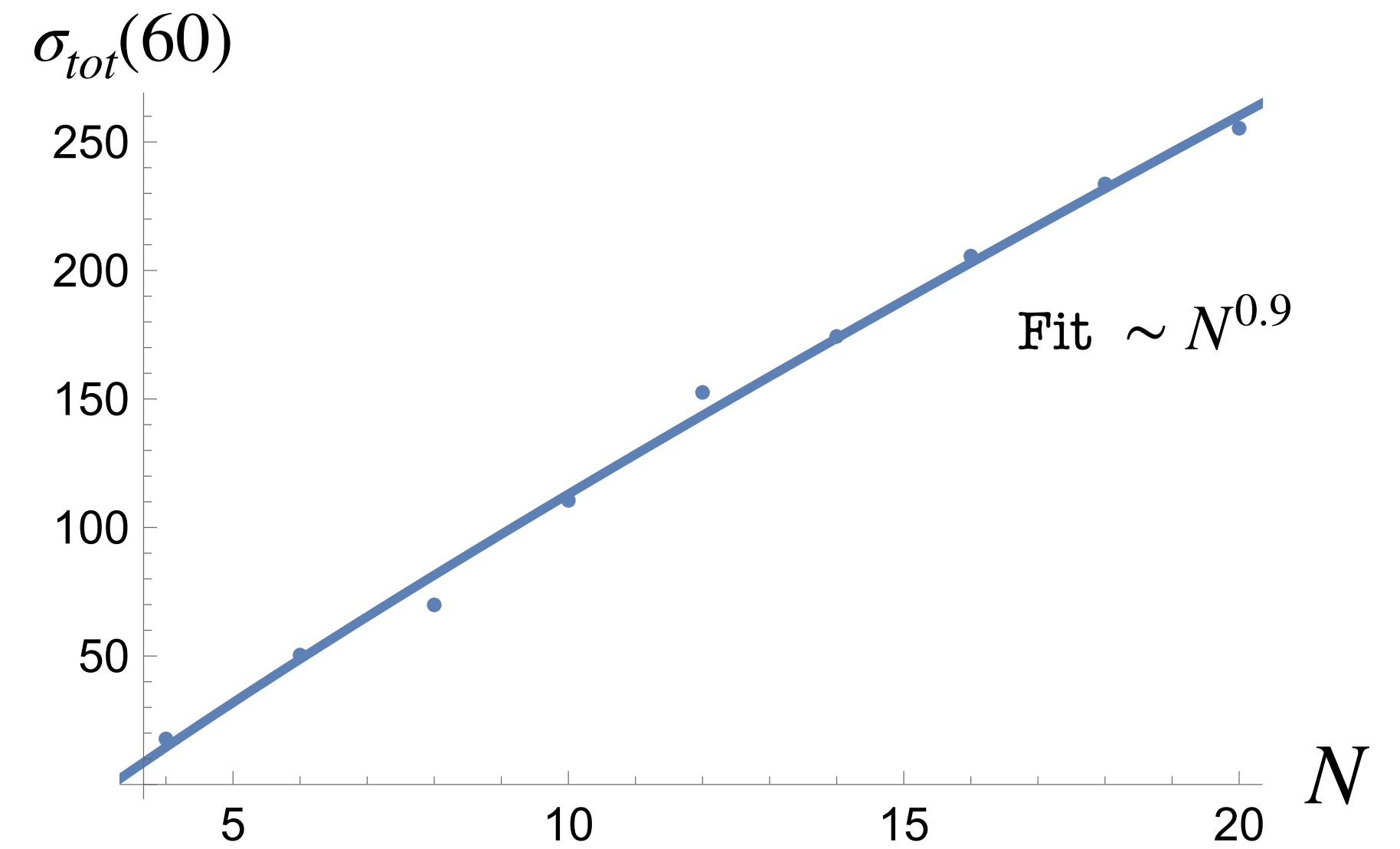
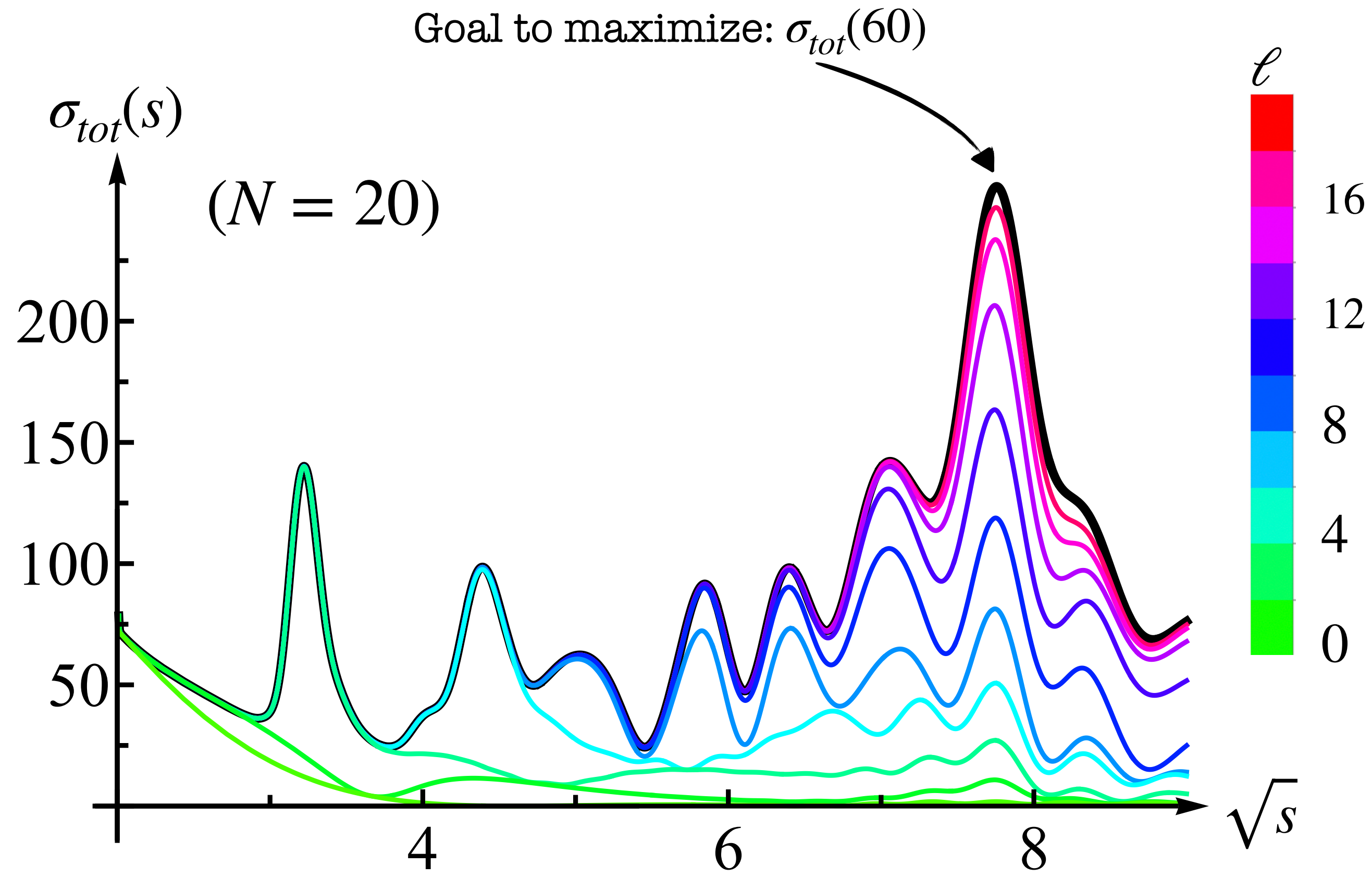
Keywords: Central collisions; Elastic scattering; Unitarity.

Inelastic overlap function

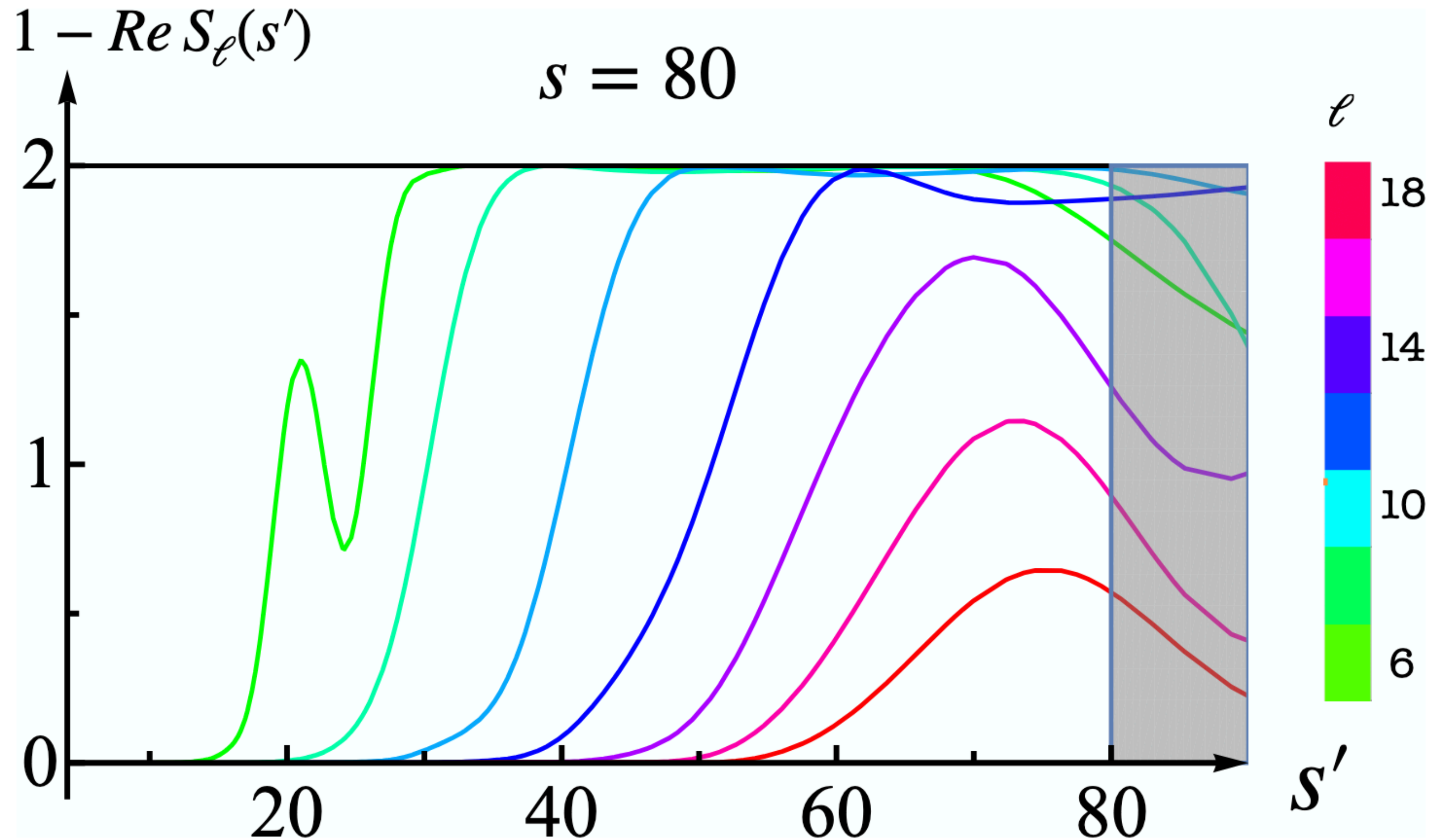


**Proton-Proton On Shell Optical Potential at High Energies
and the Hollowness Effect**

Cross-section maximization point-wise



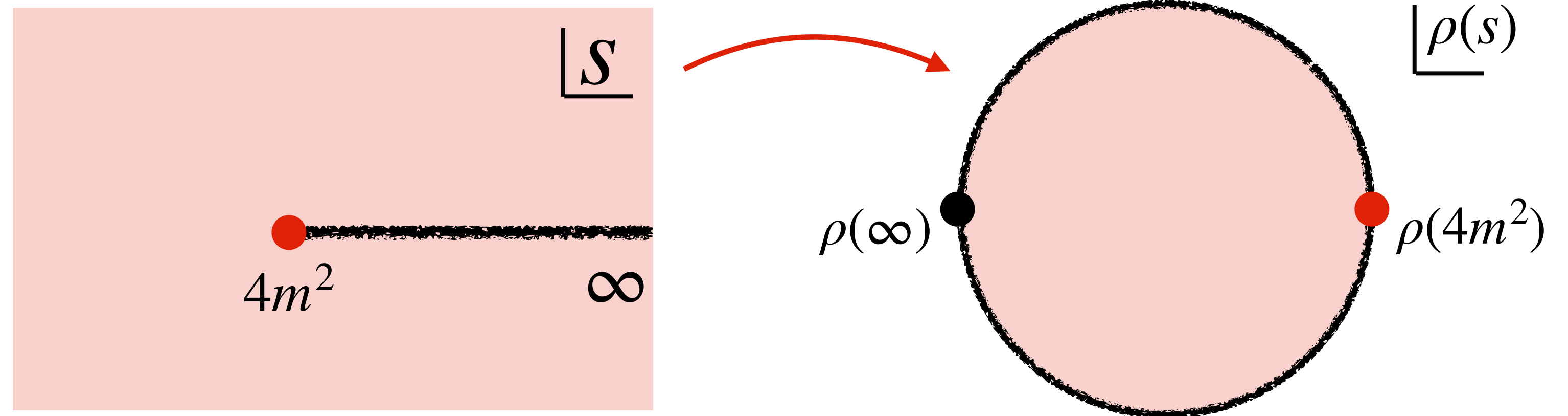
Yndurain Amplitude (partial waves)



Numerical S-matrix Bootstrap

1. Analyticity

$$\rho(s) = \frac{\sqrt{4-s_0} - \sqrt{4-s}}{\sqrt{4-s_0} + \sqrt{4-s}}$$



2. Crossing symmetry

$$T(s, t, u) = \sum_{a,b,c}^N \alpha_{(abc)} \rho^a(s) \rho^b(t) \rho^c(u)$$

3. Unitarity

$$\hat{S}^\dagger \hat{S} = \hat{1} \quad \xrightarrow{\text{partial waves}} \quad |S_\ell(s)|^2 \leq 1$$

imposed numerically using SDPB for all $\ell \leq L$

$$N, L \rightarrow \infty$$

[Simmons-Duffin; 2015]